Alma Mater Studiorum – Università di Bologna
in cotutela con Universidad Del Pais Vasco-Spagna

DOTTORATO DI RICERCA IN

CHIMICA

Ciclo 30º

Settore Concorsuale: 03 / C2

Settore Scientifico Disciplinare: CHIM / 04

TITOLO TESI

The effect of different compatibilizers agents on the nucleation and crystallization behaviour of poly(lactide)/poly(ε-caprolactone) blends

Presentata da: Matteo Rizzuto

Coordinatore Dottorato	**Supervisore**
Prof. Aldo Roda	Prof. Daniele Caretti
	Supervisore
	Prof. Alejandro J.Muller

Esame finale anno 2018

ABSTRACT (English)

In this work the effect of adding different kind of compatibilizers to poly(lactide)(PLA)/poly(ε-caprolactone)(PCL) 80/20 blends has been investigated, evaluating the results by SEM (Scanning Electron Microscopy), PLOM (Polarized Light Optical Microscopy), DSC (Differential Scanning Calorimetry) and tensile tests.

The addition of poly(lactide-ran-caprolactone), P(LA-*ran*-CL) to PLA/PCL blends does not improve the compatibility between PLA and PCL, however a plasticization effect, that increases the crystallization ability of the PLA phase, is induced. Such plasticization effect can increase the spherulitic growth rate of PLA up to two or three fold as compared to neat PLA, depending on the Tg of the random copolymer employed. At the same time copolymer incorporation in the blends leads to an anti-plasticization effect of the PCL droplets, reducing their crystallization rate.

Poly(L-lactide-block-carbonate) diblock copolymers P(LA-b-C) are effective in improving the miscibility between PLA and PCL. However, the acceleration of the cold crystallization kinetics of PLA upon blending with PCL, often reported in the literature, is not connected with the miscibility between PLA and PCL phases, as it is also present in the uncompatibilizated PLA/PCL blend, but is due to a nucleation effect induced by PCL crystals on glassy PLA. Such nuclei only become effective upon heating to PLA cold crystallization temperatures, at which PCL is already molten.

The addition of poly(ε-caprolactone)-poly(carbonate) (PCL-*co*-PC) based copolymers does not cause an increase in miscibility in PLA-PCL phases, however copolymers addition causes a reduction of molecular weight in melt mixed blends. As result, PLA phase within the blends containing PCL-PC based copolymers shows a higher tendency to crystallize during both isothermal and non-isothermal DSC experiments. The increased crystallization of PLA phase is attributed to an increase in spherulitic growth kinetics determined by PLOM analysis.

ABSTRACT (Italiano)

In questo lavoro e' stato anlizzato l'effetto dell'aggiunta di diversi tipi di compatibilizzanti in miscele di poly (lattide)(PLA) / poly (ε-caprolattone) (PCL) 80/20, valutando i risultati mediante SEM (microscopia elettronica a scansione), PLOM (microscopia ottica a luce polarizzata)), DSC (Calorimetria a scansione differenziale) e prove di trazione.

L'aggiunta di poli(lattide-ran-caprolattone), P(LA-ran-CL) in miscele di PLA/PCL non migliora la compatibilità tra PLA e PCL, tuttavia viene indotto un effetto plasticizzante in grado di aumentare la capacità di cristallizzazione della fase di PLA. Tale effetto di plasticizzazione può aumentare la velocità di crescita sferulitica del PLA fino a due o tre volte rispetto al PLA puro, a seconda della Tg del copolimero impiegato. Allo stesso tempo l'incorporazione del copolimero nelle miscele porta ad un effetto anti-plastificante delle goccie di PCL, riducendo la loro velocità di cristallizzazione.

I copolimeri diblocco poly(lattide-block-carbonato) P (LA-b-C) sono efficaci nel migliorare la miscibilità tra PLA e PCL. Tuttavia, l'aumento della cinetica di cristallizzazione a freddo del PLA dopo miscelazione con PCL, spesso riportata in letteratura, non è collegata alla miscibilità tra le fasi PLA e PCL, in quanto è presente anche nella miscela PLA / PCL non compatibilizzata. Piuttosto, è dovuto ad un effetto sulla nucleazione del PLA vetroso indotto da cristalli di PCL. Tali nuclei diventano efficaci solo durante il riscaldamento del PLA fino alla sua temperature di cristallizzazione, temperatura in cui il PCL è già fuso.

L'aggiunta di copolimeri poli (ε-caprolattone)-poli (carbonato) (PCL-co-PC) non causa un aumento della miscibilità nelle fasi PLA-PCL, tuttavia l'aggiunta di questi copolimeri causa una riduzione del peso molecolare del PLA. Come risultato, la fase PLA all'interno delle miscele contenenti copolimeri basati su PCL-PC mostra una maggiore tendenza a cristallizzare durante gli esperimenti DSC isotermici e non isotermici. L'aumentata cristallizzazione della fase PLA è attribuita ad un aumento della cinetica di crescita sferulitica determinata dall'analisi PLOM.

OVERVIEW

In this work a detailed investigation into poly(lactide) (PLA) crystallization within its immiscible blend with poly(ε-caprolactone) (PCL), upon the addition of different kind of compatibilizers, has been carried out. After a general introduction, the topic has been developed through three different chapters. Each of them is self-consistent, including all the relevant information from introduction to conclusion.

In the first chapter, *Plasticization and anti-plasticization effects caused by poly(lactide-ran-caprolactone) addition to double crystalline Poly(L-lactide)/Poly(ε-caprolactone) blends,* the crystallization behaviour of PLA/PCL has been examined upon the addition of two different kind of poly(lactide)-poly(ε-caprolactone) random copolymers, P(LA-*ran*-CL)s. The results demonstrate that the addition of P(LA-*ran*-CL) to PLA/PCL blends induce a plasticization effect that increases the crystallization ability of the PLA phase. Furthermore, a combined non-isothermal – isothermal experiment was designed in order to demonstrate that copolymer incorporation in the blends leads to an anti-plasticization effect of the PCL droplets.

In the second chapter, *Can poly(ε-caprolactone) crystals nucleate glassy polylactide?*, three different kinds of poly(L-lactide-*block*-carbonate) copolymers, PLA-*co*-PC, (varying composition and molecular weight) have been used for the first time to tune the compatibility between PLA and PCL. Cold crystallization of PLA (i.e., the crystallization of PLA during heating from the glassy state) has been investigated, both under non-isothermal and isothermal conditions. The use of specially designed thermal protocols has allowed us to successfully explain the effect of PCL on PLA crystallization nucleation.

In the third chapter, *Crystallization behaviour of poly(lactide) in immiscible blend with poly(ε-caprolactone) comparison with solution and melt-mixed blends*, two different poly(ε-caprolactone)-poly(carbonate) based copolymers, PCL-*co*-PC, (varying for the length of the sequential block units) have been used. At the same time, in order to study the effect of the blend preparation, blending has been carried out by both melt
and solvent mixing. The results indicate that crystallization rate of PLA is highly sensible to processing conditions if these ones can modify the molecular weight.

INDEX

1 INTRODUCTION

1.1 CRYSTALLIZATION IN POLYMERS

Crystallization in polymers may be considered as a phase transition process from a disorder state, in which polymer chains are distributed under a randomly coiled conformation, to an order state, in which the chains are rearranged in chain-folded lamellae.[1] The process differs from the crystallization of low molecular weight substances.

Crystallization of polymers occurs under conditions far removed from the equilibrium and mainly depends on kinetics factors, rather than thermodynamics. The crystal growth at a given temperature is the crystal with the highest growth rate, not necessarily the structure with the lowest free energy.[2]

This peculiar behaviour is due to the long chain nature of polymers, which makes difficult chain disentanglement to achieve a regular conformation within the crystal. Furthermore, instead of forming extended chain-length infinite crystals, polymer chains are folded in thin lamellae surrounded by an amorphous interface, which is formed by the folded chain interface, tie chains, entanglements, end groups, bulky substituent groups, and chain defects, all of which cannot be included into the crystalline lattice.

At the same time, being nonequilibrium structures, polymer crystals are metastable, that is, they may rearrange and modify their structure over time, depending on the temperature, pressure, stress, or solvent vapors, to which the material is exposed.

All these factors are at the origin of the semicrystalline nature of polymers: only a fraction of the units composing the long chains is able to attain the ordered arrangement required by crystallization. The amount of this fraction (i.e., degree of crystallinity) determines most of the properties of the material, as the mechanical and thermal stability, or, in the case of biodegradable polymers, the degradation rate.

In this chapter the crystallization of polymers will be briefly revised, through a summary of the crystallization process and the most common method to measure crystallization kinetics. A more detailed dissertation will be presented in next chapter, adapting the matter to the main topic of the work (see Chapter 1.1.3 CRYSTALLIZATION BEHAVIOUR OF POLY(LACTIDE)).

1.1.1 The Crystallization process

Crystallization is typically examined in terms of two independent phenomena: initial crystal nucleation and subsequent growth of crystals.

Nucleation occurs from a small group of aligned segments, or nuclei, with an appropriate surface and at enough size to constitute a stable interface between the liquid and crystal phases. Depending on the type of nuclei, nucleation may be distinguished in homogeneous and heterogeneous.[3]

Homogeneous nucleation is assumed to occur when random fluctuations of chains generates a local alignment (embryo or cluster) with appropriate size and morphology to be stable in time.[4]

On the other hand, heterogeneous nucleation is commonly originated by foreign nuclei, that is, any (low mass) particle with the correct size and surface. Heterogeneous nucleation is the most common way of nuclei formation, since it requires a much lower energy barrier than homogeneous nucleation and, at the same time, commercial polymers always contain catalytic debris and any other impurities that are left over from their synthesis and/or their first processing before the material is commercialized.[5]

At enough supercooling the formation of nuclei is followed by their growth to crystals. The growth is initially restricted to lamellae growing away from the nucleus, into the three-dimensional space. Each lamella grows linearly, creating the skeleton of semicrystalline entity. In order to fill the three-dimensional space, the lamellae must split and branch out to form a superstructure composed of lamellar stacks and intervening amorphous regions. The most common morphology encountered on solidification is the spherulite, but other superstructures, such as hedrites or dendrites, may be formed as well.[6]

A spherulite consists of lamellae, radiating from a central point (nucleus), in which chain axes are more or less perpendicular to the radius of the ordered aggregate. The three dimensional spherical shape is a result, after sufficient growth, of branching and splaying of lamellae. Non-crystallizable and less crystallizable molecules are mainly accumulated inside the spherulites, either between adjacent lamellae or between stacks of lamellae (fibrils) (Figure 1.1). In some cases, when presence of fast diffusing defective

species is coupled with slow linear growth, rejection occurs also at interspherulitic level. The primary crystallization occurs before spherulite impingement, when free growth of the superstructural units happens. After impingement, a secondary crystallization process takes place where crystallization mainly occurs in the interspherulitic regions, although some intraspherulitic crystallization is also possible (within the inter-lamellar regions).
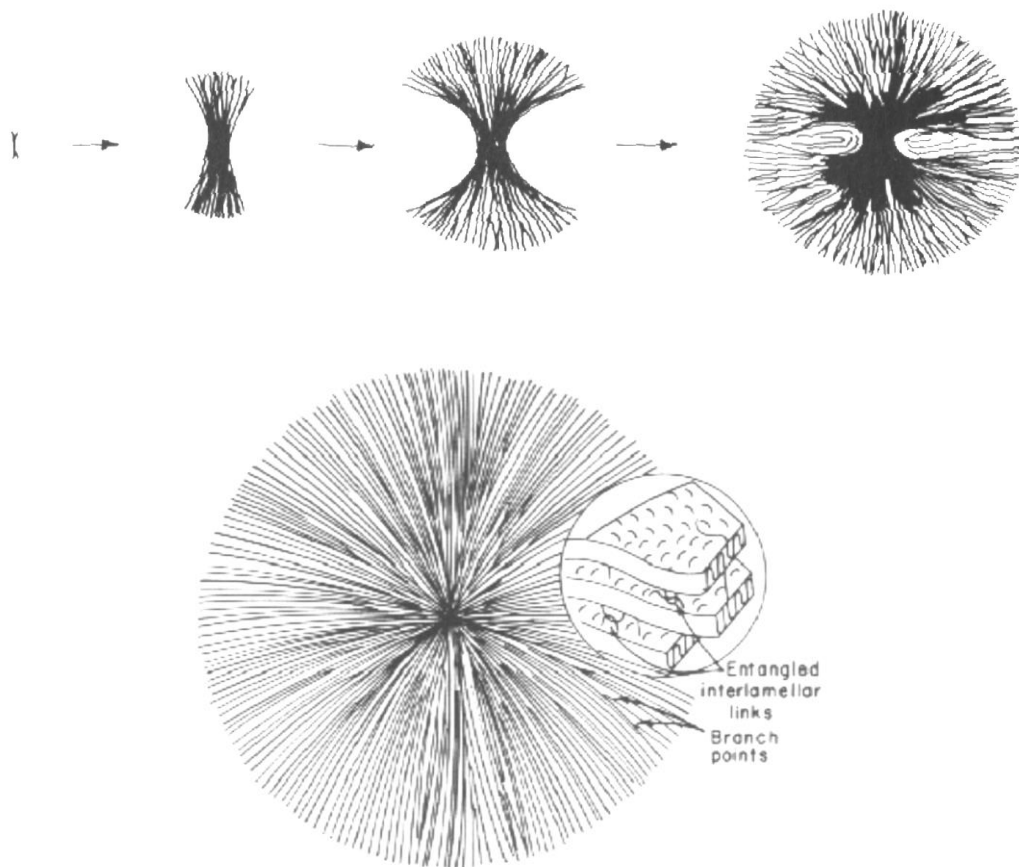

Figure 1.1: Development of spherulite from the nucleus and scheme of a spherulitic structure.

1.1.2 Crystallization kinetics

Generally, growth rates of polymers are evaluated by visually following the growth of spherulites developing at constant temperature (using PLOM). The radii of spherulites

are usually found to be a linear function of time; that is, the growth rate remains constant during isothermal crystallization.

This procedure gives accurate growth rate values, but has several limitations. Indeed, the presence of additives with high refractive indices hinder the observation of polymer samples under light transmission microscopes. At the same time, if spherulites with different growth rates are present in various concentrations during transformation (as for polymorphs and polymer blends), the measure of growth rates may not be easy, especially for less abundant spherulite types.

In order to bypass such limitations, the overall crystallization kinetics may be determined by DSC. However, in this case, both primary nucleation and crystal growth will make a contribution to the overall isothermal crystallization rate. Ideally, it would be better to determine both spherulitic growth rate and overall isothermal crystallization kinetics in separate experiments, if possible.

The Avrami Equation is one of the most common methods for obtaining information about the overall isothermal crystallization rate from isothermal DSC crystallization experiments.[7–9] The equation can be expressed as follow:

$$1 - Vc(t - t_0) = \exp[-k(t - t_0)^n]$$
$$\text{Eq. (1.1)}$$

Where t is the experimental time, t_0 is the induction time, V_c is the relative volumetric transformed fraction, k is the overall crystallization rate constant and n is the Avrami index, that assumes different values depending on the type of geometry of crystal growth and the type of nucleation. The term n, in Eq. (1) is the Avrami index, whose value is in the range between 1 and 4, depending on growth dimensions and nucleation mechanism.

Table 1.1: Values for the Avrami exponent, for various nucleation and growth process

n_n	n_g	N	nucleation and growth
1	3	4	Spherulitic growth with homogenous nuclei
0	3	3	Spherulitic growth from heterogeneous nuclei
1	2	3	Disk-like growth from homogenous nuclei
0	2	2	Disk-like growth from heterogeneous nuclei
1	1	2	Rod-like growth with homogenous nuclei
0	1	1	Rod-like growth with heterogeneous nuclei

The growth leads to a contribution of 1, 2, 3 (n_g), depending on whether one, two or three-dimensional growth occurs; nucleation brings a contribution of 0 or 1 (n_n) depending on whether it is instantaneous or sporadic. The sum of these two contributions gives the number of Avrami index n.

1.2 INTRODUCTION TO PLA BASED MATERIALS

1.2.1 The growing market of Bioplastics

With a global production close to 250 million tons per year, most of *commodities* plastics are non-degradable petroleum-based polymers.[11] However, their use has stimulated severe criticisms, resulting in a process of rethinking their role for sustainable product development.[12,13]

The main concerns related to non-degradable fossil-based polymers are economic, deriving from price variability and occasional role as a political weapon of fossil raw-materials, and environmental, deriving from solid waste disposal and contribution to climate change of current industrial polymer production.[14–18]

Bioplastics, whose production and consumption are not associated to the aforementioned drawbacks, are expected to undergo a *market boom* in next years.[12] According to the latest market data compiled by European Bioplastics, global production capacities of bioplastics is predicted to grow from around 4.16 million tonnes in 2016 to approximately 6.11 million tonnes by 2021.[19]

At the moment, mainly due to their high price level and low performance in comparison with conventional petrochemical counterparts, the number of competitive bioplastics is rather limited and only a few of those are both biodegradable and biobased.[20] Lignin, cashew nut shell liquid (CNSL) and thermoplastic starch blends (TPS) have been receiving increasing attention as a source for value-added products but are still relatively underused, mainly due to their lower performances if compared with traditional thermoplastics.[13,21]

On the other hand, Poly(Lactic acid) (PLA) and Poly(hydroxyalkanoates) (PHA) are well established biopolymers, commercially available, with a promising market increase.

In particular, PLA global production capacities is predicted to rapid growth to about 800 kt/year,[22,23] upon an increasing scientific interest attested by an impressive number of papers and reviews (see Figure 1.2).

Up-to-date, PLA production can be tailor-made into different polymer grades for processing into a wide spectrum of products and with minimal equipment modification if compared to traditional polymers. However, PLA is still relatively more expensive than most of the petroleum based polymers and often does not fit well the technical requirements of large use market.[24]

The increasing petroleum pricing and the implementation of environmental policies from the government, such as "green taxes" in countries like Germany or Japan,[12] are expected to create an economic push for the expansion of PLA in next years. At the same time, new technologies for processing PLA, such as using supercritical processes for foaming and electrospinning for producing nanofibers, are predicted to further expand the use of this polymer.[25–29]
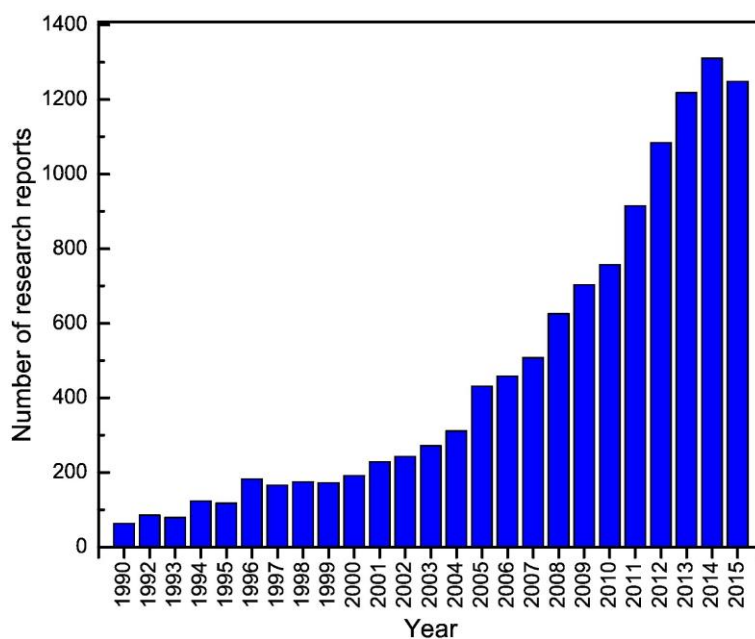
Figure 1.2: Number of research reports published since 1990 based on the *Web of Science* search using keywords "PLA", "PLLA", "PDLA", "polylactic acid", "polylactide", and "poly(lactic acid)"

1.2.2 Lactid Acid production

The basic monomer of PLA is lactic acid (LA), also named 2-hydroxy propionic acid. Lactic acid is chiral, consisting of two optical isomers. One is known as L-(+)-lactic acid and the other, its mirror image, is D-(−)-lactic acid (Figure 1.3).

(R)-2-hydroxypropanoic acid   (S)-2-hydroxypropanoic acid

D-(-)-lactic acid   L-(+)-lactic acid
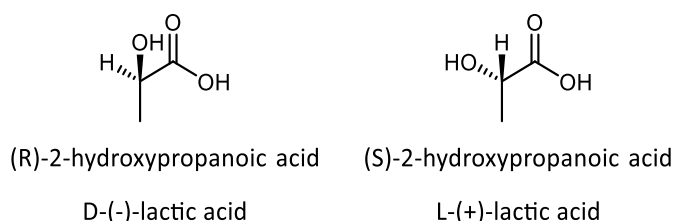
Figure 1.3: Optical isomers of Lactid Acid, L-(+)-lactic acid and D-(−)-lactic acid

The optical purity of Lactic Acid is a crucial parameter for PLA production. As the optical purity of LA is lowered, the tendency to crystallize of the corresponding PLA decreases until reaching a threshold composition of 92% beyond which the crystallization is not observed anymore.[30]

Considering that the selective isolation of enantiomers is barely performable on large scale,[31] lactid acid production for PLA synthesis need to be designed upon the aim to obtain only one of the two forms.

The two main methods to produce LA are the bacterial fermentation of carbohydrates and the chemical synthesis.[32]

Chemical synthesis is typically based on the addition of hydrogen cyanide to acetaldehyde and subsequent hydrolysis of forming lactonitrile by strong acids. The harsh reaction conditions, limited yields, high carbon footprint and, most importantly, the inability to achieve only one of the two isomeric forms, hinder the commercialization of this process, which currently covers only the 10% of the worldwide lactid acid production.[33]

The remaining 90% of the production is covered by bacterial fermentation, exploiting homolactic organisms such as *Lactobacilli Amylophilus*, which exclusively form a mixture of 99.5% of the L-isomer and 0.5% of the D-isomer.[34] Furthermore, in comparison with chemical synthesis, bacterial fermentation has other advantages, like

low cost of substrates, low production temperature, and low energy consumption.[35] The two major worldwide producers of PLA, NatureWorks LLC and Corbion, use bacterial fermentation to obtain lactic acid from starch derived from renewable resources. In the process, starch is transformed via enzymatic hydrolysis into dextrose and after into LA via homo fermentative conversion.[36]

1.2.3 PLA synthesis

There are two major routes to produce PLA from lactic acid: direct polycondensation of lactic acid[37] and ring-opening polymerization through lactide intermediate[38] (Figure 1.4). From these two routes, derives a common misleading in PLA nomenclature. Poly(Lactic acid) refers to PLA directly obtained from the lactic acid, whereas Poly(Lactide) refers to

Figure 1.4: Routes to produce PLA. Direct polycondensation of lactic acid and ring-opening polymerization through lactide intermediate.
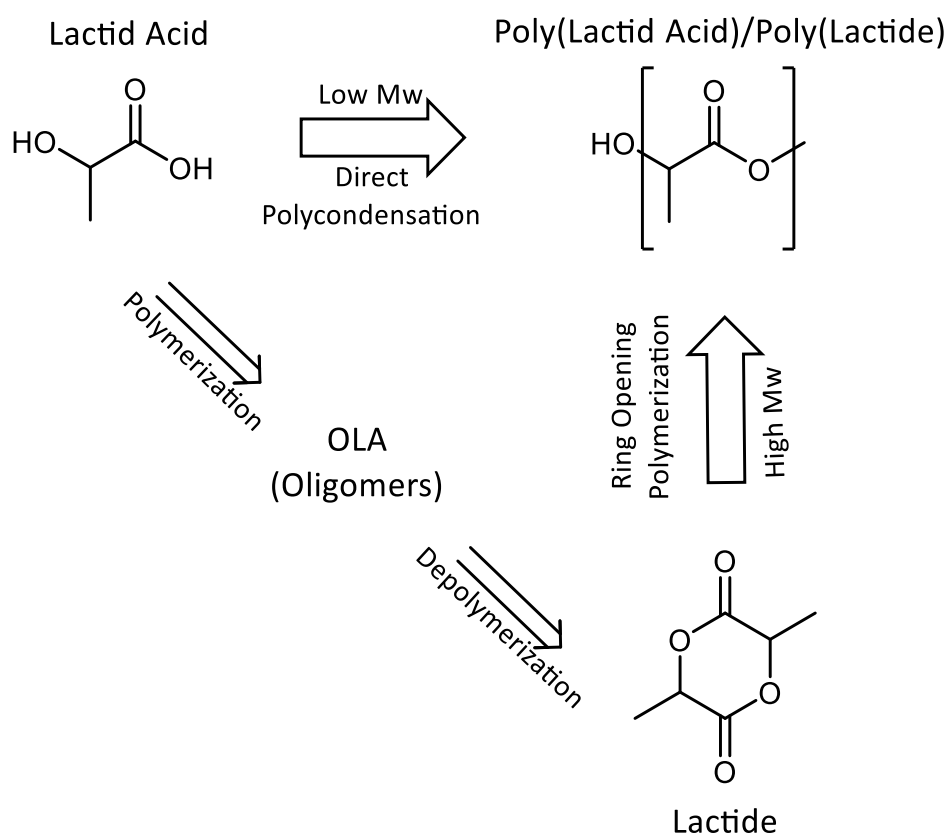
PLA obtained through lactide intermediate. The choice of one or other process depend on the balance between costs and added value on the obtained material.

Direct polycondensation of lactic acid is the least-expensive route, since it proceeds in one step. However, only low-molecular-weight PLAs can be obtained, mainly due to the viscous polymer melt, the presence of water, impurities, and the "back-biting" equilibrium reaction that forms the six-member Lactide ring during polymerization.

Such a low molecular weight PLAs are, for the most part, unusable for any applications unless external coupling agents are used. Examples of coupling agents are: bifunctional isocyanates, acid chlorides, anhydrides, epoxides, thirane, and oxazoline. However, the use of all of these is associated with lack of biodegrability, with a consequent applications restriction, of the resulting PLA.[39]

Polycondensation in an azeotropic solution yields to higher molecular weight PLAs than what happens in direct polycondensation, since equilibrium is shifted toward the formation of polymer chain by continuous water removal through azeotropic distillation. However, considerable catalyst impurities, due to the high levels needed for acceptable reaction rates, can remain in the end-use polymer. This residual catalyst may cause many problems during further processing, such as: unwanted degradation, uncontrolled or unreproducible hydrolysis rates, or, in the case of medical applications, catalyst toxicity and differing slow-release properties.[40]

It is therefore easy to understand how the major worldwide producer of PLA exploits the ring-opening polymerization (ROP) of Lactide intermediate to obtain high molecular weight PLA (Mw>100 KDa).[41] In the process, lactid acid is firstly polymerized to low molecular weight oligomers by removing water under mild conditions. Then oligomers are catalytically depolymerised to form a cyclic intermediate dimer, Lactide, which is then purified using distillation.

The stereoregularity, of the final polymer depends on the purity of the lactide.[42] Among the three potential forms in which lactide exists (see in Figure 1.5, D-lactide, L-lactide and meso-lactide) only D and L Lactide are optically active stereoisomers able to produce stereoregular PLA. The different amounts of one of the lactide isomers, depends on the lactic acid feedstock, as well as on the temperature and catalyst used during dimerization. Therefore, before polymerization the Lactide is split into a stream
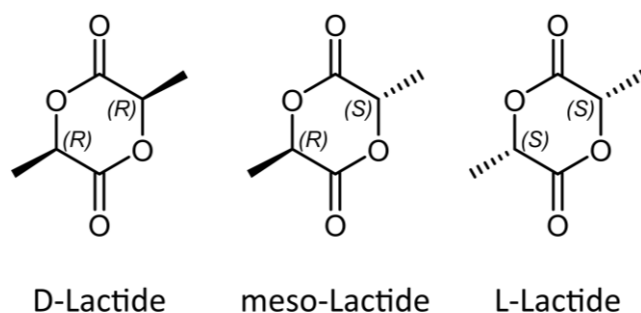
Figure 1.5: Stereoisomers of Lactide. D-lactide, meso-lactide and L-lactide.

with a high level of L-lactide and a stream with a mixture of L-lactide and isomerical impurities (D-lactide and meso-lactide).

The fraction with high L-Lactide levels can be used to produce semi-crystalline polymers whereas the other produces more amorphous materials. Applications of the meso-lactide by-product include its use as chemical intermediates in various surfactants, coatings, and copolymers.[43]

In the resulting PLA, the optical purity is determined by polarimetry in a suitable solvent, for example, chloroform, at 589 nm (reported optical rotations of enantiomerically highly pure PLLA and PDLA typically lie between |140| and |156|)[44,45] or by carbon nuclear magnetic spectroscopy (^{13}C NMR).[46,47]

By taking into account the different L/D stereoisomeric ratio a different nomenclature is typically used. PLLA refers to a Poly(lactide) containing only L-lactide. PDLA refers to a Poly(lactide) containing only D-lactide. When both the isomers are present (as it happens in many commercial grades) the term PLA should be used.

Molecular modelling suggests that two molecules of an alcohol (ROH) exchange with the octanoate ligands followed by the coordination of lactide to the metal centre. The insertion of the alcohol followed by ring-opening generates a linear monomer that subsequently starts propagation.[48] The reaction rate is increased with the increasing concentration of alcohol (typically added to the reaction mixture), since alcohol shifts the equilibrium towards the tin(II) alkoxides until finally the whole amount of Sn(Oct)$_2$ is converted into these propagating species. Also hindered amines, such as 2,6-di-tert-

butylpyridine or bis(dimethylamino)naphthalene, increase the rates of polymerization, being able to complex protons during coordination.[29]

Tin (II) octanoate (Sn(Oct)$_2$) is the most common catalyst for lactide polymerization, thanks to its solubility properties, high catalytic activity and ability to favour the formation of high molecular weight polymers with low levels of racemization (<1%).[49] Tin-based catalyst proceeds through a coordination-insertion mechanism (as shown in Figure 1.6) thermodynamically driven by the increase of entropy obtained upon ring opening of lactide.

Although Tin (II) octanoate has been approved by FDA for polymers used in coatings that contact food,[50] metal free catalysts have been proposed, mainly based on chiral organic molecules. Such organocatalysts are attracting an increasing attention, mainly due to their lower toxicity if compared to metallic counterparts. However, the high temperature required by these polymerizations and the difficulty of synthesizing perfect PLA chains at such high temperature without any racemization, transesterification reactions and macrocyclizations is currently hindering their scale up from laboratory use to large scale production.[51]
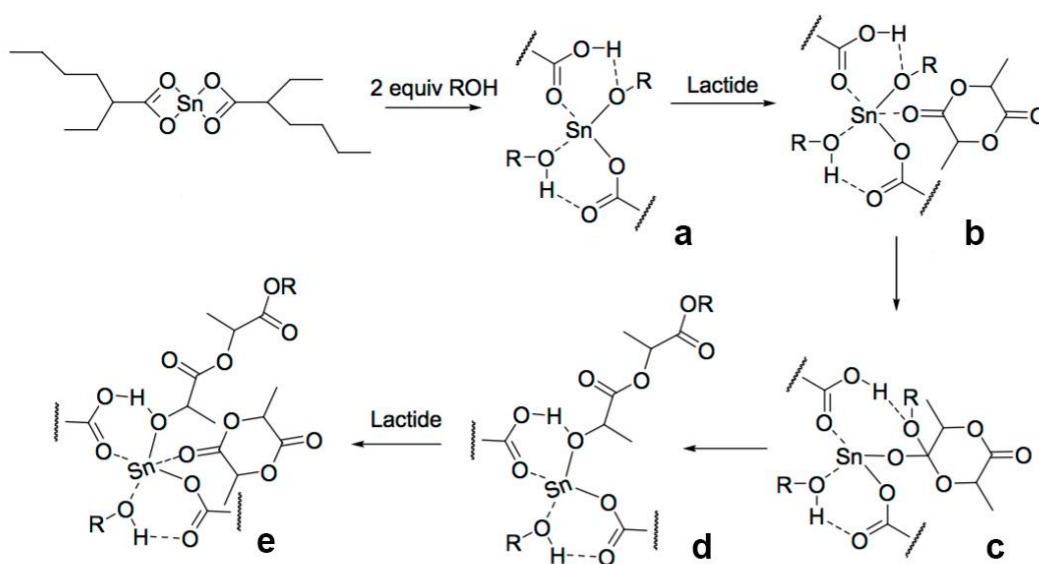
Figure 1.6: Coordination-insertion mechanism of Tin (II) octanoate catalysis. (a) Coordination of octanoate ligands (b) Coordination of lactide to the metal centre (c) Insertion of the alcohol (d) Ring-opening of Lactide (e) Chain propagation.

1.2.4 PLA processing

One of the key factors behind the increasing interest on PLA, in comparison with other bioplastic, consists in its suitability to be processed by the techniques employed with other commercial polymers, such as Polystyrene (PS) and Polyethylene Terephthalate (PET), with well-established manufacturing techniques.[52]

Typically, the main technique for conversion of high M_w PLA into end products (such as consumer goods, packaging, and other applications) is melt processing. It consists in heating the material above its melting temperature, forming the molten polymer into desired shapes, and finally cooling to stabilize its final dimensions. Extrusion is the most important technique for continuously melt processing of PLA. The plasticizing extruder can be part of the forming machine systems for injection molding, blow molding, film blowing and melt spinning.

Some of the examples of melt processed PLA are injection molded disposable cutlery, thermoformed containers and cups, injection stretch blown bottles, extruded cast and oriented films, and melt-spun fibers for nonwovens, textiles and carpets.[53]

The limiting factors for melt processing of PLA are similar to those of other commodities polymers: degradation at the upper limits of temperature and shear, and poor homogeneity at the lower limits.

Furthermore, like most of other aliphatic biopolyesters, PLA is a hygroscopic material,[54] very sensitive to high relative humidity (RH) and temperature. Hydrolytic degradation takes place when PLA is exposed to moisture: the ester groups of the main chain of the polymer are cleaved, resulting in a decrease of molecular weight and the release of soluble oligomers and monomers. The hydrolysis of PLA starts by the diffusion of water molecules into the amorphous regions, which in turn initiates the cleavage of the ester bonds. The products of the hydrolysis self-catalyze the reaction. Then, degradation continues in the boundary layer of the crystalline domains.[54,55]

In order to avoid hydrolysis, PLA should be dried to a water content less than 100 ppm (0.01%, w/w) before being processed while during industrial production it is mostly dried to values below 250 ppm water (0.025%, w/w). If PLA is processed at temperatures

higher than 240 ºC or with longer residence times, it should be dried below 50 ppm water (0.005% w/w).[56]

High temperature processing of PLA can also cause thermal degradation that it is mainly due by intramolecular transesterification reactions leading to cyclic oligomers of lactic acid and lactide. Simultaneously, there is a recombination of the cyclic oligomers with linear polyesters through insertion reactions, while molecules with longer chains lengths are favoured. Thermal degradation can be caused also by intermolecular transesterification. In this case two ester molecules exchange their radicals, leading to a variation on the distribution of molecular weights. It can be minimized by the addition of benzoyl peroxide, 1,4-dianthraquinone and other stabilizers.[56]

At the same time PLA should never be processed at temperatures above 240ºC, since it can be degraded by pyrolytic elimination, which leads to the formation of an acid moiety and a molecule with acrylic end groups, or by radical degradation, which can be assumed to start with either an alkyl-oxygen or an acyl-oxygen homolyses.

Another typical problem that can occurs during in any step preceding or following the polymerization, or during polymerization itself, is racemization of lactoyl moieties. It typically occurs at temperatures exceeding 200ºC, depending on the type of the catalyst used, leading to a reduction of the tendency to crystallize of the formed polymer.[57] Racemization must be taken especially under control if a crystalline material is desired, since, as reported in the previous paragraphs, only stereoregular PLAs are able to crystallize.

At the same time, during PLA synthesis and processing unreacted lactide monomer can evaporates if exposed at high temperature, leading to the formation of structural defects and therefore to a decline of mechanical properties of the resulting polymer. In order to solve the problem, Kimura *et al.*[58] proposed a two-step polymerization. During the first step, the polymerization of lactide is carried out in melt at 170ºC and the remaining monomer concentration is close to its equilibrium concentration, about 9%. Then, during the second step, the polymerization is continued at 120ºC, in order to crystallizes the formed polymer and separates crystalline phase from the molten monomer. In this way, the local Lactide concentration in the monomer phase is much higher than the equilibrium concentration and new polymer can be formed.

1.2.5 Comparison between PLA and other thermoplastic polymers

The physical properties of PLA, including melting temperature, crystallization behaviours, and mechanical properties strongly depend on its molecular weight and on its stereochemical composition, which determinate the price and application of commercially available PLA grades. Therefore, a punctual comparison between PLA and other materials should indicate a specific PLA grade.

As general indication it can be pointed out that, by comparison with commodity polymers such as PE, PP, PS and PET, the mechanical properties of semi-crystalline PLA are attractive, particularly its Young's modulus, making it an excellent substitute for commodity polymers. Mechanically, un-oriented PLA is quite brittle, but possesses good strength and stiffness. Oriented PLA provides better performance than oriented PS, but comparable to PET. Tensile and flexural moduli of PLA are higher than high density polyethylene (HDPE), polypropylene (PP) and PS, but the Izod impact strength and elongation at break values are smaller than those for these polymers.[59]

Notwithstanding the good mechanical properties of PLA, there are a number of areas which still need to be improved, especially in applications where PLA is intended to be used as a substitution for existing thermoplastics.

For instance, in food products where high barrier protection is important, replacement of PET by PLA packaging may not be feasible, since the barrier properties of PLA are not in par with PET.[60] At the same time, PLA biodegradability may in some cases result in unpredicted performance if the polymer is exposed to uncontrollable abusive temperature and humidity conditions.

Furthermore, PLA has a slow crystallization rate if compared with many other thermoplastics, resulting in longer processing time if semi-crystalline samples are desired. Even at high L-LA content, PLA crystallization is typically too slow to develop significant crystallinity unless the crystallization is induced by strain such as in processes used to produce biaxially oriented films or bottles. In processes such as injection moulding, where the orientation is limited, and the cooling rate is high, it is much more challenging to develop significant crystallinity and thus formulation or process changes are required.

Since the control of PLA crystallization rate constitutes one of the major drawbacks in expanding its commercial applications, a large body of literature has been focused on this topic. Next paragraph will summarize the parameters that control crystallization of PLLA, focusing also on the attention of the methods to improve it.

1.3 CRYSTALLIZATION BEHAVIOUR OF POLY(LACTIDE)

The potential large-scale expansion of PLA based materials depends on its ability to comply the technical specifications required by the market, keeping, at the same time, the production cost as low as possible. In this context, a key role is played by the control of the crystallization rate, since it influences both the duration of the molding process and the added value on the material as well.

Unless induced by strain (such as in processes used to produce biaxially oriented films or bottles), crystallization of PLA commercial grades is too slow to be developed at the cooling rate commonly employed in traditional melt processing (extrusion or injection molding).

However, the control of PLA crystallization kinetics is not a trivial issue, since it depends on the relative amount of the two stereoisomeric forms in which Lactide exists (i.e., L or D lactide). Only if one of the two forms is present in enough amount (at least more than 96–97%), PLA is able to develop significant crystallinity. The presence of low amounts of isomer co-units (L or D) in the PLA chains during structure formation leads to a reduction in the maximum achievable crystallinity and to the slowing of the crystallization process.[61] However, being L and D lactide separation difficult to achieve on a large scale,[31] most of commercial PLA grades contain a minor portion of D units.

At the same time, a wise control of PLA crystallization does not necessarily mean only an increase of the crystallization rate, but rather a tuning of the crystallization depending on the type of application. For example, enzymatic degradation rate can be reduced by more than 7 times for highly crystalline PLA as compared to amorphous samples.[62] It has also been shown that for crystallized PLA the oxygen and water vapor permeability coefficients were decreased by more than 4 and 3 times respectively, if compared to amorphous references.[63]

The following paragraph is aimed to elucidate the influence of stereosiomeric ratio and molecular weight on neat PLA isothermal crystallization, passing through the effects on both nucleation and growth of crystals, and on the relative position of melting and glass transition temperature as well.

1.3.1 PLA Crystal Structures and α - α' Polymorphism

PLA is polymorphic, therefore, depending on crystallization temperature, different crystalline structures may be obtained. Crystallization above 120ºC, from melt or solution, results in the most common and stable PLA polymorph, the α-form. This structure consists in two antiparallel 10_3 helical chain segments, packed in an orthorhombic unit cell, with 3.3 monomers per turn and a monomer repeat unit of 27.8 nm.[64]

At temperatures below 120ºC, α-form can be replaced by pseudohexagonal α'-form. In this case the molecule segments have the same 10_3 helical chain conformation adopted in α-form but with higher conformational disorder and lower packing density.[65]

More recent studies demonstrate that the α'-form crystal is preferentially formed only at crystallization temperatures below 100ºC, while at crystallization temperature between 100 and 120ºC α'-form coexist with α-form.[66]

The existence of the two different crystal modifications gives rise to a peculiar thermal behaviour. In PLA crystallized at temperatures corresponding to α'-form crystal formation, a small exotherm appears just before the single melting peak, due to the transformation of more disordered α'-form to the ordered α-form crystals. On the other hand, when PLA is crystallized at a temperature of coexistence of the two crystals forms, a double melting behaviour appears.[66] However, double melting can also be due to reorganization during the heating scan.

Analysis of the bulk enthalpies of melting of these crystals at their respective melting temperatures of 150 and 180ºC revealed values of 107 and 143 J g^{-1} for the enthalpy of melting of α' and α forms, respectively. It is worth noting that the bulk enthalpy of melting of the α´-crystals is 30–40% lower than that of the α-form, as expected from the presence of conformational defects and the lower packing density of the chain segments.[67]

The two α and α' forms have also different crystallization kinetics, which give rise to discontinuity in the PLA crystallization kinetics at around 110–120ºC.[66] This discontinuity is not connected to a change in nucleation or changes in crystal superstructural morphology, but it has been ascribed to an acceleration in spherulite growth rate of α and α' forms, which ultimately causes a bimodal distribution of the spherulite growth rate versus temperature.[67]

The two α and α' forms have also different mechanical properties, as result of the different packing of the PLA chains. As reported by Cocca *et al*,[68] α-form crystal provides a better barrier to water vapor and a higher Young's modulus, compared to α'-form, but a lower elongation at break.

Additional crystals form can be obtained in special processing condition. Hot-drawing melt-spun or solution-spun PLA fibers to a high-draw ratio leads to β-form. An orthorhombic unit cell with six chains in the frustrated helical conformation. This structure seems to be formed to accommodate the random up-down orientation of neighbour chains associated with the rapid crystallization under stretching.[69]

In the case that PLA crystals are the results of epitaxial crystallization on hexamethylbenzene substrate, γ-form is obtained. This crystal structure is characterized by two antiparallel helices in an orthorhombic unit cell. It is worth noting that the a (0.892 nm) and b (0.886 nm) axes of hexamethylbenzene crystals are close to the chain axis repeat distance of PLA γ-form. This matching induces the epitaxial growth of γ-form crystallization on hexamethylbenzene crystal surface.[70]

1.3.2 Melting and glass transition temperatures of PLA

Crystallization of macromolecules occurs at temperatures in between melting and glass transition temperatures. Below T_g no transport of chain segments across the liquid-crystal phase boundary is expected, whereas above T_m crystals are melted.[71]

The glass transition temperature T_g of a semicrystalline polymer depends on its molecular weight by the following Fox-Flory equation:[72]

$$T_g = T_g^\infty - \frac{K}{M_n}$$

Eq. (1.2)

where T_g^∞ is the glass transition temperature for infinite molecular weight, K is a constant that depends on the free volume and $\overline{M_n}$ is the number-average molecular weight. Saeidlou *et al* [73] adapted the equation to PLA sample relating the value of K with the amount of minor unit concentration X_D (defined as D-lactate in the case of a L-rich PLA and as L-lactate for a D-rich PLA):

$$K = 52.23 + 791X_D \qquad \text{Eq.(1.3)}$$

$$T_g^\infty = \frac{13.36 + 1371.68X_D}{0.22 + 24.3X_D + 0.42X_D^2} \qquad \text{Eq.(1.4)}$$

Combining equations (1.3) and (1.4) with (1.2), it gives rise to:

$$T_g = \frac{13.36 + 1371.68X_D}{0.22 + 24.3X_D + 0.42X_D^2} - \frac{52.23 + 791X_D}{\overline{M_n}} \qquad \text{Eq.(1.5)}$$

Figure 1.7 shows a graphic representation of Eq. (1.5) taking into account the influence of $\overline{M_n}$ on T_g, considering PLA with different amounts of D units. From the Figure is possible to see how T_g has an asymptotical convergence, increasing rapidly until
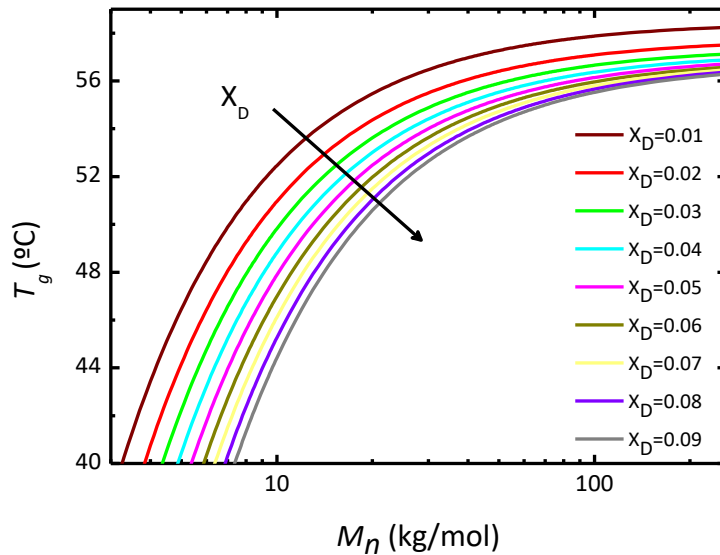
Figure 1.7: Tg vs. $\overline{M_n}$ for different D-Lactate concentration

reaching a molecular weight of 80–100 kg/mol, where approximately constant values are obtained.

Notwithstanding the described effect, it is noteworthy that most of commercial PLA grades have molecular weight in the 50–150 kg/mol range and an amount of D-Lactate between 0.01% and 0.05% wt. Therefore, in these cases the influence of $\overline{M_n}$ and X_D on T_g is negligible if compared with others parameter, such as PLA chain architecture or presence of chain extender and comonomers as well.

On the other hand, the melting temperature of PLA is highly influenced by molecular weight and D-Lactate amount. Figure 1.8 compares the melting point as a
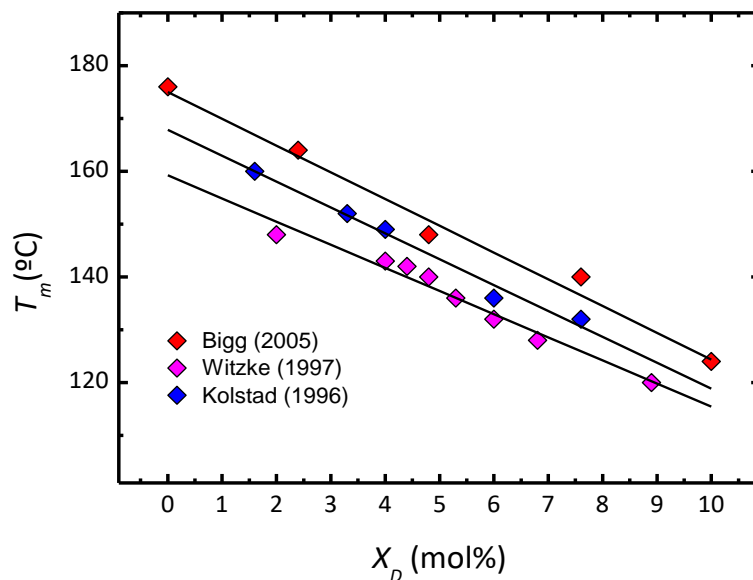
Figure 1.8: Melting temperature as a function of D-Lactide amount. Data adapted from ([61,74,75])

function of D-unit content in the polymer structure.[61,74,75] The maximum melting temperature is detected for pure PLA between 175 and 180ºC. The melting point decreases linearly with the D-lactide amount. The decrease can be linearly fitted, with a slope between −5.5 and −5.0. This means that 1% D-unit content results in approximately 5ºC reduction in melting temperature of PLA.

At the same time, also molecular weight has an influence on melting point. Figure reports the melting point variation as a function of the number averaged molecular

weight $\overline{M_n}$. The data have been compiled from previous works where PLLA with less than 1.25% minor units has been used.[30,76,77]

The melting temperature increases dramatically with molecular weight for low $\overline{M_n}$ but reaches an asymptotical value at $\overline{M_n}$ > 100 kg/mol. It is noteworthy that commercial PLA grades with a molecular weight in the 50–150 kg/mol range are in the high- molecular weight plateau region.
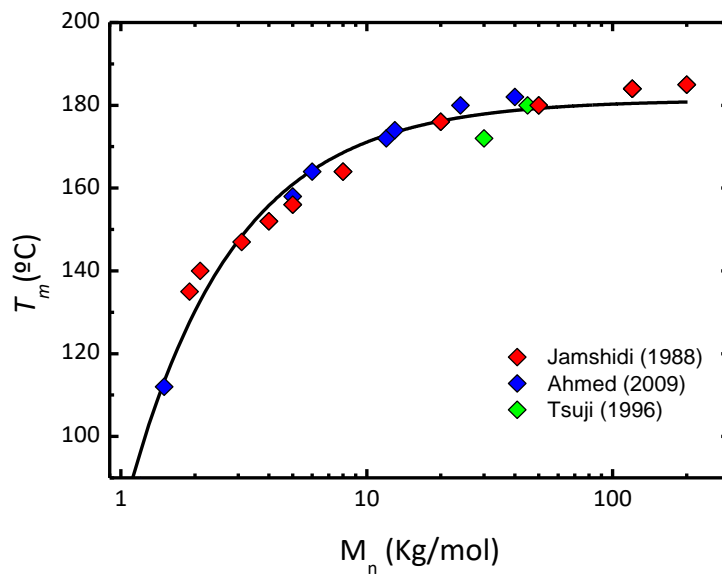
Figure 1.9: PLA Melting point as a function of molecular weight. Data adapted from ([30,76,77])

1.3.3 Nucleation and growth of crystals in PLA

Thermodynamically irreversible crystallization is the phase transformation of an unstable liquid structure or melt into stable or metastable crystals at a temperature lower than the equilibrium melting temperature T_m^0.[71] Crystallization is typically examined in terms of two independent phenomena: initial crystal nucleation and subsequent crystal growth.

Nucleation is assumed to occur from a small group of aligned segments, or nuclei, with an appropriate size to constitute a stable interface between the liquid and crystal phase. In the case of homogeneous crystal nucleation, formation of crystal nuclei occurs spontaneously in the bulk liquid phase by random fluctuations of the chains.[78] However, in most commercial polymers, nucleation is induced by heterogeneous nuclei, that is, any

(low mass) particle with the correct size and surface-like, for instance, catalytic residues and other impurities of unknown origin.[79]
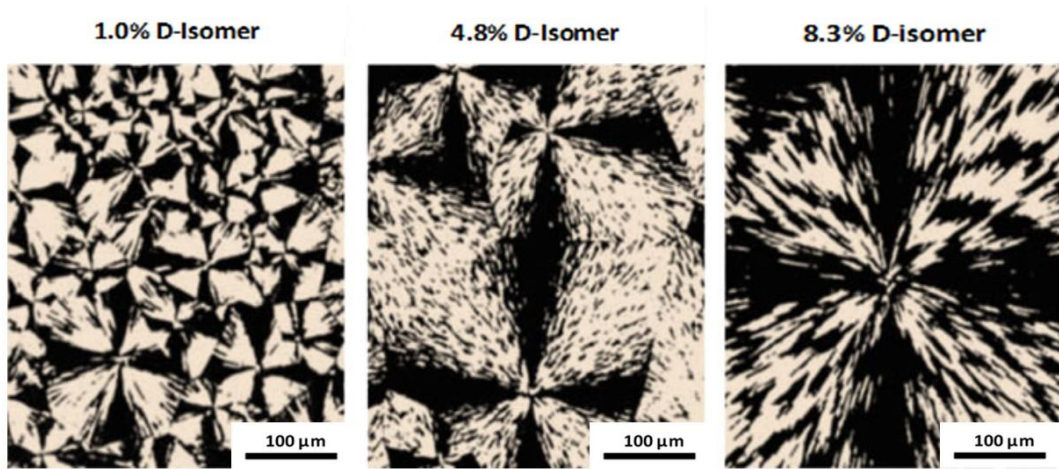
Figure 1.11: PLOM images of PLLA with D-isomer concentrations of 1.0% (left), 4.8% (center), and 8.3% (right), isothermally crystallized at 120ºC. The scale bar represents a distance of 100 µm. The PLOM images were adapted from (63)
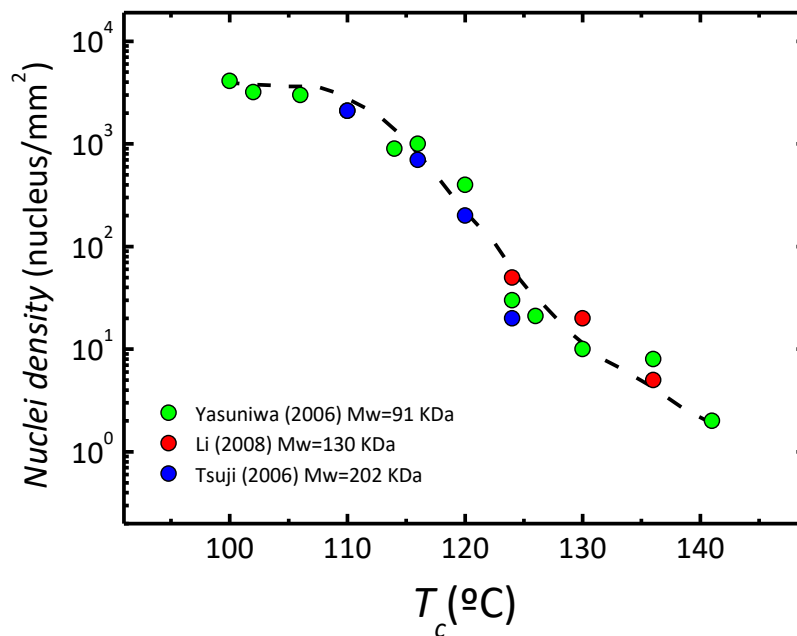
Figure 1.10: Spherulite density as a function of crystallization temperature. Data adapted from literature (60,61,62)

Subsequently to nucleation, crystals start to growth. The most common morphology encountered on solidification from the melt is the spherulite, but other superstructures, such as hedrites or dendrites, form as well. In any case, the growth is initially restricted to lamellae growing away from the nucleus, into the three-dimensional space. Each primary lamella grows linearly, creating a skeleton (of the spherical semicrystalline entity in the case of spherulite), while subsidiary lamellae are grown to fill the volume. This free growth is stopped by the, also developing, neighbouring spherulites. The interspherulitic space is then filled with lamellae whose growth is not so regular, while more subsidiary lamellae may fill the available space. These processes that occur after neighboring spherulites impinge on one another are known as secondary crystallization, while primary crystallization is usually restricted to the free growth process of spherulites before impingement.[80]

Nucleation is typically assessed by measuring the density of nuclei (number of spherulites per unit area) formed in isothermal condition, in a supercooled melt[81] Measurements of linear growth rates of polymer spherulites are generally conducted in isothermal conditions, by monitoring the growth of a spherulite radius as a function of time, until solidification is terminated by impingement on neighbouring spherulites.[82]

As a general rule, the number of stable nuclei increases with decreasing temperature, upon the increase of thermodynamic driving force for the phase transformation in supercooled condition ($T_m^0 - T_c$).[71]

Figure 1.10 shows the correlation between the number of crystallization sites (spherulite density) with crystallization temperature for PLA sample at different molecular weight. Data were adapted from literature[83–85] According to Figure 1.10 spherulite density is increasing by about three orders of magnitude on decreasing the temperature from 140 to 110ºC. By further lowering of the crystallization temperature, only a minor increase of the spherulite number is detected, suggesting a *plateau* value or the occurrence of a maximum around 90 ºC. From the Figure it is also possible to see how the influence of molar mass on the kinetics of crystal nucleation is negligible because nucleation requires mobility only at a short length scale and not large-scale cooperative mobility.

On the other hand, by increasing the content of isomer co-units (D-Lactate in the case of PLA) the nucleation density at identical temperatures decreases. Figure 1.21 shows PLOM micrographs of different PLA grades, with the similar molecular weight, containing D-isomer concentrations of 1.0, 4.8, and 8.3% after isothermal crystallization at 120 ºC.[86] For the three grades containing 1.0, 4.8, and 8.3% D-isomer co-units, spherulite densities of 180, 11, and 2 spherulites/mm^2 were measured, respectively.

The images demonstrate that, at identical crystallization temperatures, the spherulite density/nucleation rate increases with and decreasing D-isomer content. Since T_g is almost independent on the D-isomer content in the chain if it is less than 5–10%, the decrease in nucleation rate with increasing D-isomer co-unit content for crystallization at identical temperatures is a result of lower supercooling of the melt below T_m^0, which excludes differing segmental mobilities over a wide range of length.

At sufficient supercooling the formation of nuclei is followed by their growth to crystals. The temperature dependence of crystal growth rate shows a similar behaviour of nucleation. Decreasing the temperature from T_m^0 the growth rate increases as a result
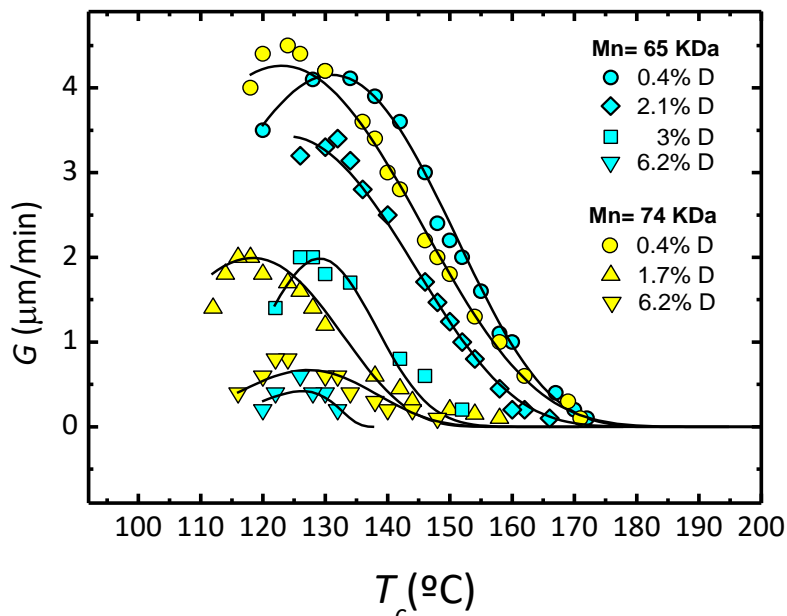
Figure 1.12: Effect of D unit concentration on the spherulite growth rate. Data adapted from (64,65)

of the increased thermodynamic driving force. At even higher supercoolings, it passes through a maximum and then decreases.

In PLA sample, the growth rate (G) is highly influenced by D- isomer content. Figure 1.2 shows spherulitic growth rate for PLA grades with different D- isomer content.[87,88] The optimum T_c (at which G is maximum) is in the 115–130ºC range. Increasing the optical impurity, the maximum spherulite growth rate decreases dramatically. It is around 4.5 µm/min for a PLLA with 0.4% D impurity and is decreased by a factor of 40 (less than 0.1 µm/min) with the addition of only 6.4% D-lactate.

The decrease in crystallization rate for PLA containing a low amount of D-isomer co-units is in accordance with rules commonly employed for describing crystallization of random copolymers.[89]
The segregation of noncrystallizable co-units at the crystal growth front leads to their enrichment in the amorphous phase during the course of crystallization, which then slows crystal growth and also contributes to the decrease in maximum achievable crystallinity, typically reported for optical copolymers of PLA.
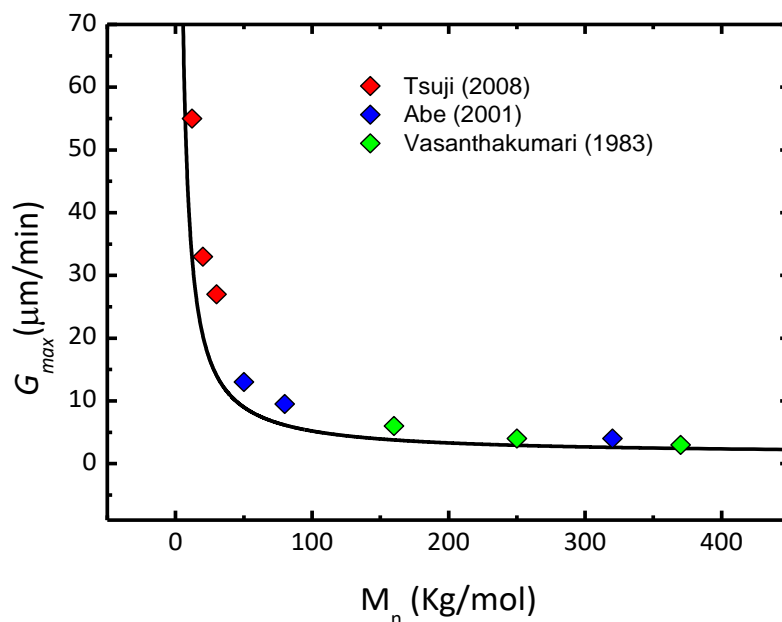
Figure 1.13: Maximum spherulite growth rate as a function of molecular weight. Data adapted from ([86,90,91])

The molecular weight's effect on the maximum growth rate is displayed in Figure 1.13, in which are shown data for PLLA having low D-unit concentration (0–1%).[86,90,91]Once more, the regression of the maximum growth rate can be fitted by the general form of Flory–Fox equation for data. The following parameters were used to draw the solid-line curve in Figure 1.:

$$G_{max} = G_{max}^{\infty} - \frac{A}{M_n}$$
Eq. (1.6)

Where G_{max}^{∞}= 1.4 μm/min and A = −3.8 ×10^5 (μm g)/(min mol).

Obviously, the growth rate decreases with increases in molecular weight as expected from more restricted chain mobility. The decrease is sharp at lower molecular weights, while in the range of molecular weights typical of commercially available polymer the effect is not dramatic as the optical purity.

1.3.4 Effect of processing on crystallization of PLA

Many studies have been recently published on the crystallization kinetics of PLA, however the effect of the processing conditions on this feature is often neglected.

Considering that PLA is extremely sensitive to processing conditions, a significant reduction in molecular weight takes place, due to thermal and mechanical degradation, could take place.[92–94] As result, crystallization kinetics may be severely altered.

Pantani et al.[95] stressed the significance of the melt processing on the crystallization kinetics: melt processing can induce a reduction in molecular weight due to mechanical and thermal degradation and this can enhance crystallization kinetics. The correspondence between molecular weight reduction has been already clarified in the previous paragraph.

In addition to the effect of the molecular weight reduction, also the effect of previous thermal history is extremely significant on the crystallization of PLA. It has been shown in literature[96–98] that PLA presents completely different crystallization behaviour when cooled from the melt (melt crystallization) or heated from the solid (cold crystallization). This aspect can be quite relevant for selecting suitable post-processing steps to increase the crystallinity inside the products.

De Santis *et al.*[96] examining the kinetics of PLA crystallization under both isothermal and non-isothermal conditions, found that, at equal molecular weights and D-isomer amounts, the crystallization kinetics of PLLA is always faster when starting from the glassy state than from the melt state. Zhang *et al.*[97] reported significant differences in infrared spectra for PLA samples obtained from melt and cold crystallization, indicative of differences in the crystal structures depending on whether the material was brought to the crystallization temperature by quenching from the melt (melt crystallization) or by heating from the glassy state (cold crystallization). Sanchez *et al.*[98] used a DSC with rapid scanning rate capabilities to examine the effect of cooling from the melt at various rates from 5 °C/min to 300 °C/min, on the cold and melt crystallization behavior of PLLA, in this study the kinetics of melt crystallization appeared to be slower than cold crystallization.

All the authors agree that the differences between cold and melt crystallization are due to the major tendency of PLLA to form active nuclei during cooling to the glassy state rather than cooling from the melt. Even if the crystal growth is nearly null when the glass transition temperature region is reached, the number of crystal nuclei should be considerable, since the nucleation rate increases with the distance to the equilibrium melting temperature. Nucleation progresses with an isothermal annealing at temperatures just above the glass transition temperature. If the temperature is then increased to the interval in which crystal growth is significant, a greater number of spherulites grow simultaneously and yield a crystalline morphology very different from that obtained by isothermal crystallization at high temperature after a temperature jump from the melt, or by slow cooling from the melt. As result, the increase in the number of nuclei is detectable by the acceleration of the crystallization kinetics.

1.4 HOW TO INCREASE CRYSTALLIZATION RATE OF POLY(LACTIDE)

1.4.1 Nucleating agents for PLA

Nucleating agents are particles with an appropriate morphology (i.e., size and surface-like) able to decrease the surface free energy barrier of polymer towards nucleation.[99] In this way induction period for nucleation is reduced, the number of primary nucleation

sites is increased and the melt crystallization upon cooling is shifted at higher temperature then in the bulk polymer.[100]

Generally, the efficiency of nucleating agents is characterized in two different ways: either in a non-isothermal experiment, by measuring the increase in crystallization temperature, or in an isothermal experiment by evaluating the reduction of the crystallization half-time, $t_{1/2}$. In both cases, comparison is made with a 'reference' which is the 'virgin polymer', the polymer with no nucleating agents but submitted to the same processing conditions used to incorporate the nucleating agents (e.g. melt blending, etc...).[101]

One of the requirements of a good nucleating agent is miscibility with the polymer melt and, ideally, upon cooling the miscible compound should phase separated (liquid-to-solid transition) prior to the crystallization of the polymer starts, providing heterogeneous nuclei for crystal growth.

Talc is one of the most common nucleating agent for PLA, so much that is commonly used as a reference to compare the nucleation ability of other additives. It was shown that talc nucleates the crystallization of polymers through an epitaxial mechanism, reducing the crystallization half-time by more than one order of magnitude to less than 1 min when 1% talc is added.

Kolstad et al.[61] found that the addition of talc at 6% increases the nucleation density of PLA by 500 times. As a result, at the optimum crystallization temperature, crystallization half-time is reduced 7 folds.

In another study, the addition of talc at 1% causes a 35-fold reduction in $t_{1/2}$, while in non-isothermal condition, the crystallization peak upon cooling (T_c) is shifted from 100 to 120 °C in presence of talc .[102]

Talc has been applied in industrial application as an effective physical nucleating agent of PLA. However, agglomeration usually occurs due to insolubility of talc in PLLA melt, leading to uncontrollable nucleating agent shape/size and nucleation efficiency.

Clay are commonly employed to improve thermal, mechanical and barrier properties of polymers. It is therefore interesting to examine their effect on the crystallization of PLA. Nam et al. reported that the crystallization rate of PLA increase around 50% in presence of 4% organically modified montmorillonite.[103]

In any case, the effect on crystallization depends on clay exfoliation. It was shown that the crystallinity and nucleation density of intercalated and flocculated samples were greater than those of nearly exfoliated clay. On the other hand, exfoliation of the silicate layers resulted in an increase by about 10°C of the crystallization temperature related to intercalated morphology.[104] Compared to talc, clay is a less efficient nucleating agent for PLA as the reduction in $t_{1/2}$ is moderate in isothermal mode and it is not effective for high cooling rates in non-isothermal crystallization.

Organic materials can also physically nucleate the crystallization of PLLA. This is typically achieved by adding a low molecular weight substance that will crystallize more rapidly and at a higher temperature than the polymer, providing organic nucleation sites, finely dispersed in molten PLLA.

Nakajima *et al.* took advantage of this point to prepare haze-free crystalline PLLA.[105] Different derivatives of 1,3,5-benzene tricarboxyamide (BTA) were solution blended with PLLA. Sheets with 1% of selected derivatives crystallized at 100°C for 5 min exhibited 44% crystallinity while the neat PLA reference showed a crystallinity of 17% in the same conditions. More interestingly, the derivative with a lower melting point (206°C) than processing temperature (235°C) and similar solubility parameter to PLLA preserved PLLA's transparency regardless of the high degree of crystallinity.

Kawamoto *et al.*[106] compared the nucleating ability of hydrazide compounds with talc using a PLLA with 99.4% optical purity. Samples containing 1% nucleating agent were completely melted and their nucleation behaviour was compared at a rate of 20 °C/min. Selected hydrazide compounds enabled complete PLA crystallization upon cooling with enthalpy of crystallization, ΔH_c, reaching 46 J/g while talc induce ΔH_c of 26 J/g in the same conditions.

p-tert-butylcalix[8]arene is another organic material that has revealed interesting nucleating effect for PLLA[107]. PLLA with 1% of this material revealed a sharp crystallization peak at 134.3°C upon cooling at a rate of 5 °C/min, 15°C higher than that of 1% talc and nearly 26°C higher than neat PLLA.

Biobased nucleants are a particular subset of interest for PLA, since they can maintain the virgin characteristic of PLLA. Harris and Lee reported a reduction in the crystallization half-time of a PLLA containing 1.4% D-PLA from 38 to 1.8 min when adding

2% of a vegetable-based ethylene bis-stearamide (EBS). Talc in the same conditions led to a lower half-time of 0.6 min. Upon cooling at 10°C/min, addition of EBS enabled some crystallization with a broad and weak exotherm centered around 97 °C but again talc was more effective revealing a sharp peak at 107 ºC .[108]

Starch is a biopolymer that has raised a lot of interest in recent years and its blends with other polymers are under extensive investigation. The effect of starch on PLLA crystallization was found to be relatively modest with a crystallization half-time reduction from 14 min to 1.8–3.2 for samples containing 1–40% starch. Again, 1% talc was found to be more efficient and decreased $t_{1/2}$ to about 0.4 min. It also shifted the optimum crystallization temperature up by around 15 °C compared to only 5 °C for starch.[102]

Cellulose nanocrystal (CNC) is another emerging material that has prompted high interest due to its high tensile properties and biobased origin. It was found that unmodified CNC, with a 15 nm diameter and 200–300 nm length, did not significantly affect PLA crystallinity. However, when its surface was partially silylated (SCNC), it had a modest positive effect on crystallinity. Used at 1%, the modified CNC increased PLLA X_c from 14% to 30% upon slow cooling at 10 °C/min. In isothermal experiments, the crystallization half-time was decreased 2-fold to around 4 min when 1% SCNC was incorporated.[109]

Orotic acid is another bio-based chemical that was recently investigated.[110] As little as 0.3% orotic acid had a significant effect on crystallinity development in non-isothermal and isothermal mode. At a cooling rate of 10 °C/min, a sharp crystallization peak at 124°C with a high crystallization enthalpy (34 J/g) was found. Besides, the $t_{1/2}$ in the 120–140°C temperature range exhibited 10–20 fold decreases down to as low as 0.64 min. Authors believed that the good match between b-spacing of PLA and a-spacing of orotic acid crystals may explain this strong nucleating effect.

Recently, carbon nanotubes have attracted attention because of their high aspect ratio and outstanding mechanical, thermal and electrical properties. Xu et al.[111] reported modest nucleating effects for multi-wall carbon nanotubes (MWCNT) solvent-mixed at very low loading (up to 0.08 wt.%) with PLLA. Upon cooling, the crystallization peak temperature, T_c, was shifted to higher temperatures but did not enable significant crystallinity development at cooling rates of 10°C/min and higher. PLLA-grafted carbon

nanotubes (PLLA-*g*-CNT) were also investigated in a PLLA with 2% D-LA units. At the moderate cooling rate of 5°C/min, crystallinity of 12–14% were attained with 5–10% PLLA-*g*-CNT .[112] Moreover, in isothermal experiments on similar material, the minimum $t_{1/2}$ was decreased from 4.2 min to 1.9 min with 5% PLLA-*g*-CNT.[113]

Mixture of PDLA and PLLA can crystallize in the form of a stereocomplex that has a melting point about 50°C higher than the PLLA or PDLA homocrystals. Because the stereocomplex will form at higher temperature upon cooling than the homocrystals, small concentrations of PLA stereocomplex may be suitable for nucleating PLLA homo-crystallization.

Brochu et al.[114] reported that in presence of the PLA stereocomplex, the spherulite density was higher and the homopolymer crystalline fraction was larger than that in the pure polymer, implying the nucleating effect of stereocomplex crystals. They concluded that PLLA crystals can form epitaxially on stereocomplex lamellae that were previously formed at higher temperatures. It was shown by measuring the crystallization temperature, T_c, for various compositions that addition of small PDLA contents (forming the stereocomplex in situ in the PLLA major phase) had a higher nucleation efficiency than talc. For example, the nucleating efficiency of 6% talc was 32% whereas that of 6 wt.% PDLA was 56%. In addition, the nucleation density with as little as 0.25 wt.% PDLA was more than 170 times that of pure PLLA. The use of 1% talc only doubled the nucleation density in the same conditions. Unfortunately, the nucleation density increase was not accompanied by an overall increase in the extent of crystallization of the PLLA. This behavior was related to the tethering effect of stereocomplex crystallites, reducing PLLA chain mobility.

Inorganic–organic hybrids are a new class of materials that include polyhedral oligomeric silsesquioxane (POSS) and layered metal phosphonates. Unlike organoclays, the organic and inorganic components of these hybrid materials are connected through covalent rather than ionic bonds. In the case of POSS, the material core is constituted of a silicon and oxygen "nanocage" grafted with organic arms that can be modified depending on requirements. In a series of studies, Qiu et al. investigated the effect of POSS with isobutyl, methyl and vinyl arms on the PLA properties. In isothermal experiments, 1% POSS with vinyl arms decreased $t_{1/2}$ from 8 to 1.2 min.[115] Upon cooling

at 5 °C/min, the crystallization temperature was increased by 10–15°C compared to neat PLA and the samples were fully crystallized within the cooling cycle. At a cooling rate of 15°C/min however, only a small crystallization exotherm appeared around 92°C for 2% POSS content. This was shifted slightly to 95 and 97°C when POSS concentration was increased to 5 and 8%, respectively.[116]

Layered metal phosphonates have also exhibited a nucleating effect on PLA. Pan et al. compared the nucleation effect of zinc phenylphosphonate (PPZn) to that of talc and PDLA at 1% nucleating agent content.[117] For crystallization upon cooling at 10 °C/min, the highest crystallization temperature, around 128°C, and the sharpest crystallization peaks were achieved for PPZn. At the same cooling rate, a very high crystallinity of 47–56% was achieved when using PPZn in the range of 0.02–15% in PLLA. The cold crystallization temperature of quenched samples was also shown to be reduced by up to 30°C when adding PPZn. In isothermal tests, PPZn was also more effective than talc and PDLA in reducing the crystallization half-time, $t_{1/2}$, of PLLA. Values as low as 0.63 min were found compared to over 6 min for talc and PDLA respectively. It was suggested that the match of the lattice parameters of PPZn and PLA α crystal explains such a great enhancement of the crystallization behavior. In another study, Wang et al. investigated the effect of metal type on PLA/layered metal phosphonate composites by comparing zinc, calcium and barium phosphonates (PPZn, PPCa and PPBa).[118] It was found that the nucleating ability decreased in the following order PPZn > PPCa > PPBa due to the different dispersion and interfacial interaction of nucleating agents with PLA matrix.

1.4.2 Plasticizers for PLA

PLLA is a brittle material, therefore the addition of plasticizers is a common solution to improve its ductility and drawability and thus broadening the range of potential applications.[119]

However, plasticization may have contrasting effects on the crystallization behaviour. On one hand, T_g depression upon plasticizer addition shifts the crystallization temperature window to lower temperatures and thus facilitates the movement of chains from the amorphous phase into the existing crystal surface. On the other hand,

plasticization may also cause melting point depression, with a consequent overall crystallization rate decrease due to the reduced degree of undercooling.[71]

Therefore, in order to measure the efficiency of a plasticizer as crystallization assistant, is convincible to consider both T_g and T_m shifting, relating the effect with other

Table 1.2: Average T_g and T_m depression of PLA as a function of plasticizer type and concentration.

Plasticizer	Abbr.	M_w (g/mol)	ΔT_g/[Plasticizer] (°C/%)	ΔT_m/[Plasticizer] (°C/%)
Polyethylene glicol	PEG	200	2.34	0.6
		400	2.33	0.46
		578	2.51	
		1000	1.91	0.16
		1500	1.55	0.1
		8000	1.87	0
Polypropylene glycol	PPG	530	2.25	
		1123	2.17	
Poly(ethylene glycol-co-propyl-ene glycol)	PEPG	12	1.78	0.13
Triphenyl phosphate	TPP	326	1.34	0.37
Dioctyl phthalate	DOP	390	1.75	0.46
Di-2-etylhexyladipate	DOA	370	1.48	0.4
Polymeric adipate	G206/2	1530	1.76	0.23
	G206/3	2000	1.96	0.4
	G206/5	2700	1.48	
	G206/7	2560-3400	1.75	0.26
Poly(1,3-butylene adipate)	PBA	1500–2000	1.03	
Triethyl citrate	TEC	276	1.45	0.81
Tributyl citrate	TBC	360	1.85	0.43
TBC- oligoester	TBC-3	980–4450	1.27	0.3
	TBC-7	2200–63600	0.6	0.2
Acetyl triethyl citrate	ATEC	318	1.28	0.39
Acetyl tributyl citrate	ATBC	402	2	0.46
Glycerol			0.33	0.78
Oligomeric lactic acid	OLA	–	2.05	0.9
Poly(1,3-butanediol)	PBOH	2100	1.2	0.12
Acetyl glycerol monolaurate	AGM	358	1.54	0.36
Dibutylsebacate	DBS	314	1.53	0.45
Diethyl bishydroxymethylmalo-nate	DBM	220	1.67	0.57
DBM-oligoester	DBM-A-8	4200	0.87	0.2

parameters that are directly associated, as spherulite growth rate. Table 1.1 reports the effect on Tg and Tm of the most common used plasticizers for PLLA.

Polyethylene glycol (PEG) is the most investigated plasticizer for PLLA. The addition of PEG reduces the T_g by approximately 2°C per % plasticizer, depending on its molecular weight, while it does not affect melting point significantly.[120,121]

However, if used in high concentration (i.e., 30 wt%) in blends with PLLA, it could undergo phase separation at ambient temperature, due to epitaxial crystallization of PEG on the edge of the PLA spherulites.[121]

Polypropylene glycol (PPG) is another oligomeric plasticizer, with effects similar to PEG on PLLA T_g. However, PPG is less miscible than PEG with PLLA, and phase separation occurs at only 12.5% of PPG.[121] At the same, basing on the spherulite size measurements with a small angle light scattering (SALS) technique, it was shown that the growth rate and nucleation density were greater with PEG than with PPG.

Among the low molecular weight plasticizers for PLA, citrate esters are the most investigated ones. The intrinsic advantage of this plasticizers is their bio-based, bio-compatible and biodegradable nature, which limit PLA application. These materials are as effective as PEG for reducing the glass transition temperature but induce a higher melting point reduction. Among common citrates, tributyl citrate and acetyl triethyl citrate were found to be more efficient than triethyl citrate and acetyl tributyl citrate.[122]

Triphenyl phosphate and dioctyl phthalate are commonly used to enhance PLA crystallization.[123] In particular, in the case of triphenyl phosphate, the plasticizer used at 10, 20 and 30% reduces significantly the T_g of PLLA by 14, 26 and 39°C, respectively, and increases the spherulite growth rate of two or three time fold if used in high concentration (i.e., 20 and 30 wt%).[124]

Adipates are another family of PLA plasticizers, however, this group of plasticizers lead to a T_g decreases with plasticizer concentration only up to concentration of 10% probably due to limited miscibility with PLA. Accordingly, only modest crystallization enhancements were found.[125,126]

Even though it cannot be used as a conventional plasticizer because of its high volatility, carbon dioxide has shown outstanding plasticization and crystallization enhancement effects on PLA, due his highly solubility. On a weight-basis, CO_2 is much

more effective in reducing T_g than the plasticizers above mentioned, however the use of this technology is restricted to only few applications, as in the extrusion foaming process where CO_2 can be used as a physical blowing agent for PLA.[127,128]

1.5 INTRODUCTION TO POLYMER BLENDS

Polymer blending covers more than 20% of the total annual consumption of engineering polymers, with a world market increase of 50 million tons per year.[129] This growing interest is driven by the possibility of design the end-use properties of the resulting blend, according to the requirements of specific applications and at a lower cost than the complex and expensive synthesis of new polymers.

The thermal, mechanical and rheological properties of a polymer blend depend on the miscibility between the components. Depending on the number of favourable specific interactions between the counterparts, a miscible or an immiscible blend may be obtained.[130]

In a miscible blend, a single-phase system, which combines the properties of the components, is formed. Therefore, the tendency to crystallize of one component can either increase or decrease, according to the changes of the equilibrium melting and glass transition temperature expected upon blending.

In immiscible blends, the components are separated in microdomains with contacts at their interfaces. Although the crystallization of each component takes place in separated domains and thus the crystal growth rates are not expected to be influenced by blending, significant deviations of the overall crystallization kinetics may still take place, as nucleation of one phase on the other can occur.

In this chapter the thermodynamics behind miscibility in polymer blends and its effect on crystallization behaviour will be analysed, taking into account both miscible and immiscible blends. Furthermore, the most common methods to compatibilize an immiscible blend will be reviewed.

1.5.1 Thermodynamics of polymer blends

According to the general principles of thermodynamics, the Gibbs free energy (ΔG) energy of mixing (ΔG$_m$) of a binary polymer system is defined as:

$$\Delta G_m = \Delta H_m - T\Delta S_m$$

Eq. (1.7)

Where ΔH$_m$ and ΔS$_m$ are, respectively, the variations of enthalpy and entropy produced upon blending. At constant temperature and pressure, the necessary condition for miscibility is ΔG$_m$ < 0, which is fulfilled when |ΔH$_m$| > |TΔS$_m$| if ΔH$_m$ < 0 and ΔS$_m$ < 0; ΔH$_m$ < 0 and ΔS$_m$ > 0; or |TΔS$_m$| > |ΔH$_m$| if ΔH$_m$ > 0 and ΔS$_m$ > 0.

For polymer blends comprising polymers A and B, the Gibbs free energy of mixing may be calculated by Flory-Huggins equation:[131]

$$\Delta G_m = (RTV/V_r)\left[\left((\varphi_A/r_A)/(ln\varphi_A)\right) + \left((\varphi_B/r_B)/(ln\varphi_B)\right) + \chi_{(AB)}\varphi_A\varphi_B\right]$$

Eq. (1.8)

where T is the absolute temperature, V is the total volume of the mixture (V$_A$ + V$_B$), V$_r$ is the reference volume (the volume of a segment in the lattice cell, equal to the volume of the repeating unit of the polymer chain, assuming it is identical for both polymers), φ_i is the volume fraction of each polymer, r_i is the number of segments (i.e., the polymerization degree) for each polymer, $\chi_{(AB)}$ is the thermodynamic interaction parameter that is associated with the intermolecular and intramolecular interaction energy (ε) between segments and can calculated by:

$$\chi_{(AB)} = (\varepsilon_A + \varepsilon_B - 2\varepsilon_{AB})/(k_BT) = z\Delta\varepsilon r_i/k_BTV_i$$

Eq. (1.9)

Where k_B is the Boltzman constant, z is the coordination number of the lattice, and Δε is the energy of formation of AB contacts, which is calculated from the algebraic sum of the interaction energies:

$$\Delta\varepsilon = \varepsilon_{AB} - \frac{(\varepsilon_{AA} + \varepsilon_{BB})}{2}$$

Eq. (1.10)

$$\varepsilon_{AB} = \sqrt{\varepsilon_{AA}\,\varepsilon_{BB}}$$

Eq. (1.11)

Because the contribution to the combinatorial entropy of mixing in Eq. (1.8) becomes negligible when the molecular weight of the components increases, Eq. (1.8) can be simplified into:

$$\Delta G_m \approx \Delta H_m = B\varphi_A\varphi_B \qquad \text{Eq. (1.12)}$$

$$\text{B} = \chi_{AB}\, RTV/V_r \qquad \text{Eq. (1.13)}$$

Where B is the interaction energy density and the parameter contains both an enthalpic and a noncombinatorial entropic contribution. Values of χ_{AB} can be determined using a semiempirical method based on Hildebrand solubility parameters:[132]

$$\chi_{AB} = \frac{(V_r)}{RT}(\delta_A - \delta_B)^2 \qquad \text{Eq. (1.14)}$$

$$\delta = \left(\frac{\rho\Sigma F_i}{M}\right) \qquad \text{Eq. (1.15)}$$

Where δ is the solubility parameter, F_i is the molar attraction constants of all the chemical groups in the repeating unit of the polymer, and M is the molecular weight of the polymer.

1.5.2 Compatibilization strategies of polymers blends

Compatibilization is a process of modification of immiscible polymer blends that allows a reduction of the interfacial tension between the polymer phases and the formation and stabilization of a stable morphology. In this way, the adhesion between the polymer phases of the blend in the solid state could be enhanced and thus the stress transfer under strain is facilitated. As result, a useless mixture of polymer is converted into a blend with desired set of performance characteristics.[130,133,134]

In order to be effective in reducing the interfacial tension between the phases, compatibilizers must be miscible with both phases. In this contest, the most used technique of compatibilization are the addition of premade molecules miscible with both phases (i.e., block, random or grafted copolymers or nanoparticles) or the in-situ generation of compatibilizers directly during the blending process (i.e., reactive blending). [130,133,134]

Block copolymers, with one constituent block miscible with one component and a second block miscible with the other component are among the most widely used premade compatibilizers. Random copolymers can also effective as they usually have some sequential comonomer units, although some can be completely random. This sequential comonomer units can be regarded as short blocks which are miscible with corresponding blend components.[135]

Since the key requirement is miscibility, it is not necessary for the compatibilizing copolymer to have identical chain segments as those of the main polymers. It suffices that the copolymer has segments having specific interactions with the main polymeric components (i.e., hydrogen bonding, dipole-dipole, dipole-ionic, Lewis acid-base), since emulsification between the phases occurs due to the entanglement of each block with the corresponding blend component. [130,133,134] Figure 1.14 presents a schematic picture of the supposed conformation of some compatibilizer molecules at the interface of a
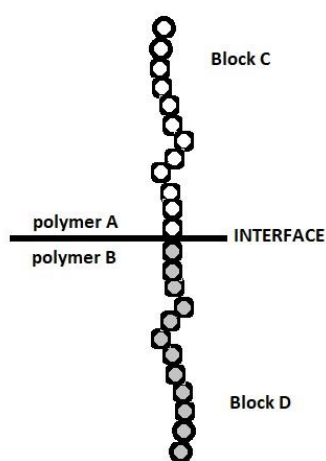

Figure 1.14*:* Schematic picture of the supposed conformation of a block copolymer at the interface of a polymer blend. An immiscible blend of polymers A and B is compatibilized by a diblock copolymer poly (C-b-D)

polymer blend. An immiscible blend of polymers A and B is compatibilized by a diblock copolymer poly (C-b-D), provided that block C is miscible with polymer A (therefore block C can also be polymer A) and that block D is miscible with polymer B (so block D can also be polymer B). One of the disadvantages of this method is the tendency of the added copolymers to form micelles. These increase the blend viscosity, reduce the efficiency of the compatibilizer and may lessen the mechanical performance.[135]

For this reason, the copolymer concentration should not exceed the 10% wt with respect to the minor phase. At the same time, the molecular weight must be minimised just to about the entanglement molecular weight for each interacting block.

An alternative way of improving compatibility of an immiscible blend is the addition of nanoparticles. These compatibilizers usually locate at the interface of the components, acting as a physical barrier that can prevent coalescence stabilizing the morphology of the blend.[136]

Unlike polymer compatibilizers, nanoparticles are unspecific to the nature of immiscible blend components, and easily incorporated via blending. In addition, exploiting nanoparticles it is possible to generate high-performance materials that combine the advantages of polymer blends and the merits of polymer nanocomposites. Therefore, this method represents a universal way of preparing compatible polymer blend nanocomposites with improved physical properties.

The second, and today the dominant method, of compatibilization is based on specific chemical reaction between two polymeric components during mechanical blending, as addition of reactive polymers. There are many advantages on addition of reactive polymers over addition of premade copolymers.[137]

Firstly, by reactive blending copolymers are generated only at the location where they are needed, at the interface of the immiscible blends, which should increase the efficiency in compatibilization if compared with the addition of premade copolymers. It is worth noting that formation of a copolymer at the interface immediately suggests that, by contrast with the compatibilization by addition, here the highest M_W copolymer is the most desirable, since the copolymer is formed within the interphase where it should stay.

Secondly, reactive polymers usually show lower melt viscosity than premade copolymers, which makes the reactive polymer diffuse towards the interface of

immiscible blends much faster than the premade copolymer. This is extremely important with respect to the short processing time during reactive blending which is usually of the order of a minute or even less. In some cases, the reactive polymers may not be initially miscible with either component of the blend, but they can also be used as compatibilizers if they are reactive towards the functional groups of both blend components.

Addition of reactive polymers has some other advantages. Compared to block copolymers, reactive polymers are easier to produce with simple techniques, and some reactive polymers have even been commercialized.

However, this technique also has some disadvantages. In fact, reactive polymers with functional groups may be harmful, which would cause some potential injuries to operators. At the same time, the inevitable residue of some poisonous functional groups if remaining would cause some safety problems of the resulting blends.

1.5.3 Crystallization behaviour of polymers blends

In order to analyse the crystallization behaviour of components within polymer blends, it is suitable to distinguish between miscible and immiscible blends.

In a miscible blend, a single-phase system, which combines the properties of both the components, is formed. On the other hand, in immiscible blends, the components are separated in microdomains with contacts at their interfaces. Although the crystallization of each component takes place in separated domains, significant deviations of the overall crystallization kinetics may still take place.[1]

In any case, the crystallization will take place in a defined temperature range, between the values of the glass transition temperature, T_g, and equilibrium melting temperature, T_m^0. Below T_g chain mobility is inhibited, while at temperatures near T_m^0, the crystal nucleation does not occur. Therefore, taking in account the variation of these temperatures upon blending, it is possible to predict the crystallization behaviour.

For a binary amorphous/crystalline miscible blend (A: amorphous polymer, B: crystalline polymer) the glass transition is intermediate between those of plain

components and thus the crystallization range, as the crystallization behaviour, will depend on the glass transition of the amorphous component (T_{gA}).

If T_{gA} is lower than T_{gB}, the "crystallization window" of the blend is larger than that of the neat crystallizable component and thus its ability to crystallize is enhanced.

On the other hand, if T_{gA} is higher than T_{gB}, the glass transition of the blend is increased and the crystallization window is reduced. In the extreme case that $T_{gA} \geq T_{mB}^0$, the crystallization can be completely inhibited.

When demixing phenomena are induced by the crystallization of one component, the amorphous component will be rejected from the crystallization front and will diffuse away into the melt, while the crystallizing molecules are migrating from the melt to the growth front.

The mode of segregation of the amorphous component is controlled by the ratio between the diffusion coefficient (D) of the amorphous component into the melt and the growth rate (G) of the crystals, δ = D/G defined as "segregation distance".[2]

When δ »1, the amorphous component moves along with the crystal growth front forming separated domains in interspherulitic zones, or within intraspherulitic regions when δ ≈ 1. Otherwise, if δ « 1, the noncrystallizing molecules can remain trapped into the growing spherulites between the crystalline lamellae (δ < 10 nm) or between the fibrils. In the latter case, which is usually found for melt miscible systems, the amorphous interlamellar regions are constituted by a homogeneous mixture of the two components.[129]

In crystalline/crystalline miscible blends the components may crystallize simultaneously or separately, depending on the difference in their crystallization rates and crystallization temperatures range.

In the blend systems in which the difference in T_m between the two semicrystalline components is large, the high-T_m component crystallizes faster than the low-T_m component; due to the increased degree of supercooling. Therefore, the high-T_m component usually crystallizes first at a higher temperature between the T_m's of the two components, whereas the low-T_m component acts as a temporary amorphous diluent. In this case, the melt-miscible semicrystalline/semicrystalline polymer blends are

actually melt-miscible semicrystalline/amorphous blends, as the low-T_m component is still in the melt during the crystallization process of the high-T_m component. Therefore, the morphological patterns of the blend system are governed by the distance over which the low-T_m component is expelled, which may show the following three basic types of separation, i.e., interlamellar, interfibrillar or interspherulitic segregations.

In the blend systems in which the difference in T_m between the two semicrystalline components is small, they can crystallize separately or simultaneously depending on the difference in their crystallization rates. If it is large, the two components crystallize separately. In this case component with a faster crystallization rate crystallizes first with its spherulites filling the whole volume, whereas the other component with a slower crystallization rate crystallizes later as tiny crystals at the same orientation as the crystallites of the host spherulites formed by the rapidly growing component.

On the other hand, if the difference in their crystallization rates is small the two components can crystallize simultaneously at the same T_c. In this case, two different types of spherulites from each component may appear and grow simultaneously; usually forming a unique crystalline morphology of interpenetrating spherulites. If the polymer chains of the components are isomorphous, that is, they give rise to a single crystal phase. In the latter case, besides the melt miscibility, a close similarity of chain conformation, crystal lattice symmetry and dimensions are necessary.

For immiscible polymer blends the properties are strictly controlled by their phase morphology, depending on the processing conditions, molecular characteristics, and interfacial properties.

The simplest case is that of complete phase separation between the two components and when, to a large extent, the two phases act independently in terms of crystallization.

In such systems, in the absence of interactions at the interphase, the crystallization characteristics are essentially those of the pure components: same melting temperature (T_m; independent of the composition), same lamellar thickness (for a given degree of supercooling) and same growth rate. However, significant deviations of the overall crystallization kinetics may still take place.

Changes in the primary nucleation density and nucleating activity of the matrix may be found due to the occurrence of migration of heterogeneities between the phases in the melt (impurities, catalysts, crystal residues from incomplete melting).

The migration of heterogeneities occurs when the interfacial free energy of the impurities within their melt phase is higher than the interfacial energy of those impurities within the other melt phase of the blend present into the melt. Thus, during the cooling different types of heterogeneities become active for nucleation and this, consequently, will affect the spherulite size and the nucleation density.

At the same time, when in a blend the minor phase is finely dispersed in droplets within an immiscible matrix, its crystallization may take place in several steps (fractionated crystallization) corresponding to different undercoolings, larger than the usual undercooling for the crystallization of the neat polymer.

This so-called *fractionated crystallization* happens if the number of dispersed droplets is greater than the number of active heterogeneities originally present in the bulk crystallizing phase. The smaller the droplets, the lower is the probability to find active heterogeneities in each droplet and thus the crystallization is shifted at lower temperature.[138]

As result, DSC cooling curves of such systems exhibit multiple crystallization exotherms: the lowest temperature exotherm with the largest undercooling is usually associated with homogeneous or surface nucleation, the highest temperature exotherm with the highest undercooling is usually associated with heterogeneous nucleation.

Coincident crystallization of the components has been reported for blends in which the matrix phase has a crystallization temperature lower than that of the dispersed component, and this latter does not crystallize at its usual undercooling, owing to its very fine dispersion into the blend, which causes a lack of heterogeneities that is able to initiate the crystallization of the droplets at their characteristic T_c .

In such case, on cooling from the melt, the molten dispersed phase can crystallize coincidently with the matrix, either at the same T_c of the matrix or at a somewhat higher T_c (intermediate between those of the neat components), acting as nucleating substrate for the matrix polymer.

In immiscible blend where there is a significant degree of intermixing between the components, the crystallization behaviour is more complicated. In this case two T_g are still observed, but they vary as a function of composition, indicating that the phase separation does not give pure A and B phases but a phase A in which a certain amount of B is dispersed and vice versa.

This intermixing necessarily influences the nucleation step and has broad consequences on the subsequent crystallization events because nucleation not only proceeds uniquely on the heterogeneities present in the crystallizable phase but can also occur on aggregates formed by the dispersed polymer.

The final morphology depends on the respective T_m, (and, therefore, on the crystallization temperatures).

If the difference in T_m is small, both polymers can crystallize over the same temperature range.

On the other hand, If the difference between the two T_m's is large, the high-T_m polymer will crystallize first in contact with the melt of the second polymer. When the second polymer subsequently crystallizes, at lower temperatures, it does in contact with a rigid phase because of the semicrystalline nature, at that point, of the second phase.

2 PLASTICIZATION AND ANTI-PLASTICIZATION EFFECTS CAUSED BY POLY(LACTIDE-*RAN*-CAPROLACTONE) ADDITION TO DOUBLE CRYSTALLINE POLY(L-LACTIDE)/POLY(E-CAPROLACTONE) BLENDS

2.1 INTRODUCTION

Polylactide (PLA) is a biodegradable, biocompatible and bio-based aliphatic polyester with good mechanical properties for specific applications.[139] However it suffers from several drawbacks that limit its use.

One bottleneck for extending PLA usage is the control of its crystallization rate. Typically, commercial PLA materials have low crystallization rate resulting in long processing time and low production efficiency.[73,140] Commercial PLAs contain predominantly L stereo-isomer units, typically more than 94%, and a minor proportion of D units, which act as defects to hinder the crystallization of L segments within the chains. In fact, many PLA commercial grades are rendered completely amorphous when fast cooling rates are employed, such as those applied during injection or extrusion moulding. The useful properties of the material are then limited by the upper boundary established by the glass transition temperature.

Both crystallinity and crystallization rate of PLAs depend on the relative amount of the two isomeric forms (i.e., L or D lactide). When either one of the two isomeric forms is present in high contents, PLA is able to crystallize. However high purity PLA is barely obtainable.[31] Therefore, in order to improve the crystallization rate of commercial PLAs, other methods are required.[73,140]

A practical way to improve the crystallization rate of PLA, and at the same time tailor its properties, can be achieved by blending it with other polymers. The properties of a polymer blend depend on the miscibility of the components and on the specific properties and relative amount of each component. Depending on the number of favourable specific interactions that could be established between the components of the blend, it is possible to obtain a miscible or immiscible system.[130,141]

In immiscible polymer blends, the absence of these favourable interactions causes the separation of the components in microdomains, in contact at their interface. The crystallizable components of immiscible blends can experience a retardation effect on their crystallization rate depending on the nature of blend components and composition.[142] However, a nucleation effect can also be promoted by blending that can enhance the overall crystallization process of a given blend component. Two possibilities may occur to induce nucleation. One component can nucleate the other, or during mixing in the melt or solution, a migration of active heterogeneities can also occur from one phase to the other.[130]

Recently, Sakai *et al.* proposed that in immiscible poly(L-lactide)(PLLA)/poly(ε-caprolactone)(PCL) blends a locally depressed glass transition temperature (Tg) of PLA at the interface with PCL domains can accelerate the nucleation of PLA during its cold crystallization.[143] However, in immiscible polymer blends, the absence of specific interactions should not allow effects on chain mobility, and the authors do not provide evidences for miscibility. On the other hand, when a miscible polymer is added to a crystallizable second component, it can either increase or decrease its tendency to crystallize, since a change is expected upon blending on its glass transition and equilibrium melting point.[144] PLA is a brittle polymer with an high Tg (circa 60°C), therefore miscible blends of PLA with more flexible polymers are among the most studied. For instance, it is reported that poly(ethylene glycol), PEG, can accelerate the spherulite growth rate of PLA by increasing molecular diffusion.[145]

PLA/PCL blends have been extensively investigated for practical applications, since PCL is a biodegradable and biocompatible flexible polyester that could be effective in improving the properties of PLA without limiting its traditional applications.[135,146,147]

Although in PLA/PCL blends the mismatch between the solubility parameters is not large (10.1 (cal/cm^3)$^{1/2}$ for PLA vs. 9.2 (cal/cm^3)$^{1/2}$ for PCL)[141] there are no specific interactions between the polymer chains that can induce miscibility. In fact, several publications[148–155] have considered PLA/PCL blends as immiscible based on their morphology[148–150] or on the lack of Tg change.[151–155]

Several methods have been employed to enhance the compatibility between PLA and PCL.[135] These include the addition of block copolymers as polymeric compatibilizers[151,156,157] and reactive compatibilization/mixing.[118,158,159] The addition of P(LA-ran-CL) random copolymers have also been reported.[160–162] This strategy is attractive in view of its lower cost, as compared to the other compatibilization methods reported in the literature.[135]

In this work, a detailed investigation into the effect of P(LA-*ran*-CL) addition on the morphology, crystallization and mechanical properties of an immiscible 80/20 PLA/PCL blend is presented. Particular emphasis is made on spherulitic growth kinetics and overall isothermal crystallization kinetics of the PLA phase, aspects which have not been previously reported for PLA/PCL/P(LA-*ran*-CL) blends. Furthermore, the crystallization of the PCL phase, another novel aspect in these type of blends, has also been explored. The results obtained have allowed us to postulate a selective dissolution of the copolymer chains in both blend phases. Thanks to the plasticizing effect of the P(LA-*ran*-CL) copolymer on the PLA phase and a nucleating effect of the PCL phase, a synergistic effect is obtained on PLA crystallization rate. Finally, the effects of P(LA-ran-CL) on the compatibility between the phases as well as on the crystallization of the matrix have been correlated with the mechanical properties of the samples.

2.2 EXPERIMENTAL

2.2.1 Materials and methods

Poly(L-lactide) PLA (Ingeo index: 4032D, 1.2-1.6 % of D-LA isomer, Mw= 200 KDa) was purchased from NatureWorks™ and was dried overnight under vacuum at 60°C before processing to avoid degradation reactions induced by moisture. Poly(ε-caprolactone) PCL (CAPA 6800 Mw= 80 KDa) was purchased from Solvay™ and was used as received.

Two different random copolymers of DL-lactide and ε-Caprolactone were used (Table 2.1) The first one, denoted P(LA-*ran*-CL)LMw was synthesized, according to a procedure previously reported[30], by ring opening polymerization in bulk at 140 ºC with stannous (II) octanoate as catalyst (for synthesis details, see next paragraph-Synthesis of P(LA-

ran-CL)LMw random copolymer). The second one, called P(LA-*ran*-CL)HMw, was purchased from Sigma Aldrich™ (Substance ID: 24869375) and was used as received.

2.2.2 Synthesis of P(LA-ran-CL)LMw random copolymer

P(LA-*ran*-CL)LMw was synthesized, according to the literature,[163] by ring opening polymerization (ROP) of ε-caprolactone and D,L-lactide in the presence of tin(II)octanoate. The reaction was carried out overnight in an oil bath at 140°C and stopped by quenching it in an ice bath. The crude product was dissolved in a minimum volume of CHCl$_3$, followed by precipitation into a 10-fold excess of methanol. The copolymer is recovered by filtration and after drying under vacuum.

The analysis of the ^{1}H-NMR spectrum (Figure 2.1) was performed using the work of Peponi *et al*. as reference. The multiplet from 5.05 to 5.25 ppm is assigned to methine proton of polymerized lactide (f). The multiplet from 4.08 to 4.18 ppm is due to the CL proton (a) that linked to LA molecule, while the triplet at 4.05 ppm indicates that the CL proton (a) is linked to another CL molecule. The multiplet between 2.34 to 2.44 ppm is due to the CL proton (e) that linked to a LA molecule, while the triplet at 2.30 indicates that the CL proton € is linked to another CL molecule. For the rest of the spectrum, multiplets at 1.66 ppm and 1.39 ppm are related to the CL protons (b), (d), and (c), respectively, and the multiplet at 1.56 ppm, to the LA methyl protons (g). So, the ratio of the LA signals to the CL signals results in a molar composition of the copolymers

Table 2.1: Compositions (CL/LA), average molecular weights (Mw), polydispersity (D), and glass transition temperatures (Tg) of the two P(LA-*ran*-CL) random copolymers

Sample	CL/LA (mol/mol)[a]	Mw (kDa)[b]	D[c]	Tg (ºC)[d]
P(LA-*ran*-CL)LMw	48/52	31.8	1.72	-16
P(LA-*ran*-CL)HMw	65/35	116.1	1.92	-38

[a]Determined by ^{1}H NMR [b]Determined by SEC (THF) with PS standards [c]Determined as Mw/Mn
[d]Determined by DSC, heating curves at 20°C/min
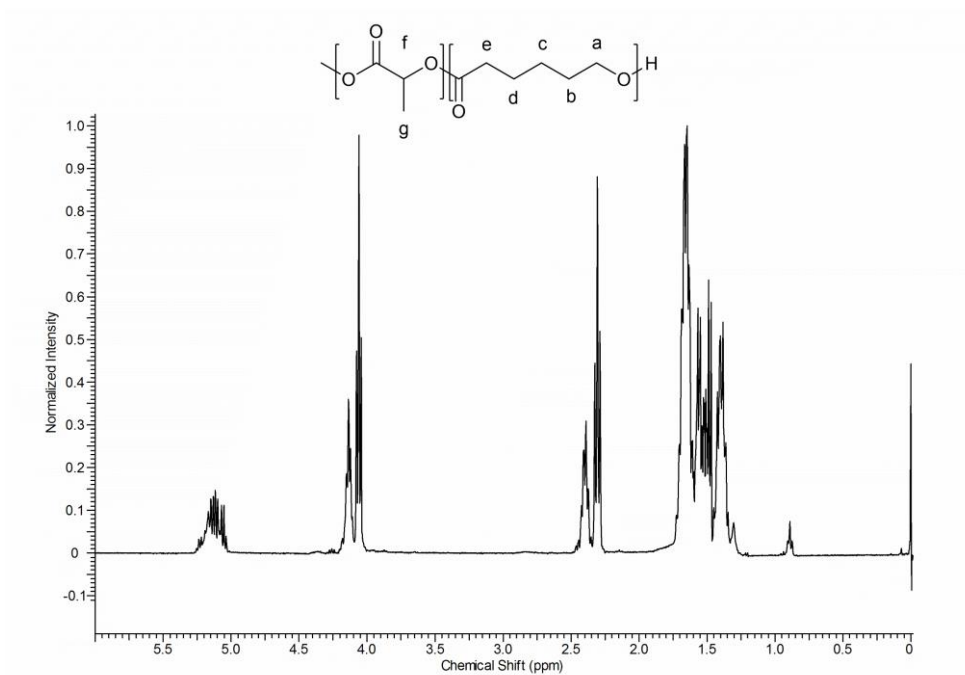
Figure 2.1: ^{1}H-NMR spectrum and chemical structure of the P(LA-*ran*-CL) random copolymer

2.2.3 Blend Preparation

A constant PLA/PCL weight ratio of 80/20 was employed. The blends containing random copolymers were prepared by adding 10% of copolymer with respect to the minor phase, so that the final blend approximate ratio was: 80/20/2 PLA/PCL/P(LA-*ran*-CL), see Table 2.2.

Melt blending was performed in a Collin twin-screw extruder (Teachline, L/D ratio 18, screw diameter: 25 mm) at a screw speed of 200 rpm, at a temperature of 180°C,

Table 2.2: Composition of the prepared blends

Sample	PLA (w/w %)	PCL (w/w %)	P(LA-*ran*-CL)LMw (w/w %)	P(LA-*ran*-CL)HMw (w/w %)
PLA	100	-	-	-
PCL	-	100	-	-
PLA/PCL	80	20	-	-
PLA/PCL/P(LA-*ran*-CL)LMw	78.4	19.6	2	-
PLA/PCL/P(LA-*ran*-CL)HMw	78.4	19.6	-	2

with a residence time of approximately 1 minute. The extruded filaments were quenched in a water bath and pelletized. The pellets were dried overnight in a dehumidifier at 80 ° and were compression molded in a Collin P-200-E compression molding machine at 200°C (3 minutes without pressure followed by 3 minutes at 100 bar). Tensile testing specimens (ASTM D 638 type IV, average thickness 1.84 mm) of both homopolymers and blends were obtained. The compositions of all the samples used in this work are reported in Table 2.2.

2.2.4 Morphological Analysis

The tensile test specimens were cryogenically fractured after 3 hours of immersion in liquid nitrogen. Fracture surfaces were observed by Scanning Electron Microscopy (SEM), after gold coating under vacuum, using a Hitachi S-2700 electron microscope.

Micrographs of the most representative inner regions of the specimens were achieved. PCL droplets diameters were measured on at least 100 particles. Number (dn) and volume (dv) average diameters and particle size polydispersity (D) were calculated by the following equations:[138]

$$d_n = \frac{\sum n_i d_i}{\sum n_i} \qquad\qquad \text{Eq. (2.1)}$$

$$d_v = \frac{\sum n_i d_i^4}{\sum n_i \, d_i^3} \qquad\qquad \text{Eq. (2.2)}$$

$$D = \frac{d_v}{d_n} \qquad\qquad \text{Eq. (2.3)}$$

Where ni is the number of droplets "i" of diameter di.

Polarized Light Optical Microscopy (PLOM) was employed to observe the morphology and growth of PLA spherulites. Micrographs were recorded by a LEICA DC 420 camera on film samples with a thickness of approximately 10 µm, cut from tensile test specimens. By using a METTLER FP35Hz hot stage, the films were firstly held at 200°C for 3 minutes, to erase previous thermal histories, then they were cooled to the crystallization temperature and the isothermal spherulitic growth was followed by PLOM.

2.2.5 Thermal Analysis

The thermal behavior of the blends was studied by Differential Scanning Calorimetry (DSC) using a Perkin Elmer DSC Pyris 1 calorimeter calibrated with indium and tin. All measurements were performed under nitrogen atmosphere and using sample masses of approximately 5 mg.

For non-isothermal DSC measurements, the samples were first heated to 200°C for 3 minutes in order to erase crystalline thermal history. Then they were cooled at 10°C/min until -20°C while the corresponding cooling scans were recorded. Finally, the samples were reheated to 200°C at the same rate to register the subsequent heating scans.

The isothermal DSC experiments were performed following closely the procedure recommended by Lorenzo et al.[164] The samples were first heated to 200°C and kept at that temperature for 3 min to erase thermal history. Then they were cooled at a controlled rate of 60°C/min to the chosen isothermal crystallization temperatures (Tc). The isothermal crystallization temperature range was determined by preliminary tests to ensure that no crystallization occurred during the cooling step.[164]

In order to avoid degradation reactions, each sample was dried overnight at 60°C under vacuum before DSC measurements, and it was not used for more than two isothermal experiments.

2.2.6 Mechanical Properties

Tensile tests were performed with an Instron 4301 universal testing machine. Young's modulus, yield strength and the elongation at break were measured at a crosshead speed of 10 mm/min by means of an extensometer. A minimum of five tensile specimens were tested for each reported value.

The degree of crystallinity $X_C(\%)$ of the PLA phase was calculated from the first DSC heating scans of samples taken from tensile testing specimens (these DSC scans are not reported here), and using the following formula:

$$X_C(\%) = \frac{(\Delta H_m - \Delta H_{cc})}{(\Delta H_m^\circ w_f)} \qquad \text{Eq. (2.4)}$$

Where ΔH_m and ΔH_{cc} are the measured enthalpies of melting and cold crystalliza-tion, ΔH_m° is the melting enthalpy of 100% crystalline PLLA (93.6 J/g according to the lit-erature[64]) and w_f is the weight fraction of PLA in the sample.

2.3 RESULTS AND DISCUSSIONS

2.3.1 SEM Micrographs

Figure 2.2 shows SEM micrographs for cryogenically fractured surfaces of PLA/PCL, PLA/PCL/P(LA-*ran*-CL)LMw and PLA/PCL/P(LA-*ran*-CL)HMw blends. In all cases, a sea-is-land morphology, which is typical of immiscible blends, is observed. PLA conforms the matrix while PCL is finely dispersed in droplet. The immiscibility of PLA/PCL blends has been well documented. [148–155] Wu et al. reported that the blend morphology changed from fibrillar for the 60/40 composition to spherical for the 80/20 composition.[151]

For neat PLA/PCL blend (Figure 2.2-a), a large number of cavities are observed, as a result of interfacial debonding between PCL and PLA during cryogenic fracture. After copolymer addition, debonding is reduced, and the number of cavities for P(LA-ran-CL)LMw (Figure 2.2-b) and especially for P(LA-ran-CL)HMw (Figure 2.2-c) is lowered. The differences can be correlated with the degree of crystallinity of the PLA matrix in the blends (Table 2.5). When the PLA matrix crystallizes in the blend, it experiences a larger volume contraction upon solidification, as compared to when it remains amorphous, dur-ing cryogenic fracture.

Table 2.3: Number-average (d_n) and volume average (d_v) particle diameters and particle size distributions (D) of the PCL phase in the blends prepared by compression moulding

Sample	d_n (µm)	d_v (µm)	D
PLA/PCL	0.48	3.38	7
PLA/PCL/P(LA-*ran*-CL)LMw	1.84	16.9	9.2
PLA/PCL/P(LA-*ran*-CL)HMw	0.45	3.09	6.9
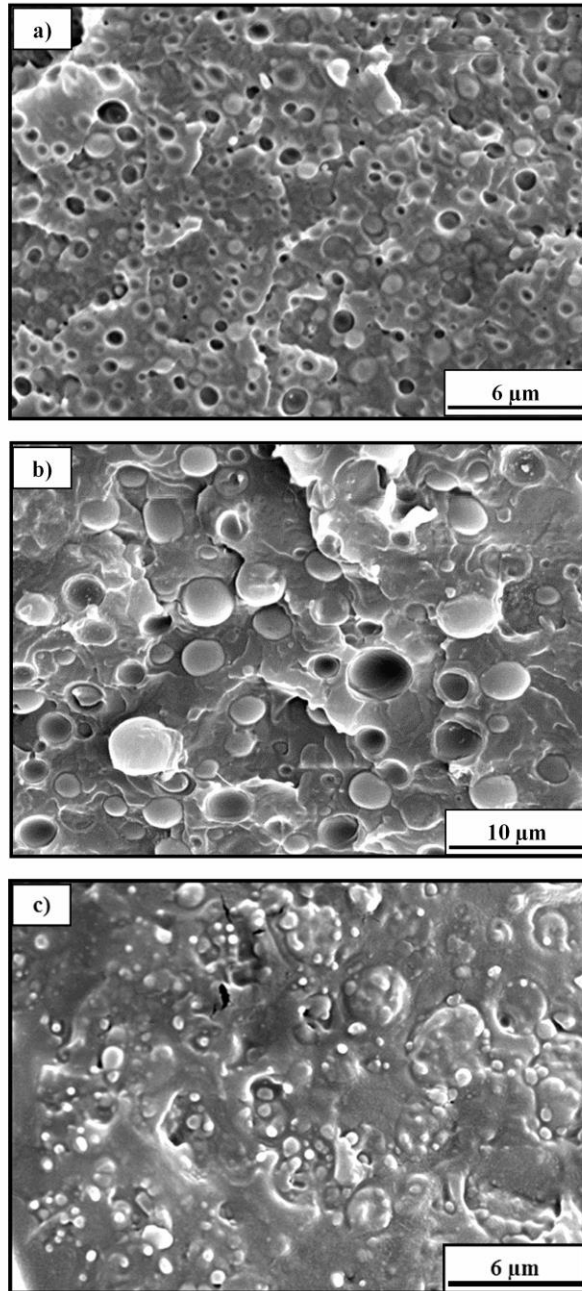
Figure 2.2: SEM micrographs for the cryogenically fractured surfaces of: a) PLA/PCL, b) PLA/PCL/P(LA-*ran*-CL)LMw, c) PLA/PCL/P(LA-*ran*-CL)HMw.

Table 2.3 reports average diameters and particle size distributions of PCL droplets in the blends. Copolymer addition does not reduce PCL average particle size in the blends. These results indicate that P(LA-*ran*-CL) copolymers do not significantly reduce the interfacial tension between PCL and PLA since they are not migrating to the interfacial regions between the components, as would have been expected for an effective compatibilizer

action. Choi et al. reported a decrease in PCL particle size from 10 μm to 3 μm upon 5 wt% addition of a P(LA-ran-CL) copolymer in solvent casted 70/30 PLA/PCL blends.[161] However, it should be noted that in our case the blends were obtained by melt blending, in place of solvent casting, and thus the processing conditions used to extrude and to mould the blends are sufficiently effective to create a fine droplet dispersion, even without the addition of a compabilizating agent.

2.3.2 Non-isothermal DSC experiments

Figure 2.3 shows DSC cooling scans from the melt and subsequent heating scans for all the blends while Table 2.4 lists the characteristic temperatures and enthalpies derived from them.

As shown in Figure 2.3-a, neat PCL crystallizes at 26°C with a sharp exotherm.
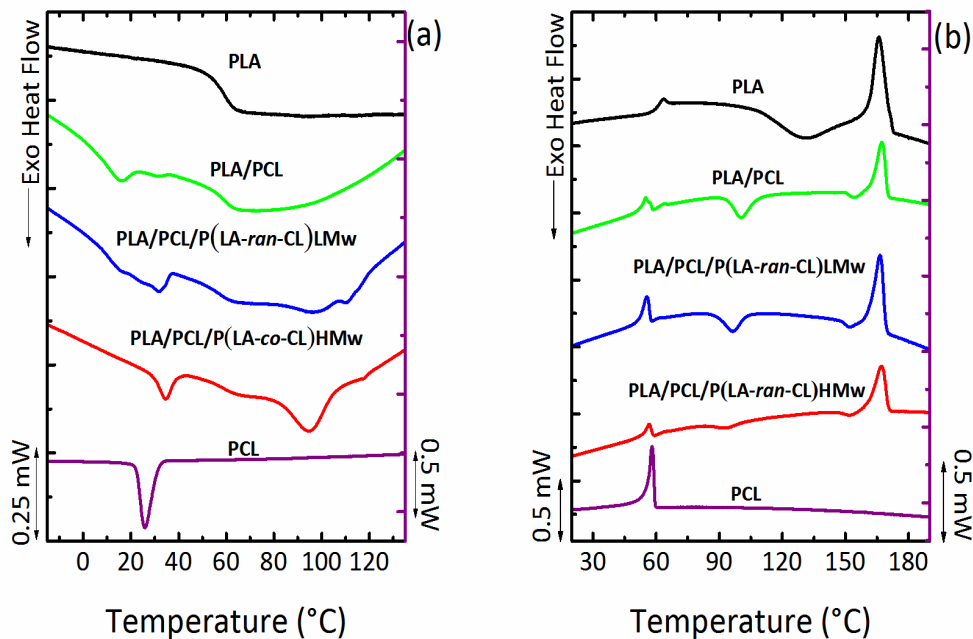
Figure 2.3: Non-isothermal DSC experiments. Cooling curves (a) at 10°C/min from the melt state and subsequent heating curves (b) at 10°C/min. The curves have been normalized by the weight of the samples.

However, when PCL is dispersed in the PLA matrix in the form of droplets (within the 80/20 PLA/PCL blends, see Figure 2.3-a), its crystallization is fractionated into two peaks at 32.1°C and 15.8°C. Fractionated crystallization is a common occurrence in immiscible

Table 2.4: Thermal properties obtained from non-isothermal DSC, cooling and second heating curves. The enthalpies of crystallization and melting have been normalizated by the weight fraction of the sample.

Sample	Cooling				2nd Heating					
	T_{cPCL} (ºC)	ΔH_{cPCL} (J/g)	T_{cPLA} (ºC)	ΔH_{cPLA} (J/g)	$T_{m\,PCL}$ (ºC)	ΔH_{mPCL} (J/g)	$T_{cc\,PLA}$ (ºC)	ΔH_{ccPLA} (J/g)	T_{mPLA} (ºC)	ΔH_{mPLA} (J/g)
PLA	-	-	-	-	-	-	128.1	30.3	165.9	30.4
PCL	25.9	45.7	-	-	55.3	46.6	-	-	-	-
PLA/PCL	15.8/32.1	29.6/2.8	-	-	55.1	31.1	100.5/154	37.5/2.5	167.4	41.1
PLA/PCL/P(LA-*ran*-CL)LMw	15.3/31.6	14.3/27.4	110.8	6.3	55.6	38.7	96.3/151.5	26.2/2.4	167.2	38.4
PLA/PCL/P(LA-*ran*-CL)HMw	34.7	22.8	95.8	17.5	56.7	24.5	93.4/152.2	13.7/3.4	167.1	39.1

blends. It happens when the number of droplets of a crystallizable phase is larger or of the same order of magnitude as the number of active heterogeneities present in the bulk polymer before being dispersed. More about fractionated crystallization can be found elsewhere.[138,165,166]The first crystallization exotherm at 32.1°C corresponds to the crystallization of PCL droplets that have been nucleated by the PLA matrix, since their crystallization occurs at higher temperatures than that of bulk PCL. On the other hand, another PCL droplet population crystallizes at lower Tc values (15.8°C) probably nucleated by less active heterogeneities (see refs. 31,33,34). PLA/PCL/P(LA-ran-CL)LMw also exhibits fractionated crystallization of PCL (Figure 2.3-a). However, in this case PCL droplets are larger than in neat PLA/PCL blends (Table 2.3), therefore, the enthalpy of crystallization (ΔH_{cPCL}) of the high temperature peak is larger than the low temperature one. This is due to the lower number of droplets available to distribute the heterogeneous nuclei originally present in bulk PCL.

On the other hand, PLA/PCL/P(LA-ran-CL)HMw only exhibits a single PCL crystallization exotherm at 34°C, even when the particle size is roughly the same as in neat PLA/PCL blends (Table 2.3). All PCL droplets are in this case crystallizing at higher temperatures in comparison to bulk PCL, therefore they have all been nucleated by the PLA matrix. It should be taken into account that according to Figure 2.3-a, in this blend the PLA phase crystallizes to a much larger extent than in any other sample. Therefore, in this case the probability of PLA nucleation on all PCL droplets is far larger.

According to Figure 2.3, neat PLA does not crystallize during cooling at the scanning rate employed (10°C/min). The reason for this well-known behaviour is the D-LA isomer content of 1.2-1.6 % present in PLA 4032D. In the subsequent heating (Figure 2.3-b), neat PLA undergoes cold-crystallization during the scan and later fusion of the produced crystals. Table 2.4 indicates that the enthalpy of cold crystallization is identical to the enthalpy of melting, confirming that the PLA phase was completely amorphous. A similar behaviour can be observed for the PLA phase within PLA/PCL blends. On the other hand, the PLA/PCL/P(LA-ran-CL)HMw blend developed a significant crystallinity.

As a consequence, the cold crystallization enthalpies for the PLA phase of the PLA/PCL/P(LA-ran-CL)HMw blend is reduced during the second DSC heating scan (Figure 2.3-b and Table 2.4). This enhancement of the crystallization ability of the PLA phase in a PLA/PCL blend by a random copolymer addition, has not been reported in the literature for similar systems.[64,87,88] This positive effect of copolymer addition to the blends on PLA crystallization under non-isothermal conditions will be further analysed under isothermal conditions in the next sections.

2.3.3 Spherulitic growth kinetics of PLA and the PLA component of the blends

Figure 2.4 shows the spherulitic morphology of neat PLA and of the PLA component within the blends at 132.5°C. PLA spherulites show the typical Maltese cross morphology with a negative sign. The Maltese cross extinction patterns tend to get fuzzy upon blending while the spherulites appear to have a rougher morphology.

This trend is more pronounced in the blends in which the copolymers P(LA-ran-CL)LMw and P(LA-ran-CL)HMw are added as compatibilisers. Small PCL droplets can be observed in the melt surrounding the spherulities indicating that there are two phases in the molten state. In the blends containing copolymers, PCL droplets can be seen inside the spherulities. This evidence indicates that, although the two polymers are immiscible, a certain degree of compatibility is achieved during blending.
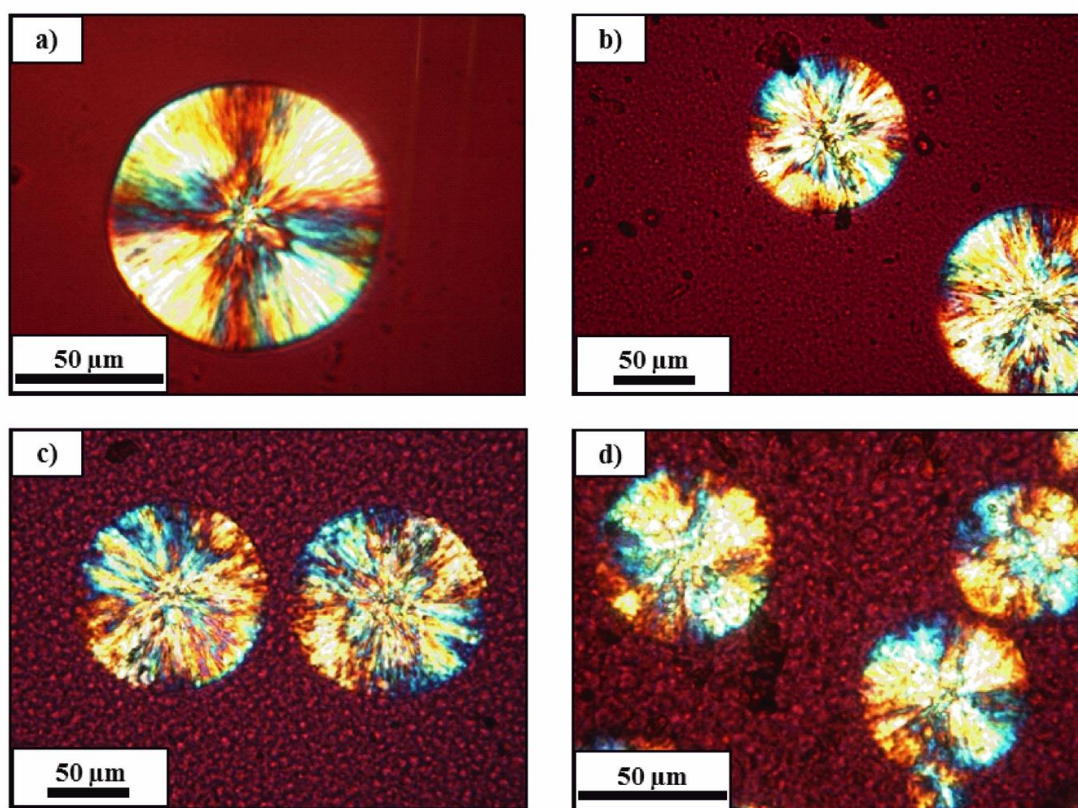
Figure 2.4: PLOM micrographs of a) PLA, b) PLA/PCL, c) PLA/PCL/P(LA-*ran*-CL)LMw, d) PLA/PCL/P(LA-*ran*-CL)HMw. The film samples have a thickness of approximately 10 μm and were taken at 132.5°C, after erasing the crystalline thermal history at 200°C for 3 minutes.

In all samples prepared here, PLA spherulites grow linearly with time indicating that no diffusion problems at the growth front were induced by blending.[66,144] The spherulitic growth rate G (μm/min) was thus calculated from the slope of the line obtained from the plotting of the spherulitic radius (μm) against time (min). The values of G at different crystallization temperatures were fitted by an arbitrary function to guide the eye in Figure 2.5.

The results of Figure 2.5 clearly indicate that neat PLA and PLA in the PLA/PCL blends develop spherulites that grow at the same rates in all the temperature range examined. This finding is consistent with the results of Sakai et al.[143] The authors observed that, as in our case, although PCL could enhance the nucleation of PLA, no influence on the spherulitic growth rate is detected.

If there would be any miscibility between PLA and PCL, a change in spherulitic growth kinetics of PLA would be detected, as any amount of dissolved PCL chains within a PLA rich phase would enhance molecular diffusion (as PCL is a very flexible polymer characterized by a Tg of approximately -60°C). The insensibility of PLA spherulitic growth rate to the addition of PCL is another evidence attesting for the immiscibility of our 80/20 PLA/PCL blends.

A more interesting result can be seen in Figure 2.5 for the blends with P(LA-ran-CL) copolymers. At temperatures of 120°C, the blends with PLA/PCL/P(LA-ran-CL)LMw and PLA/PCL/P(LA-ran-CL)HMw exhibit spherulitic growth rates that are two or three times, respectively, larger than those characteristic of neat PLA. Similar increases in spherulitic growth rates are typically reported for plasticized PLA.[121,167] Miscible plasticizers interact with PLA, increasing chain mobility and reducing the energy barrier required for crystallization
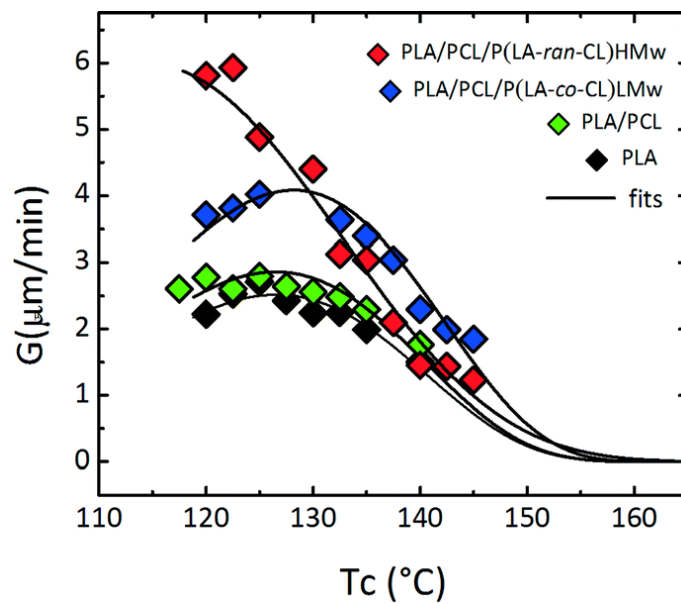

Figure 2.5: Spherulitic growth rate G as a Function of isothermal crystallization temperature T_c for neat PLA and the blends. The solid lines represent arbitrary fits to guide the eye.

Since, as indicated in Table 2.3, PCL droplet size is not reduced by copolymer addition, we assume that P(LA-ran-CL) copolymers do not migrate to the PLA-PCL interface. It is then conceivable that the copolymers can dissolve at least in the PLA phase, or even more likely in both PLA and PCL phases. In this way, the lower Tg (as compared to PLA) miscible P(LA-ran-CL) copolymer chains can interact with PLA, increasing its chain mobility and thus promoting spherulitic growth rate.

Figure 2.5 clearly shows that G values for the PLA phase are higher in PLA/PCL/P(LA-ran-CL)LMw blends than in PLA/PCL/P(LA-ran-CL)HMw blends, notwithstanding that thermodynamic conditions assert that the lower molecular weight copolymer should be more miscible in PLA than the high molecular weight one and thus could be a better plasticizer agent.[144] However, the different composition of the two copolymers must also be considered. In fact, P(LA-ran-CL)HMw has, according to Table 2.1, a 65 wt% of PCL and thus a Tg of -38°C, a value substantially lower than that of P(LA-ran-CL)LMw (Tg=-16°C) containing 48% of PCL.

Assuming that at least part of the copolymers can dissolve in the PLA phase, the higher Mw copolymer probably acts as a better plasticizer agent than the lower molecular weight one, in spite of its higher molecular weight, because of its lower Tg value determined by copolymer composition.

2.3.4 Overall crystallization rate

The inverse of the half-crystallization time, determined by isothermal crystallization from the melt employing DSC, provides an experimental measure of the overall crystallization rate, which includes both nucleation and spherulitic growth.

Figure 2.6 shows plots of the overall crystallization rate (expressed as the inverse of half-crystallization time) as a function of the temperature for neat PLA and for the blends. The solid lines correspond to arbitrary fits performed to guide the eye. All the samples display the typical bell-shape trend, where the crystallization rate goes through a maximum as the kinetics changes from nucleation control at higher temperatures to diffusion control at lower temperatures.

The isothermal crystallization experiments were conducted after quenching the sample from the melt state (by controlled cooling in the DSC at a rate of 60°C/min). The

PLA employed here crystallizes very slowly from the melt. Neat PLA completes its crystallization, at the temperature where the crystallization rate is maximum (Tc=113°C), only after 30 minutes. This result is consistent with the non-isothermal DSC cooling experiments, in which no crystallization of PLA was detected during cooling at 10°C/ min from the melt state. Taking neat PLA as reference material, an enhancement effect on the crystallization rate is clearly evident by blending the material with only PCL (see Figure 2.6). Considering that PLA spherulitic growth is not affected by PCL addition (see Figure 2.5 and its discussion), the increase in overall crystallization rate must be due to the nucleation effect of PCL.

In the case of the blends that contain copolymers, both nucleation and growth rate increases should be expected for the PLA phase. The results are consistent with our hypothesis that the copolymers are miscible (at least in part) with the PLA phase. The PLA/PCL/P(LA-ran-CL)HMw copolymer which has the lowest Tg value is a more effective
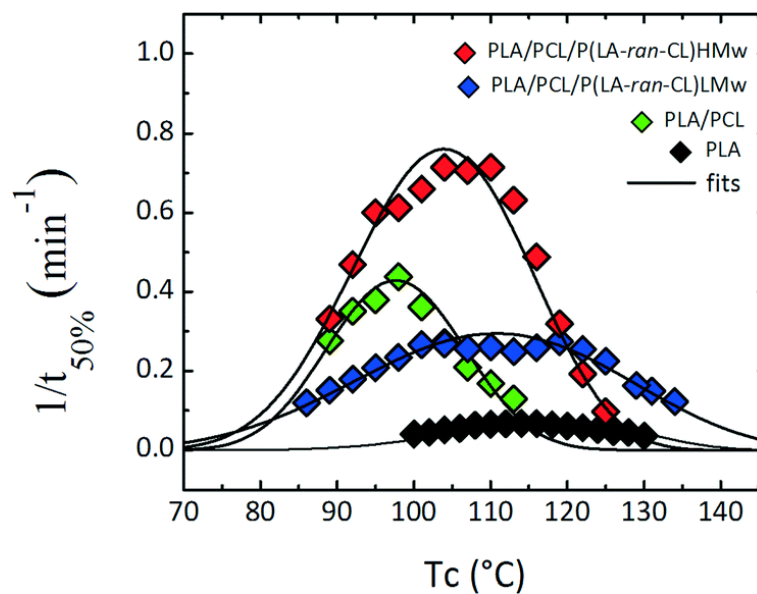

Figure 2.6: Isothermal crystallization experiments conducted after quenching the samples from the melt state. Overall crystallization rate ($1/t_{50\%}$) as a function of isothermal crystallization temperature T_c in neat PLA and the blends. The solid lines represent arbitrary fits to guide the eye.

plasticizer for the PLA phase and leads to a remarkable enhancement of overall crystallization rate in Figure 2.6.

In fact, at an isothermal crystallization temperature of 113°C, the PLA phase within PLA/PCL/P(LA-ran-CL)HMw crystallizes in only 2.8 minutes, roughly 10 times faster than neat PLA. These results are consistent with the non-isothermal results presented in Figure 2.3.

The isothermal crystallization data obtained by DSC were analysed using the Avrami equation.[168] The fits to the Avrami equation were performed using the Origin® plug in, developed by Lorenzo et al.[164]

Firstly, it allows the baseline to be established and later calculate the integral of the calorimetric isothermal curve. Secondly, the linear fit according to the Avrami equation and the evaluation of fitting errors can be performed. V_c (relative volume fraction crystallinity) is calculated according to Eq. 2.4, whereas V_c range is selected from 0.03 to 0.20 in order to obtain the best fit within the primary crystallization range.

$$Vc = \frac{Wc}{Wc + \frac{\rho_c}{\rho_a}(1 - Wc)} \qquad \text{Eq. (2.5)}$$

$$Vc = \frac{Wc}{Wc + \frac{\rho_c}{\rho_a}(1 - Wc)}$$

ρ_c and ρ_a are the fully crystalline and fully amorphous polymer densities, respectively. For all calculations, ρ_a=1.25 g/cm^3 and ρ_c=1.359 g/cm^3 were used for PLA. The relative crystalline mass fraction W_c is calculated as:

$$Wc = \frac{\Delta H_{(t)}}{\Delta H_{TOT}} \qquad \text{Eq. (2.6)}$$

Where ΔH(t) and ΔH$_{total}$ are the enthalpy as a function of crystallization time and the maximum enthalpy after completion of the crystallization process.

Finally, the Avrami equation is rearranged as follows:

$$\log[-\ln(1 - Vc)] = \log(k) + n\log(t - t_0) \qquad \text{Eq. (2.7)}$$

Where *n* is the Avrami index and *K* is the overall crystallization rate constant. The experimental and predicted half–crystallization time $\tau_{50\%}$ can be also determined by this Origin® plugin. According to the Avrami equation, $\tau_{50\%}$ is:

$$\tau_{50\%} = \left[-\frac{\ln[1 - V_c]}{K} \right]^{1/n} \qquad \text{Eq. (2.8)}$$

Then, depending on the goodness of the fit (up to 50% conversion) there may be a difference between the experimental and predicted values of $\tau_{50\%}$. The parameters obtained by Avrami Fits are collected in Table 2.5 (sample of neat PLA), Table 2.6 (sample PLA/PCL), Table 2.7 (sample PLA/PCL/P(LA-*ran*-CL)LMw and Table 2.8 (sample PLA/PCL/P(LA-*ran*-CL)HMw.

Table 2.5: Parameters obtained by fitting the Avrami theory to PLA

Tc	$t_{50\%\ theo}$ (min)	$t_{50\%\ exp}$ (min)	n	K (min^{-n})	R^2	$1/t_{50\ exp}$ (min^{-1})
130	29.029	28.384	3.28	1.10E-05	1.0000	0.0308
128	22.449	22.567	3.59	9.73E-06	1.0000	0.0402
126	21.191	21.234	3.3	2.94E-05	1.0000	0.0423
124	19.715	19.313	3.24	4.47E-05	0.9997	0.0454
122	18.052	17.686	3.23	6.01E-05	0.9993	0.0493
120	16.645	16.317	3.03	1.40E-04	0.9995	0.0535
118	15.856	15.567	3.12	1.26E-04	0.9998	0.0563
116	15.195	14.866	2.97	2.12E-04	1.0000	0.0580
114	15.125	14.717	2.84	3.06E-04	0.9999	0.0579
112	15.837	15.033	2.7	3.98E-04	1.0000	0.0550
110	15.816	15.317	2.68	4.21E-04	0.9998	0.0550
130	29.029	28.384	3.28	1.10E-05	0.9998	0.0308
128	22.449	22.567	3.59	9.73E-06	1.0000	0.0402
126	21.191	21.234	3.3	2.94E-05	0.9998	0.0423
124	19.715	19.313	3.24	4.47E-05	0.9997	0.0454
122	18.052	17.686	3.23	6.01E-05	0.9993	0.0493

Table 2.6: Parameters obtained by fitting the Avrami theory to PLA/PCL

Tc	$t_{50\%\ theo}$ (min)	$t_{50\%\ exp}$ (min)	n	K (min^{-n})	R^2	$1/t_{50\ exp}$ (min^{-1})
113	8.307	7.733	2.3	0.00503	0.9997	0.1293
110	6.415	5.933	2.36	0.00858	0.9993	0.1685
107	5.049	4.783	2.54	0.0114	0.9995	0.2091
104	3.756	3.684	2.97	0.0137	0.9998	0.2714

101	2.737	2.766	3.81	0.0149	1.0000	0.3615
98	2.271	2.283	3.58	0.0367	0.9999	0.4380
95	2.593	2.633	4.32	0.0113	1.0000	0.3798
92	2.843	2.85	3.8	0.0131	0.9998	0.3509
89	3.62	3.617	3.71	0.0059	0.9998	0.2765
86	5.587	5.633	4.04	0.00062	1.0000	0.1775
83	8.219	8.133	3.6	0.000352	0.9998	0.1230

Table 2.7: Parameters obtained by fitting the Avrami theory to PLA/PCL/P(LA-*ran*-CL)LMw

T_c	$t_{50\% theo}$ (min)	$t_{50\% exp}$ (min)	n	K (min^{-n})	R^2	$1/t_{50 exp}$ (min^{-1})
134	7.864	8.133	3.1	0.00116	0.9999	0.1230
131	6.473	6.717	3	0.00257	1.0000	0.1489
129	5.932	6.117	2.84	0.00443	1.0000	0.1635
125	4.325	4.45	2.92	0.00962	1.0000	0.2247
122	3.874	3.934	2.63	0.0197	1.0000	0.2542
119	3.635	3.65	2.55	0.0257	0.9999	0.2740
116	3.836	3.867	2.65	0.0197	1.0000	0.2586
113	4.031	4.017	2.54	0.02	1.0000	0.2489
110	3.994	3.833	2.25	0.0306	0.9998	0.2609
107	4.008	3.9	2.3	0.0286	1.0000	0.2564
104	3.784	3.734	2.32	0.0315	1.0000	0.2678
101	3.883	3.75	2.4	0.0266	0.9999	0.2667
98	4.421	4.266	2.42	0.0191	0.9999	0.2344
95	4.942	4.8	2.56	0.0117	0.9998	0.2083
92	5.629	5.567	2.85	0.00553	0.9999	0.1796
89	6.607	6.617	2.99	0.00244	0.9998	0.1511

Table 2.8: Parameters obtained by fitting the Avrami theory to PLA/PCL/P(LA-*ran*-CL)HMw

| T_c	$t_{50\% theo}$ (min)	$t_{50\% exp}$ (min)	n	K (min^{-n})	R^2	$1/t_{50 exp}$ (min^{-1})
125	10,251	10,3	3,4	0,000253	1,0000	0,0971
122	5,121	5,184	3,09	0,00448	1,0000	0,1929
119	3,057	3,133	3,09	0,022	1,0000	0,3192
116	1,999	2,05	3,14	0,078	1,0000	0,4878
113	1,526	1,583	3,7	0,145	1,0000	0,6317
110	1,344	1,4	3,47	0,248	1,0000	0,7143
107	1,414	1,415	4,31	0,156	1,0000	0,7067
104	1,38	1,4	3,88	0,199	0,9998	0,7143
101	1,491	1,516	3,95	0,143	0,9999	0,6596
98	1,645	1,633	3,44	0,125	0,9996	0,6124
95	1,711	1,667	3,04	0,136	0,9996	0,5999
92	2,198	2,134	2,92	0,0695	0,9996	0,4686
89	3,121	3,017	2,89	0,00844	0,9996	0,3315
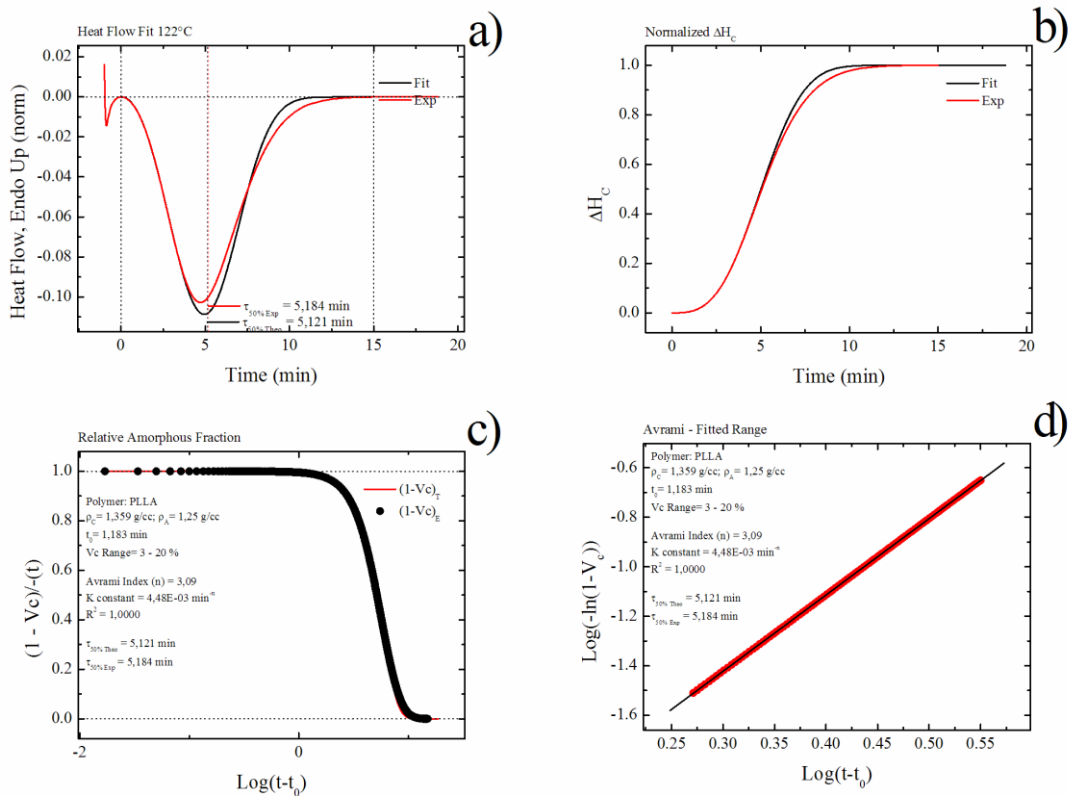
Figure 2.7: Avrami plots obtained by the Origin® plugin developed by Lorenzo *et al.* (a) Experimental DSC crystallization isotherm of PLA/PCL/P(LA-*ran*-CL)HMw at 122°C and its fitting with the Avrami equation. The experimental crystallization half–time is indicated. (b) Relative enthalpy of crystallization (Ec. 2) as a function of time. (c) Evolution of the normalized volumetric fraction of the amorphous phase as a function of crystallization time. (d) Linear fitting of the Avrami equation in the primary crystallization range, where the slope indicates the Avrami index and the intercept the overall crystallization rate constant.

The Avrami index values (n) for the isothermal crystallization of PLA or the PLA phase within all prepared blends oscillated between 2.5 and 4 (although in some isolated cases values closer to 2 were obtained). As spherulites were always observed by PLOM, values of 3-4 are expected, since n=3 corresponds to instantaneously nucleated spherulites and n=4 to sporadically nucleated spherulites. As Tc increases the Avrami index tends to increase. This is a typical trend, since nucleation becomes more sporadic as temperature increases. No other specific trends or differences between the blends were observed.

2.3.5 Effect of P(LA-ran-CL) copolymers on the crystallization of the PCL phase

The random copolymers employed in this work have 48 % and 65 % PCL repeating units within them (see Table 2.1). In previous sections we showed evidences indicating that these copolymers (at least in part) are probably dissolved in the PLA phase when they are added to the 80/20 PLA/PCL blends. It is reasonable to assume that part of the copolymer chains may also dissolve in the PCL phase or that in other words, during the melt mixing procedure, a partition of the copolymer chains occurs, as the copolymers are probably miscible with both phases. If this hypothesis is true, then a reduction of the PCL phase crystallization should occur as a result of adding copolymer chains that have a higher Tg value (see Table 2.1).

The Tg values of the copolymers according to Table 2.1 are 16°C and -38°C for the low and the high molecular weight copolymer respectively. PLA has an approximate Tg value of 60°C and therefore the addition of miscible P(LA-ran-CL)s produces a plasticization of the PLA chains, as demonstrated in previous section. On the other hand, PCL has a Tg of -60°C and therefore the addition of P(LA-ran-CL)s, if miscible, should cause an anti-plasticization of the PCL chains.
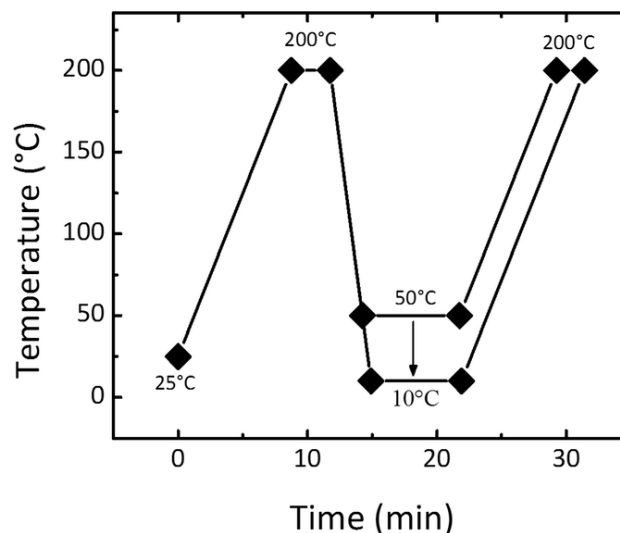

Figure 2.8: Combined isothermal-non-isothermal experiment on PCL crystallization. First heating from room temperature to 200°C, quenching at 60°C/min until certain isothermal crystallization temperatures (T_c) between 50°C and 10°C and subsequent reheating at 20°C/min to 200°C.

Attempts were made to determine the isothermal crystallization rate of the PCL phase within our blends. Unfortunately it was experimentally not possible by the usual techniques. In the blends, PCL particles are too small to appreciate the spherulitic growth by PLOM isothermal experiments. The overall crystallization rate of PCL is so fast, that it crystallizes upon cooling from the melt in the DSC to the crystallization temperature, even when cooling rates of 60°C/min are employed. To overcome these difficulties, a combined non-isothermal – isothermal experiment was designed in order to have a measurement of the crystallization ability of the PCL droplets within the blends as depicted in Figure 2.8.

According to Figure 2.8, the samples were first heated to 200°C and kept at that temperature for 3 minutes, in order to erase thermal history. Then they were cooled at 60°C/min until an isothermal crystallization temperature (T_c) between 50°C and 10°C, was reached. After an isothermal crystallization time of 7 minutes was elapsed, the samples were heated at 20°C/min while the DSC scan was registered. The melting enthalpy of PCL during this second heating corresponds to the sum of the crystallization enthalpy obtained during cooling to T_c plus the isothermal crystallization enthalpy obtained during the isothermal crystallization period.
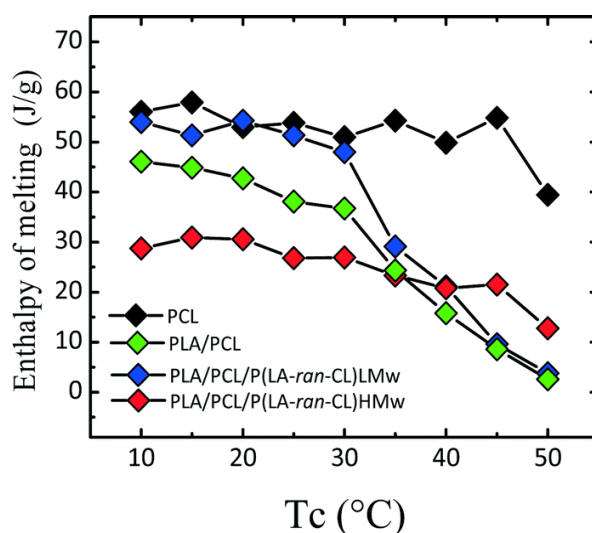

Figure 2.9: Combinated isothermal-non-isothermal experiment on PCL crystallization. PCL enthalpy of melting as a function of crystallization temperature for neat PCL and for the blends. The melting enthalpy corresponds to the sum of enthalpy of the isothermal and non-isothermal crystallization. The curves have been normalized by the weight of the samples.

Figure 2.9 shows the PCL enthalpy of melting (registered during the final heating step of the protocol indicated in Figure 2.8) as a function of crystallization temperature for neat PCL and for the blends. Neat PCL exhibits a lack of dependence of the enthalpy of melting on the isothermal crystallization temperature. After the 7 minutes at the different crystallization temperatures, a value of around 55 J/g is always obtained. This means that neat PCL crystallizes during the previous non-isothermal cooling (at 60°C/min) from the melt to Tc, regardless of the Tc employed.

In the case of PCL droplets within 80/20 PLA/PCL blends, the enthalpy of melting for the PCL component has a different behaviour. The enthalpy of melting decreases with Tc, especially for Tc values larger than 30°C. This means that in this blend, PCL reaches its maximum crystallization rate at temperatures below 30°C. The differences between bulk PCL behaviour (in neat PCL) and PCL droplets behaviour within this blend agree with the non-isothermal DSC results, where a fractionated crystallization was detected and part of the droplets crystallizing at lower temperatures than bulk PCL. A similar behavior can be observed in Figure 2.9 for PCL droplets within PLA/PCL/P(LA-ran-CL)LMw blend.

For PLA/PCL/P(LA-ran-CL)HMw blend (Figure 2.9), the melting enthalpy of PCL droplets is lower and has a weak dependence on Tc. For this blend, the anti-plasticization of PCL chains by the incorporation of miscible PLA/PCL/P(LA-ran-CL)HMw seems to be dominant, and PCL droplets can only develop half the crystallinity value as compared to neat PCL or even the PCL component in the other blends, when the comparison is made at low Tc values (for instance Tc=10°C in Figure 2.9)

2.3.6 Mechanical Properties

Table 2.9 reports results from tensile tests performed on compression moulded specimens. Neat PLA displays a typical brittle behavior,[38] with an elongation at break of 2 % and a stress at break of 56 MPa.[11] Neat PCL shows a typical ductile behavior,[38] with an elongation at break of 516 %, a yield strength of 11 MPa and a stress at break of 28 MPa.

Uncompatibilized PLA/PCL blends exhibit a better balance in tensile properties, as compared to the blends prepared with copolymer addition. For instance, they exhibit an elongation at break of 68%, while the other blends are either brittle (PLA/PCL/P(LA-ran-

CL)LMw exhibits only 4% elongation at break) or significantly less ductile (PLA/PCL/P(LA-ran-CL)HMw displays 18% elongation at break).

The results shown in Table 2.9 are in agreement with SEM measurements that indicate a lack of compatibilizing action of the PLA-ran-PCL copolymers, since they do not reduce particle size and they do not improve the mechanical properties of neat PLA/PCL blends.

It must be noted that the crystallinity of the PLA matrix has a great influence on the mechanical properties. In view of the plasticizing action of copolymer addition, the PLA matrix in the blends containing copolymer has a significantly higher crystallinity degree as compared to neat PLA/PCL blends. For instance, in PLA/PCL/P(LA-ran-CL)HMw the crystallinity of the PLA matrix is 19% and thus this sample has a Young's Modulus of 2910 MPa, higher than that of PLA/PCL (Young's Modulus 2370 MPa) that displays a PLA crystallinity of 5% .

Table 2.9: Mechanical properties of neat PLA, neat PCL and blends. Tensile test at room temperature at 10 mm/min on the compression moulded sheets

Sample	Young's Modulus (MPa)	Yield stress (MPa)	Yield strain (%)	Stress at break (MPa)	Strain at break (%)	PLA Xc (%)
PLA	3380±113	-	-	56±5	2.3±0.3	2
PCL	303±51	11.4±0.1	9.8±0.2	28±2	516±70	-
PLA/PCL	2370±33	39.6±0.7	2.1±0.1	22±2	68±4	5
PLA/PCL/P(LA-ran-CL)LMw	2240±196	30±3	1.6±0.1	27±4	4±1	15
PLA/PCL/P(LA-ran-CL)HMw	2910±50	39.7±0.8	1.6 ±0.1	26±3	18±6	19

2.4 CONCLUSIONS

The addition of P(LA-*ran*-CL) to PLA/PCL blends induce a plasticization effect that increases the crystallization ability of the PLA phase. Such plasticization effect can increase the spherulitic growth rate of PLA two or three fold as compared to neat PLA depending on the Tg of the random copolymer employed.

The copolymer with the higher amount of ε-Caprolactone, and with a lower Tg, produces a larger plasticization effect in comparison with the other copolymer used

(characterized by a higher amount of PLA) and can significantly increase the overall crystallization rate of PLA up to an order of magnitude.

A combined non-isothermal – isothermal experiment was designed in order to demonstrate that copolymer incorporation in the blends leads to an anti-plasticization effect of the PCL droplets. The mechanical properties of the blends are greatly influenced by the crystallinity of the PLA matrix.

3 CAN POLY(Ε-CAPROLACTONE) CRYSTALS NUCLEATE GLASSY POLYLACTIDE?

3.1 INTRODUCTION

Polylactide (PLA), is one of best candidates to replace conventional petroleum based polymers because it is bio-based, biodegradable and biocompatible. Even if its useful properties have already been employed for specific applications, such as biomedical devices[169] or food packaging,[170] its development as large-scale commodity material is still limited by several drawbacks. Among them, the upper temperature boundary for practical applications of amorphous PLA established by its low glass transition temperature (i.e., circa 60°C) and its mechanically brittle behavior.[73,119,171–174] Extending its temperature range of applications requires that the polymer crystallizes, but its crystallization rate is much slower than the cooling rates employed during processing.

The control of PLA crystallization kinetics is not a trivial issue, since it depends on the relative amount of the two stereoisomeric forms in which lactide exists (i.e., L or D Lactide) and on its molecular weight. Only if one of the two forms is present in a high enough amount (at least more than 96-97%), PLA is able to develop significant crystallinity. However, being directly produced from natural feedstock, most of commercial PLA grades contain a minor portion of D units that is enough to render the material completely amorphous at the fast cooling rates applied during processing (i.e., during extrusion or injection molding).[73,119,171–174] The enhancement of crystallization rate up to levels where the material can crystallize during processing would also imply a transformation from the liquid to the solid state at higher temperatures and therefore with faster molding cycles, saving energy and production times.

Because the separation of L and D Lactide is difficult to achieve on a large scale,[31] an increasing effort has been made to improve the crystallization kinetics of commercial PLAs without varying its stereoisomeric composition.[27,31,73,75,119,171–176] These include: polymer blending,[175] copolymerization,[75] addition of additives[27] or surface modifications,[176]

among which blending is the most versatile. Blending can in principle be tailored to accelerate crystallization kinetics and at the same time improve the mechanical properties of PLA, depending on the components present in the formulation.

In a polymer blend the miscibility between the components is the key factor that determines the phase Behavior and thus the final properties of the resulting blended material.[130] Depending on the favorable specific interaction between the polymeric counterparts, a miscible or an immiscible blend may be obtained.[177]

In a miscible blend, a single-phase system, which combines the properties of the components, is formed. Therefore, the tendency to crystallize of one component can either increase or decrease, depending on the changes of the glass transition and equilibrium melting temperature produced by blending.[178] Considering the inherent brittleness of PLA, below its Tg value (i.e., 60° C), its blends with miscible low Tg polymers, like poly(ethylene oxide)(PEO),[179,180] have been frequently reported. In this case, PLA growth rate increases in view of the plasticizing ability of PEO chains.[144]

In immiscible blends, the components are separated in microdomains with contact at their interfaces. Although the crystallization of each components takes place in separated domains and thus the crystal growth rates are not expected to be influenced by blending, significant deviations of the overall crystallization kinetics may still take place.[177] Generally, two possibility may occur. One component can nucleate the other trough interface-assisted nucleation mechanisms.[181] Otherwise, the nucleation kinetics may be increased by the migration of active heterogeneities from one component to the other during blending.[182] Also the morphology of the blend may have a pivotal role. When in a blend the minoritary phase is finely dispersed in droplets within an immiscible matrix, its crystallization may take place in several steps, the so-called fractionated crystallization, this happen if the number of dispersed droplets is greater than the number of active heterogeneities originally present in the bulk crystallizing phase.[138,166,183]

Blends of PLA with poly(ε-caprolactone) (PCL) have been extensively investigated, as PCL is a flexible, biodegradable and biocompatible polyester, that could be useful in compensating the brittleness of PLA. Although the solubility parameters of PLA and PCL are quite close (i.e., 10.1 $(cal/cm^3)^{1/2}$ for PLA vs. 9.2 $(cal/cm^3)^{1/2}$ for PCL),[149] there are not favorable interactions and miscibility does not occur. Therefore the two polymers are

immiscible over a wide range of temperature, composition and molecular weight, as confirmed by many previous studies where the polymers were mixed in solution[184–186] or in the melt.[148,154,155,187] A large body of literature has been devoted to try to enhance phase adhesion and thus improve blend properties.[135,152,156–158,160–162,188–195] Different kinds of compatibilizers have been proposed, including: random copolymers,[160–162,188] block copolymers[156,157,189,190] as well as reactive compatibilization/mixing.[158,191–195]

Notwithstanding the extensive literature on phase structure, morphology, and mechanical properties of PLA/PCL blends;[24–52] the effect of PCL on the crystallization kinetics of PLA is still not completely understood. In blends where PCL conforms the minor phase, PLA melt crystallization is not greatly influenced by blending, unless a migration of heterogeneities from one phase to the other may occur. On the other hand, if proceeding from the glassy state, PLA crystallization (i.e., cold crystallization) may be strongly enhanced upon PCL addition. [46–51] This effect cannot be trivially explained unless deriving from an increased miscibility between the phases upon the addition of a compatibilizer, as result of an enhanced PLA chain mobility imposed by miscible PCL chains.[46–48] However, an increase of PLA cold crystallization kinetics has also been observed in uncompatibilized blends, as a result of a nucleation effect of PCL on PLA which up to now has not been satisfactorily explained in the literature. [143,198,199]

Sakai et al[143] observed that, even in small amounts (i.e., 1-5 wt %), PCL addition enhances the nucleation rate of PLA during cold crystallization but has an insignificant effect on its melt crystallization and crystal growth, probably due to the immiscibility of the blends. The authors proposed that this improvement of the nucleation rate is due to a local increase of PLA chains mobility at the interface with PCL domains. However, this mechanism cannot explain why the effect is detectable only during cold crystallization, whereas it has no relevance during melt crystallization. At the same time, it is not clear why annealing the blends at temperatures well below the *Tg* of PLA an increase in PLA nuclei density upon subsequent heating is detected.

More recently, Derakhshended et al.[198] attributed the enhanced cold crystallization of PLA in PLA/PCL blends, to precursors transfer from PCL-rich phase into PLA-rich phase during spinodal decomposition of the blend. According to these authors, once the

temperature is increased above the melting temperature of PCL, some residual crystallization precursors, which consist in highly aligned PCL chains, could migrate into PLA phase providing additional sites for nucleation. However, this explanation requires that some miscibility between PLA and PCL exists, a fact that has not been conclusively demonstrated so far in the literature. In fact, most reports of uncompatibilized PCL/PLA blends do not find any influence of blend composition on the thermal transitions of the two components. In fact, constant Tm and Tg values (located at identical temperatures to those of the homopolymers) at different composition have been found, indicating total immiscibility in these blends. Nevertheless, decreases in the cold crystallization temperature of PLA during heating can still be observed in such uncompatibilized blends. [148,154,155,184–187]

Despite the great interest attracted by PLA/PCL blends, the effect of PCL on PLA crystallization and its relationship with blend compatibility remain an open issues. In this work, the cold crystallization of PLA (i.e., the crystallization of PLA during heating from the glassy state) within 80/20 PLA/PCL blends, with different degrees of compatibilization, has been investigated, both under non-isothermal and isothermal conditions. Three different kinds of poly(L-lactide-*block*-carbonate) copolymers (varying composition and molecular weight) have been used for the first time to tune the compatibility between PLA and PCL. The use of specially designed thermal protocols have allowed us to obtain results that can successfully explain, for the first time, why the cold crystallization of PLA is promoted by PCL addition and how compatibilization can also play a role in this phenomenon.

3.2 EXPERIMENTAL PART

3.2.1 Materials and methods

Polylactide (PLA, Ingeo index: 4032D, with 1.2-1.6% D-LA isomer content, M_w = 200 Kda, Tg = 60°C) was purchased from NatureWorksTM and was dried overnight under vacuum at 60°C before use, in order to avoid degradation reactions induced by moisture. Poly(ε-Caprolactone) (PCL, CAPA 6500, M_w = 45 Kda, Tg= -60°C) was purchased from SolvayTM

and was used as received. Polycarbonate (PC, TARFLON® IV1900R, *Tg* = 140°C) was purchased from Idemitsu Chemicals Europe.

Three different poly(lactide-*block*-carbonate) copolymers, PLA-*b*-PC, were tested as compatibilizers. The synthesis of these copolymers was carried out by ring opening polymerization in toluene at 95°C, using stannous (II) octanoate as catalyst (details of the synthesis are described in the next paragraph). Composition (LA/C), weight average molecular weights (M_w), polydispersity (*D*) and glass transition temperatures (Tg) of the block copolymers are reported in Table 3.1.

Table 3.1: Composition (*LA/C*), average molecular weights (M_w), polydispersity (D) and glass transition temperatures (*Tg*) of the block copolymers

Sample	LA/C (w/w)[a]	M_w (Da)[b]	D[c]
PLA-*b*-PC80-20	80/20	6400	1.4
PLA-*b*-PC50-50	50/50	5200	1.9
PLA-*b*-PC15-85	15/85	5700	2.0

[a]Composition weight ratio between lactide unit (*LA*) and carbonate unit determined by ^{1}H-NMR. [b] Determined by SEC (THF) with PS standard. [c] Determined as: M_w/M_n.

3.2.2 Synthesis of PLA-b-PC copolymer

In a typical procedure, L-lactide and polycarbonate were charged to a three-neck flask equipped with a condenser under nitrogen atmosphere (by following the composition of the copolymer and at total amount of 1g) containing stannous 2-ethylhexanoate (0.1% mol/mol with respect to L-lactide amount) and toluene (10 ml). The reaction was carried out at 95°C for 24 hours under nitrogen and stopped by quenching it in an ice bath.

The crude product was dissolved in a minimum volume of dichloromethane, followed by precipitation into a 10-fold excess of methanol. The copolymers were recovered by filtration and after drying under vacuum.

^{1}H-NMR (400 MHz, CDCl3): δ = 5.15 (br, 1H, lactide-unit), 1.68 (br, 3H, lactide-unit), 7.25 (br, 2H, carbonate-unit), 7.17 (br, 2H, carbonate-unit) and 1.66 (br, 6H, carbonate-unit) ppm.
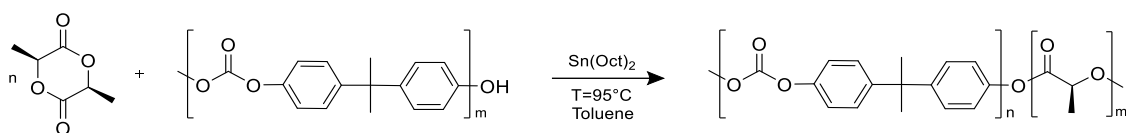
Figure 3.1. Synthesis of PLA-*b*-PC copolymer, from L-lactide and polycarbonate olygomers
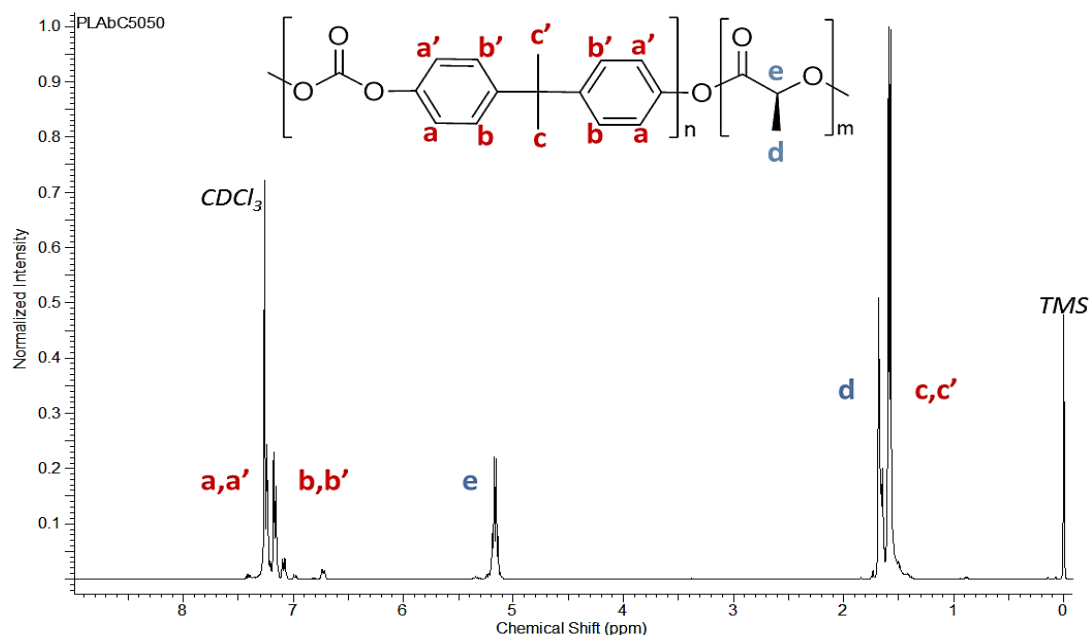

Figure 3.2: ^{1}H-NMR spectrum(400 MHz, CDCl3) and chemical structure of PLA-b-PC50-50

3.2.3 Blends preparation

All the blends were prepared by solution mixing and subsequent solvent casting. By the same technique, also neat PLA and neat PCL films were prepared. Neat homopolymers and the compatibilizers were dissolved in dichloromethane, at the total concentration of 1 g/dL following the compositions in Table 3.2, and stirred at room temperature for 3 hours. The film forming solutions were cast in Petri dishes (diameter= 5 cm). The obtained films were dried for 24 hours at room temperature, and for additional times at 60 °C under vacuum until a constant weight was reached.

A constant PLA/PCL weight ratio of 80/20 was employed. PLA-*b*-PC copolymers and neat PC were tested as compatibilizers by adding them at 10% with respect to the minor phase. Thus, the final blends have an approximate composition of 80/20/2, weight

ratio, PLA/PCL/Compatibilizer. By using the same method, PLA/PC blends were also prepared with weight ratios of: 99/1, 98/2 and 95/5. The compositions of all the blends used in this work are reported in Table 3.2.

Table 3.2: Composition of PLA/PCL, PLA/PCL/Compatibilizer and PLA/PC blends

Sample name	PLA (wt%)	PCL (wt%)	PLA-*b*-PC 80-20 (wt%)	PLA-*b*-PC 50-50(wt%)	PLA-*b*-PC 15-85(wt%)	PC (wt%)
PLA/PCL	80	20	-	-	-	-
PLA/PCL/PLA-*b*-PC 80-20	79	19	2	-	-	-
PLA/PCL/PLA-*b*-PC 50-50	79	19	-	2	-	-
PLA/PCL/PLA-*b*-PC 15-85	79	19	-	-	2	-
PLA/PCL/PC	79	19	-	-	-	2
PLA/PC 99-1	99	-	-	-	-	1
PLA/PC 98-2	98	-	-	-	-	2
PLA/PC 95-5	95	-	-	-	-	5

3.2.4 Morphological analysis

Specimens of the blends were cryogenically fractured after 3 hours of immersion in liquid nitrogen. Fracture surfaces were observed by Scanning Electron Microscopy (SEM) after gold coating under vacuum, using a Hitachi S-2700 electron microscope.

Micrographs of the most representative inner regions of the specimens were achieved. PCL droplet diameters were measured by counting at least 100 particles. Number (d_n) and volume (d_v) average diameters and particle size polydispersity (D_p) were calculated by the following equations[138]

$$d_n = \frac{\sum n_i d_i}{\sum n_i}$$

Eq. (3.1)

$$d_v = \frac{\sum n_i d_i^4}{\sum n_i d_i^3}$$
<div align="right">Eq. (3.2)</div>

$$D = \frac{d_v}{d_n}$$
<div align="right">Eq. (3.3)</div>

Polarized Light Optical Microscopy (PLOM) was employed to observe the morphology and measure the growth rate of PLA crystals. Micrographs were recorded with a LEICA DC 420 camera on film samples with a thickness of approximately 10 µm. A METTLER FP35Hz hot stage was employed to thermally treat the samples with different methods as a function of the designed experiment.

The isothermal spherulitic growth rate of neat PLA and the PLA phase within the blends was measured. The samples were first heated to 200 °C for 3 minutes, to erase previous thermal history, and then cooled to the designated crystallization temperature, at which spherulitic growth was followed by PLOM.

3.2.5 DSC experiments

The thermal behavior of the blends was studied by Differential Scanning Calorimetry (DSC) using a Perkin Elmer DSC Pyris 1 calorimeter, equipped with a refrigerated cooling system Intracooler 2P and calibrated with indium and tin. All measurements were performed under nitrogen atmosphere and using sample masses of approximately 5 mg. The analyses were conducted with different methods as a function of the experiment.

In non-isothermal analysis, the samples were first heated from 25 °C to 200 °C at 10 °C/min and held at 200 °C for 3 minutes, in order to erase their thermal history. Then they were cooled at 10 °C/min from 200°C to -20°C, while the corresponding cooling scan was registered. Finally, they were reheated at 10 °C/min from -20°C to 200 °C to register the subsequent second heating scan. The isothermal DSC experiments of the PLA phase from the glassy state, were performed closely following the procedure recommended by Lorenzo *et al.*[7] The samples were firstly heated from 25°C to 200°C at 20 °C/min and held at this temperature for 3 minutes, in order to erase thermal history.
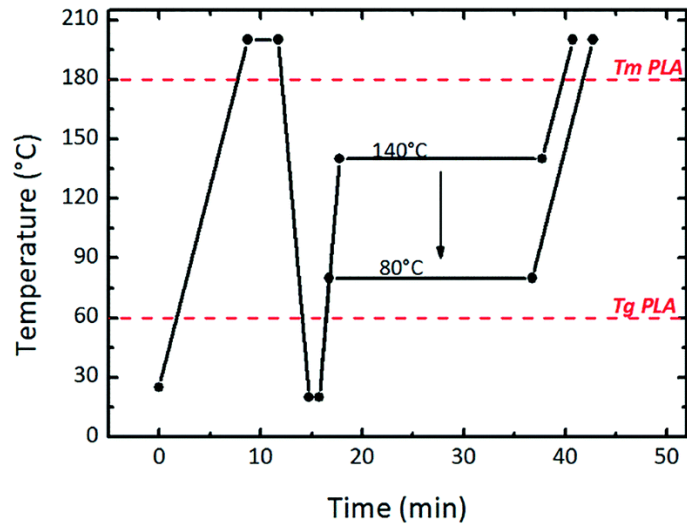
Figure 3.3: Thermal protocol used for isothermal crystallization experiments starting from the glassy state of PLA. The continuous line indicates the thermal scans while the dashed line corresponds to the thermal transitions of the PLA phases

Figure 3.4: Thermal program used for DSC annealing test. The continuous line indicates the thermal scans while the dashed line corresponds to the thermal transitions of the PLA and PCL phases. The grey frame indicates the crystallization temperature ranges of the PLA and PCL phases.
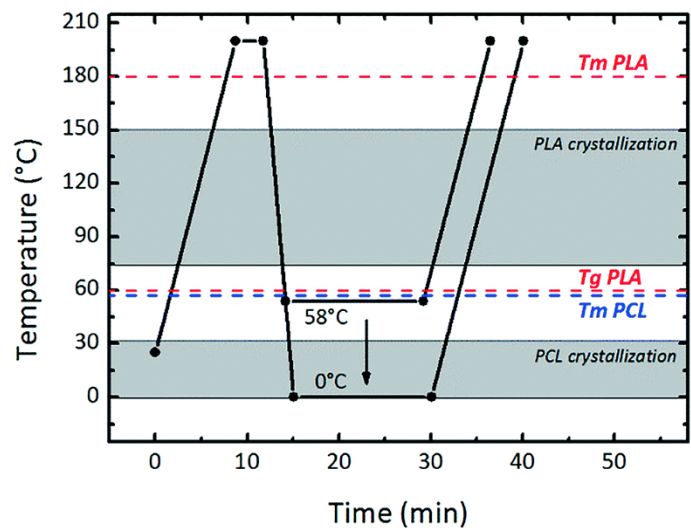
Then they were cooled at 60°C/min (in order to avoid PLA crystallization) from 200°C to 20°C (a temperature well below the Tg of PLA) and annealed at this temperature for 1

minute. From 20°C they were heated at 60°C/min to the chosen isothermal crystallization temperatures (Tc), in a range between 80°C and 140°C, and held at Tc until the crystallization saturated (i.e., at least 20 min) (Figure 3.3). The isothermal crystallization temperature range was determined by preliminary tests to ensure that no crystallization occurred during the cooling step or during the subsequent heating scan.

A special annealing experiment was subsequently designed. The samples were firstly heated from 25°C to 200°C and held at this temperature for 3 minutes in order to erase thermal history. Then they were cooled at 60°C/min (in order to avoid PLA crystallization during cooling) until specific annealing temperatures (T_a), between 58°C and 0°C, below the Tg of PLA, and held at these temperatures for 15 minutes. Following this procedure it is possible to study the effect of annealing below the Tg of PLA on the subsequent cold crystallization temperature of PLA (Tcc) by reheating the samples from T_a to 200°C (at 20°C/min) (see Figure 3.4).

3.3 RESULTS AND DISCUSSION

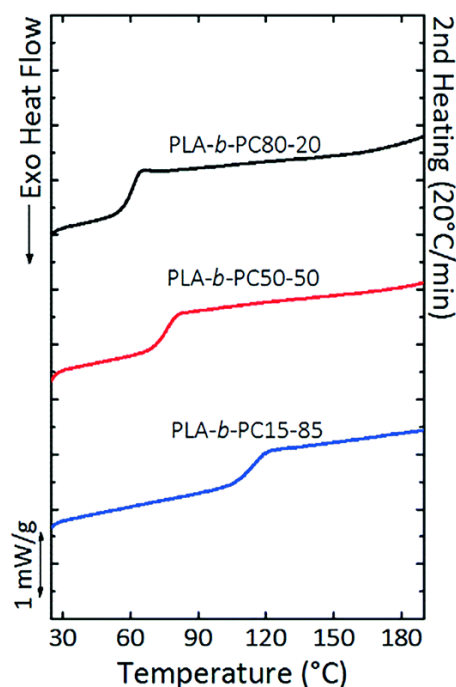### 3.3.1 Characterization of the block copolymer

Figure 3.5: DSC heating curves of PLA-*b*-PC copolymers at 20°C/min. The curves have been normalized by the weight of the samples.

Table 3.3 : Molecular characteristics of PLA-*b*-PC copolymers.

Sample	$T_g(°C)^{a)}$	$T_g*(°C)^{b)}$	$N^{c)}$	$\chi N^{d)}$
PLA-*b*-PC80-20	66	72	27	3.5
PLA-*b*-PC50-50	76	92	12	1.6
PLA-*b*-PC15-85	115	118	11	1.4

[a)]Determined by DSC, second heating curves [b)]Calculated by the Fox equation, using as T_g reference values: 60°C for the PLA block and 130°C for the PCL block. [c)]Calculated by M_n/M_o. Where M_n is the number average molecular weight of the entire copolymer and M_o the molecular weight of the repeating unit (taking into account the molar composition of the copolymer) [d)]The Flory–Huggins enthalpic segmental interaction parameter, $\chi = 0.13$, was calculated by Imre *et al.*[207] according to the group contribution theory of Hoftyzer and Van Krevelen

Figure 3.5 shows DSC heating scans of the synthesized PLA-*b*-PC copolymers, while Table 3.3 lists the corresponding glass transition temperatures (Tg) derived from them. The curves have been registered after erasing the thermal history and the subsequent cooling from the melt state to room temperature at 20°C/min.

The structure of the block copolymer microdomains in the melt state depends on their segregation strength given by χN[178,200] (where χ is the Flory–Huggins interaction parameter[130,149] between different blocks and N the overall polymerization degree of the entire block copolymer). When χN is lower than 10, a single-phase melt is usually formed.

According to Table 3.3, for all copolymers χN is lower than 5. As a result, a single Tg, indicating that the copolymers form a single phase was obtained for all copolymers. Furthermore, the Tg values vary with composition in agreement with the values predicted by the Fox equation.

It is therefore reasonable to assume that PLA-*b*-PC form a single phase material which could be dissolved in one or both PLA and PCL phases.

3.3.2 Compatibilization of the Blends

Figure 3.6 shows SEM micrographs of cryogenically fractured surfaces of PLA/PCL, PLA/PCL/PC and PLA/PCL/PLA-*b*-PCs blends. A *sea island* morphology, typical of immiscible blends, is observed in all cases, confirming previous results on PLA/PCL 80/20 blends.[148,149,154,155,184–187] PLA conforms the matrix while PCL is dispersed in droplets. The size of these droplets correlates with the degree of compabilization between PLA and PCL
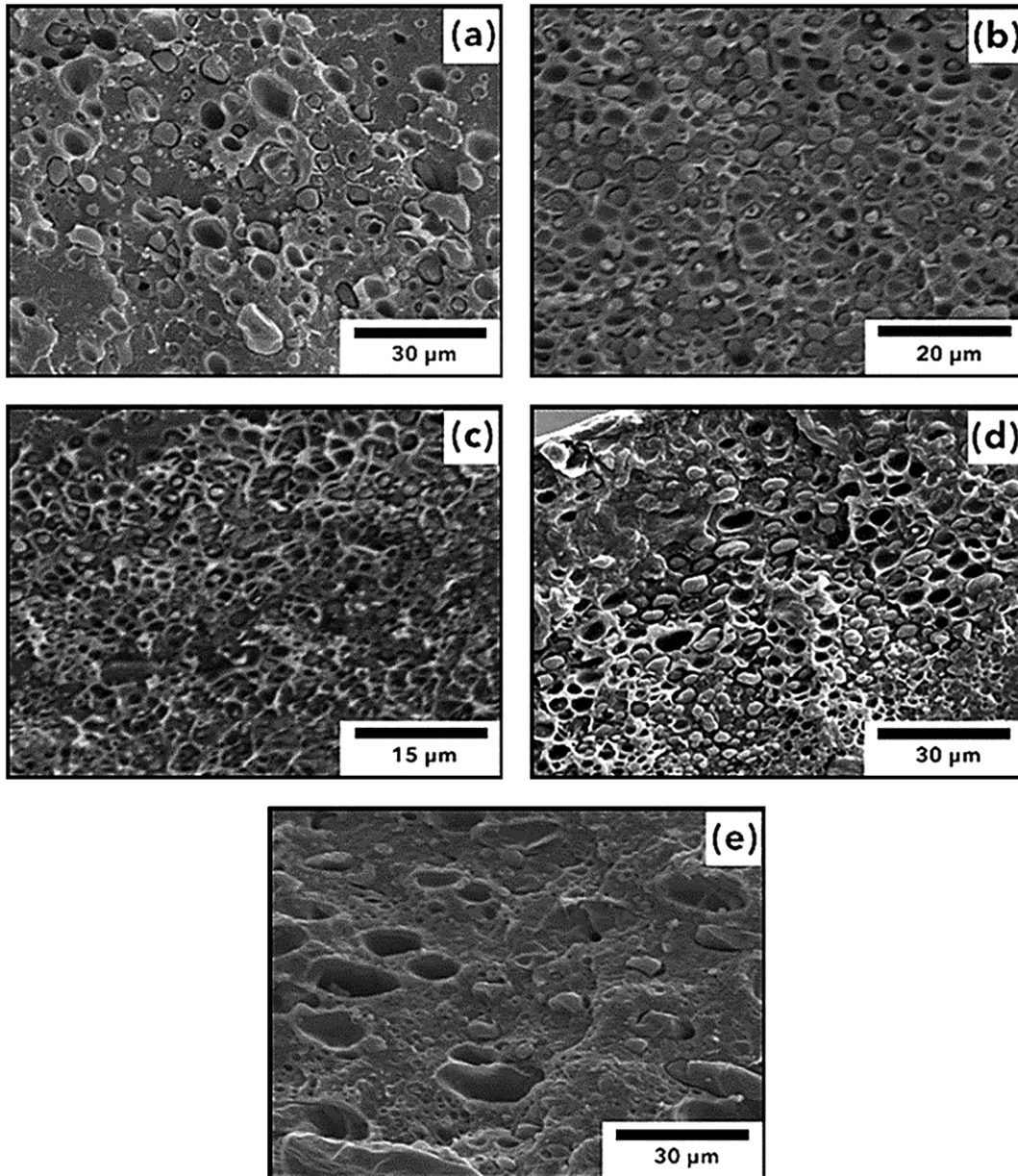
Figure 3.6 SEM micrographs of the cryogenically fractured surfaces of (a) PLA/PCL (b) PLA/PCL/PLA-*b*-PC80-20   (c)   PLA/PCL/PLA-*b*-PC50-50   (d)   PLA/PCL/PLA-*b*-PC15-85   (e) PLA/PCL/PC blends

phases.[201] The cavities observed on the micrographs are the result of interfacial debonding between PCL and PLA during cryogenic fracture, a sign of immiscibility between phases.

Table 3.4 reports average PCL particle size within the blends, measured by counting at least 100 particles. PCL particle size clearly decreases upon PLA-*b*-PC copolymers addition. In particular, upon addition of the PLA-*b*-PC50-50, the PCL particle size is reduced threefold in comparison with the blend without copolymers (i.e., for PLA/PCL d_n=2.48 µm,

Table 3.4. Number average (d_n) and volume average (d_v) particle diameters, particle size distributions (D) and standard deviation (SD) of the PCL phase in PLA/PCL and PLA/PCL/Compatibilizer, blends by solution mixing.

Sample	d_n (μm)	d_v (μm)	D_p	SD
PLA/PCL	2.48	4.34	1.75	0.64
PLA/PCL/PLA-*b*-PC80-20	1.72	2.12	1.23	0.22
PLA/PCL/PLA-*b*-PC50-50	0.79	0.91	1.15	0.01
PLA/PCL/PLA-*b*-PC15-85	2.23	2.94	1.32	0.34
PLA/PCL/PC	2.21	6.42	2.90	0.80

whereas for PLA/PCL/PLA-*b*-PC50-50 d_n= 0.79 μm). On the other hand, neat PC does not cause any significant reduction of the PCL particle size when it is added to the blend. The different size of the PCL particles within the blends has an effect on the temperatures and enthalpies of PCL crystallization.

Figure 3.7 shows DSC cooling scans at 10°C/min from the melt state for all the blends in comparison with neat PLA and neat PCL, while in Table 3.5 the characteristic temperatures and enthalpies derived from them are listed. Neat PCL crystallizes at 29°C, in one single sharp peak. While, if PCL is dispersed in a PLA matrix (within PLA/PCL blend, see Figure 3.6), PCL crystallization is fractionated into two peaks at 32°C and 22°C.

In immiscible blends, the fractionation of the crystallization peak of the minor phase is a common occurrence and mainly reflects its dispersion in droplets. It happens when the number of droplets is larger or of the same order of magnitude as the number of most active heterogeneities present in the bulk polymer before being dispersed. The smaller the droplets, the lower the probability to find active heterogeneities in each droplet.[138,166,183]

In PLA/PCL the first crystallization exotherm at 32°C corresponds to the crystallization of PCL droplets that have been nucleated by the same active heterogeneities present in the bulk polymer, since their crystallization occurs at the same temperature than bulk PCL. On the other hand, another PCL droplet population crystallizes at lower *Tc* values (22°C) probably nucleated by less active heterogeneities (for more on fractionated crystallization the reader is refer to the following references[138,166,183]). It is worth noting that the enthalpy of the exotherm at 32°C is clearly higher than the enthalpy of the exotherm at 21.7°C, indicating that a larger fraction of particles have a sufficient size to
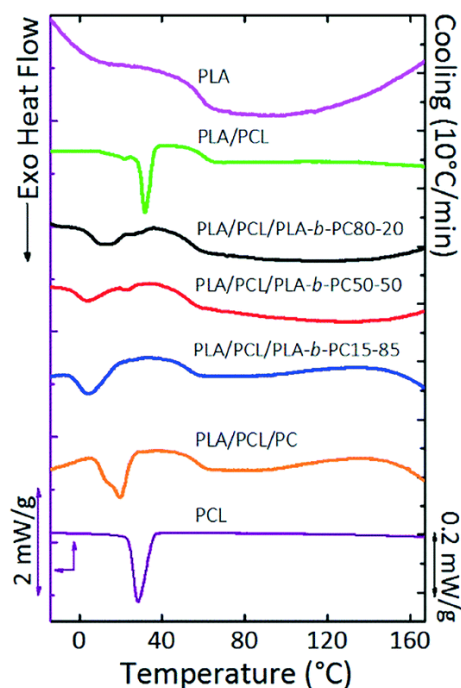
Figure 3.7: Non-isothermal DSC experiments. Cooling curves at 10°C/min from the melt state. The curves have been normalized by the weight of the samples.

contain at least one highly active heterogeneity able to activate the crystallization at the same temperature as in bulk PCL.

PLA/PCL/PLA-*b*-PCs blends also exhibit fractionated crystallization of PCL (Figure 3.7). However, in this case, PCL droplets are smaller than in neat PLA/PCL blends (Table 3.4), therefore, their number per unit volume is higher. As a result, the crystallization peaks are shifted to lower temperatures and the enthalpy of crystallization (see Table 3.5) of the lower temperature peak is larger than the higher one. This is due to the much

Table 3.5: Thermal properties obtained from non-isothermal DSC cooling at 10°C/min. The enthalpies of crystallization and melting have been normalized by the weight fraction of the samples.

Sample	Comp. (w/w)	PCL		PLA		
		T_c (°C)	ΔH_c (J/g)	T_g (°C)	T_c (°C)	ΔH_c (J/g)
PLA	100	-	-	59	-	-
PLA/PCL	80/20	21.7/31.8	2.6/45	58	-	-
PLA/PCL/PLA-*b*-PC80-20	80/20/2	11/26.9	28.7/4.8	52	-	-
PLA/PCL/PLA-*b*-PC50-50	80/20/2	4.6/23.1	23.5/3.9	48	119.2	3.1
PLA/PCL/PLA-*b*-PC15-85	80/20/2	5	35.4	51	93.1	1.8
PLA/PCL/PC	80/20/2	12/19.7	15.3/33.5	57	93.1	1.7
PCL	100	28.8	57.2	-	-	-

higher number of droplets available to distribute the same number density of heterogeneous nuclei originally present in bulk PCL.

Table 3.5 also lists the glass transition temperatures (Tg) of the PLA phase within the blends and neat PLA. The values were registered during cooling at 10°C/min, since during the subsequent heating (Figure 3.8) the glass transition overlaps with PCL melting.

The Tg of the PLA phase is depressed upon copolymer addition in the blends. According to Table 3.5, neat PLA exhibits a Tg of 59°C. Blending with PCL, the Tg of PLA phase remains constant within the error involved in the measurements (+/- 1°C) (i.e., Tg = 58°C in PLA/PCL). On the other hand, upon PLA-*b*-PCs addition to the blend, the Tg of the PLA phase is decreased to 52°C in PLA/PCL/PLA-*b*-PC80-20, to 51°C in PLA/PCL/PLA-*b*-PC15-85 and even to 48°C in PLA/PCL/PLA-*b*-PC50-50. It is worth noting that, the largest PLA phase Tg reduction is observed when PLA-*b*-PC50-50 was used. The same PLA-*b*-PC50-50 block copolymer causes the highest reduction of the PCL droplet size (Table 3.4).

Considering that all copolymers have a higher Tg than neat PLA (see Table 3.3), a *Tg* depression of the PLA phase can only be explained by a partial miscibility between PLA and PCL induced by the copolymer compatibilization effect. This partial miscibility maximizes the interaction between the phases and thus provokes a plasticization of PLA by
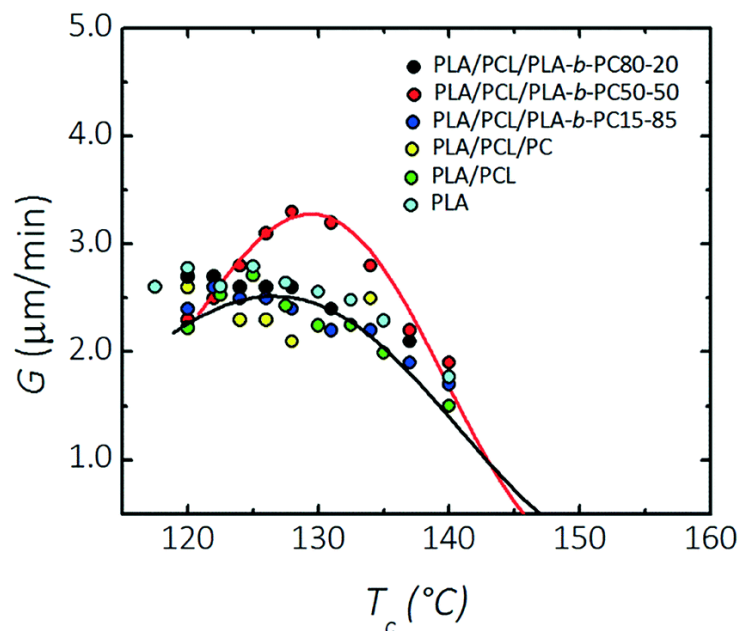

Figure 3.8: Spherulitic growth rate *G* as a function of isothermal crystallization temperature T_c for neat PLA and PLA phase within PLA/PCL and PLA/PCL/Compatibilizer blends. The solid lines represent arbitrary fits to guide the eye.

PCL chains (as PCL is a very flexible polymer, characterized by a Tg of approximately −60 °C).

Figure 3.8 shows spherulitic growth rate values (G) at different isothermal crystallization temperatures (Tc) fitted by an arbitrary function to guide the eye. A selection of
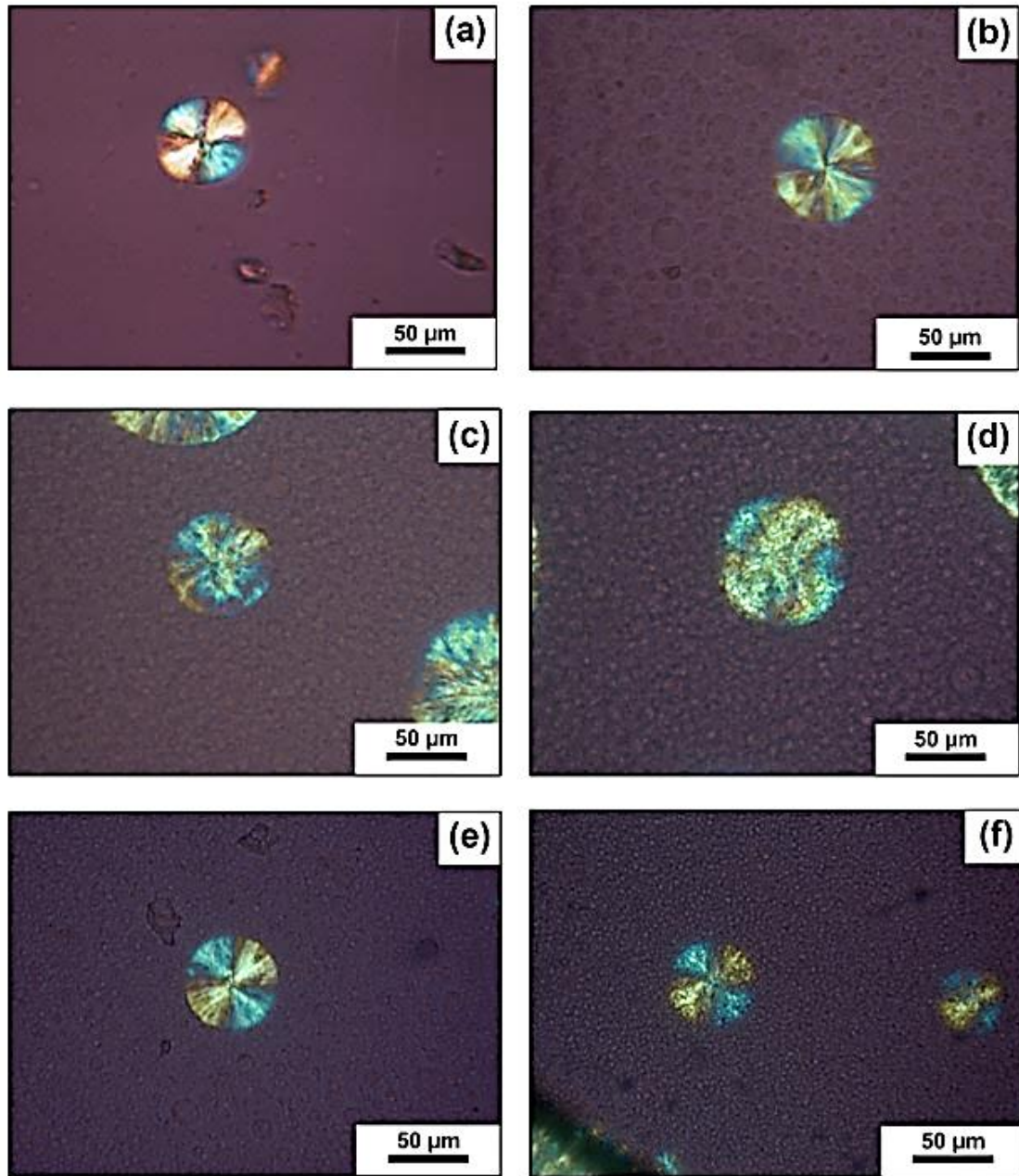

Figure 3.9: PLOM micrographs of (a) PLA (b) PLA/PCL (c) PLA/PCL/PLA-*b*-PC80-20 (d) PLA/PCL/PLA-*b*-PC50-50 (e) PLA/PCL/PLA-*b*-PC15-85 (f) PLA/PCL/PC recorded at 128°C and after 5 minutes from the begin of the crystallization from the melt state.

the most representative micrographs is reported in Figure 3.9. PLA spherulites show the typical Maltese cross morphology with a negative sign. In all the samples, PLA spherulites grow linearly with time, indicating that no diffusion problems at the growth front are induced by blending.[144] The spherulitic growth rate G (µm min^{-1}) was thus calculated from the slope of the line obtained from the spherulitic radius (µm) against time (min).

Figure 3.8 shows that all the samples approximately exhibit the well-known *bell-shaped* trend due to the dependence of the spherulites growth rate (G) with the crystallization temperature.[144] At temperatures lower than 120°C, it is not possible to collect any more data since the nucleation rate is too high and the spherulites immediately impinged with one another. Figure 3.8 also shows that G values for the PLA phase within neat PLA/PCL blends (without any compatibilizer) are close to those obtained for neat PLA within the experimental data scattering obtained. This result confirms the observed immiscibility of PLA with PCL. Otherwise, a change in spherulitic growth kinetics of PLA would be detected, as any amount of dissolved PCL chains within a PLA-rich phase would enhance molecular diffusion.[144]

On the other hand, when PLA-*b*-PC50-50 is added to the blend, the PLA spherulitic growth rate increases. At a temperature of 130°C, the G value in PLA/PCL/ PLA-*b*-PC50-50 is 3.25 µm min^{-1} while in neat PLA is 2.50 µm min^{-1}. It means that, in agreement with the results presented above (i.e., reduction in PCL particle size and PLA Tg depression when this PLA-*b*-PC50-50 block copolymer is added to the blend), PLA-*b*-PC50-50 is the best compatibilizer to increase the interaction between the phases, thereby promoting the plasticization of PLA by PCL chains. In the case of the other copolymers, the change in Tg of the PLA phase is not so pronounced and correspondingly, their effect on the spherulitic growth rate is not so significant (it is in fact within the error of the data plotted in Figure 3.8).

It is worth noting that for the PLA/PCL/PLA-*b*-PC50-50 blend, the increase of the spherulitic growth rate of the PLA phase is consistent with a small increase in the crystallization rate during cooling from the melt state detected by DSC non-isothermal experiments. In fact, neat PLA does not exhibit any crystallization during cooling from the melt, while upon PLA-*b*-PC50-50 addition to the blend, a small crystallization exotherm is detected (in Figure 3.7 the scale used does not allow a clear visualization of the PLA phase

broad crystallization exotherm, but it is clear using a different scale). The crystallization of the PLA phase within the blends will be analyzed in more detail below.

3.3.3 Cold crystallization of PLA and PLA phase within the blends, during non-isothermal and isothermal experiments

Figure 3.10 shows DSC heating scans at 10°C/min, subsequent to the cooling curves reported in Figure 3.7, for all samples, while in Table 3.6 the characteristic temperatures and enthalpies derived from these curves are listed.

Figure 3.7 shows that in the samples containing PCL, an overlap occurs between the Tg of the PLA component and the melting peak of the PCL phase. Neat PLA does not crystallize during cooling from the melt state, since the amount of D-LA isomer (PLA 4032D present 1.2-1.6 % of D-LA isomer) inhibits the crystallization at the scanning rate employed (10°C/min).[73] On the other hand, in the subsequent heating scan (Figure 3.10), neat PLA undergoes cold crystallization followed by fusion of the produced crystals. It is worth noting that the heat of fusion of formed PLA crystals is equal (within the error
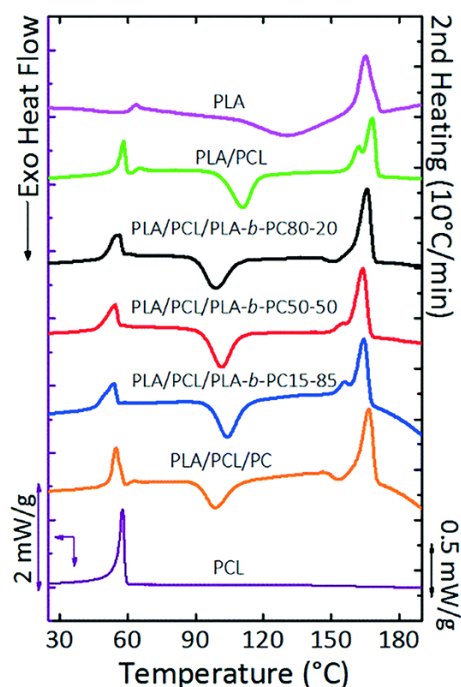

Figure 3.10: Non-isothermal DSC experiments. Second heating curves of neat PLA, neat PCL, PLA/PCL blends, and PLA/PCL/Compatibilizer blends at 10°C/min. The curves have been normalized by the weight of the samples.

involved in the measurements) to the heat that is released during cold crystallization (Table 3.6), confirming that all PLA crystallization occurs during heating.

This result reflects a common occurrence in PLA based materials. [96,202–205] If PLA is cooled below Tg from the melt state at a cooling rate fast enough to prevent crystallization during cooling (as it happens in Figure 3.7), nucleation occurs during fast cooling specially during vitrification. De Santis *et al.*[96] examining the kinetics of crystallization of PLA in both isothermal and non-isothermal conditions, found that, at equal molecular weights and D-isomer amounts, the crystallization kinetics of PLA is always faster starting from the glassy state than from the melt state.

The PLA phase within all blends also undergoes cold crystallization (Figure 3.10) during heating from the glassy state. However, in this case, the cold crystallization exotherms are sharper and shifted to lower temperatures (as compared the values of Tcc for neat PLA), indicating a nucleating effect promoted PCL addition. According to Figure 3.10, while for neat PLA a broad exotherm around 130°C is detected, for PLA/PCL the

Table 3.6: Thermal properties obtained from non-isothermal DSC heating at 10°C/min. The enthalpies of crystallization and melting have been normalized by the weight fraction of the samples.

Sample	Comp. (w/w)	PCL		PLA			
		T_m (°C)	ΔH_m (J/g)	T_{cc} (°C)	ΔH_{cc} (J/g)	T_m (°C)	ΔH_m (J/g)
PLA	100	-	-	129.1	31.8	165.6	33.3
PLA/PCL	80/20	58.2	49	110.8	30.9	162.4/167.8	15.6/16.6
PLA/PCL/PLA-*b*-PC80-20	80/20/2	56	39.1	98.9	32.5	165.9	35.9
PLA/PCL/PLA-*b*-PC50-50	80/20/2	54.4	38.7	101.5	30.9	155/164	4.4/30.8
PLA/PCL/PLA-*b*-PC15-85	80/20/2	53.9	47.8	103.9	29.2	156/164	6.1/26.9
PLA/PCL/PC	80/20/2	54.7	47.3	98.7	34	166.7	36.1
PCL	100	57.8	63.2	-	-	-	-

exotherm appears sharper and its position is shifted down to 110°C. Interestingly, upon PLA-*b*-PCs or PC addition within the blends, the cold crystallization of PLA is shifted to even lower temperatures. Indeed Table 3.6 shows that Tcc of PLA phase within PLA/PCL/PLA-*b*-PCs and PLA/PCL/PC blends is further reduced to values around 100°C.

The results agree with previous works where PLA cold crystallization is favored by PCL addition.[46–51] Several authors have attributed the enhancement of the cold crystallization to an increased PLA chain mobility, as a result of partial miscibility with PCL.[46–48]

However, in the present work, neat PLA/PCL blends were found to be immiscible. Nevertheless, Table 3.6 shows that the Tcc of the PLA component is decreased in neat PLA/PCL blends, even though, no changes in Tg value or spherulitic growth rate were detected as compared to neat PLA. Therefore, the decrease in Tcc of PLA upon blending with PCL can only result from a nucleation effect of PCL on PLA during its crystallization upon heating from the glassy state.

In an effort to find a clear mechanism that can correlate PCL addition with the enhancement of PLA cold crystallization, the overall isothermal crystallization of the PLA component was studied. The samples were first rapidly cooled to the glassy state (i.e., 20°C) at 60°C/min to prevent the crystallization of the PLA or PLA component in the blends, and then rapidly heated (at 60°C/min) to the isothermal crystallization temperature of choice, making sure that the material did not crystallize neither during cooling nor during heating to Tc.

Figure 3.11 shows the inverse of half-crystallization time as a function of crystallization temperature for neat PLA and for the blends. The inverse of half-crystallization time at a given temperature is proportional to the overall crystallization rate. The data points follow the classical trend of a *bell shape* curve, which originates from the competition between secondary nucleation (that is dominant in the right hand side of the curve) and molecular diffusion (which predominates in the left hand side of the curve as the temperature approaches Tg).

According to Figure 3.11, neat PLA completes its transformation to the semi-crystalline state (i.e., achieves its maximum relative crystallinity) in 8 minutes at Tc = 120°C, i.e., at the Tc value that corresponds to the maximum crystallization rate. Taking PLA as reference material, an acceleration of the overall crystallization rate of the PLA component is evident in its blends with PCL. Within the 80/20 PLA/PCL blend, the PLA phase completes its crystallization at Tc = 120°C in 1.5 minutes.

A further increase in the crystallization rate of the PLA phase upon PC or PLA-*b*-PC80-20 additions to the blend is detected. In PLA/PCL/PLA-*b*-PC80-20, PLA phase crystallizes at 116°C ten times faster than neat PLA, while in PLA/PCL/PC at 120°C the crystallization rate of the PLA phase is even fifteen times higher than neat PLA. On the other hand, the addition of PLA-*b*-PC15-85 gives rise to a reduction of the crystallization rate in comparison with the values obtained for the blends with the same amount of PCL.

The data obtained by isothermal DSC measurements were fitted to the Avrami equation using the Origin® plug in, developed by Lorenzo *et al.*[7] The procedure employed and examples of the results are reported in the previous chapter. The data obtained shows that most of the Avrami indexes are close to 3 for neat PLA, a value that correspond to the instantaneous nucleation of spherulites. On the other hand, the *n* value for the crystallization of PLA in the blends is always close to 2, a value characteristic of 2D lamellar aggregates that nucleate instantaneously in the case of polymers. The reason of this behavior is connected to the high nucleation rate that avoids the evolution of 3D superstructures (i.e., spherulites), as they quickly impinged on one another when they grow. A
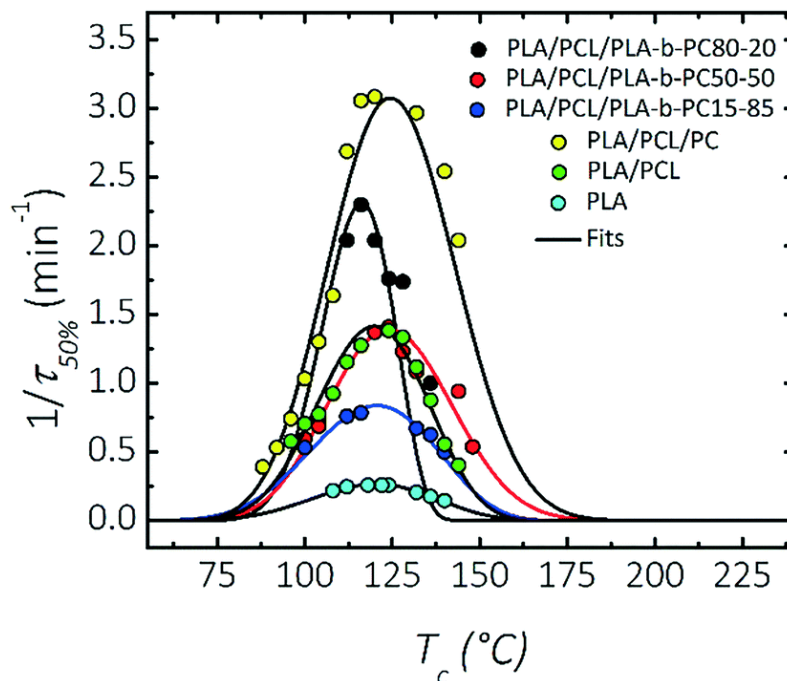

Figure 3.11: Isothermal crystallization experiments performed after heating the samples from the glassy state to T_c. Overall crystallization rate ($1/t_{50\%}$) as a function of isothermal crystallization temperature T_c in neat PLA and PLA phase within PLA/PCL and PLA/PCL/Compatibilizer blends. The solid lines represent arbitrary fits to guide the eye.

very high nucleation rate is expected for these samples, as they were first quenched to the glassy state and then reheated to the T_c value at which the crystallization rate was measured.[206]

When the materials are cooled from the melt, spherulites can develop their 3D superstructures, and the spherulitic growth rates can be determined (see Figure 3.11). However, after the crystallization from the glassy state, the texture observed in the optical microscope is that of very small birefringent superstructures, whose growth cannot be measured.

It is worth noting that an increase in the nucleation rate of PLA upon blending with PCL can explain the results obtained in the case of the neat blends. As already presented above, for the PLA component spherulitic growth rate is not affected by PCL addition (see Figure 3.11 and its discussion), therefore, the aforementioned increase in overall crystallization rate shown in Figure 3.11 (which includes nucleation and growth) must be due to an increase in PLA nucleation rate.

In an effort to investigate the manner by which the nucleation of PLA within the blends is enhanced, further analysis were performed. In particular, considering that the blend containing PC (i.e.=PLA/PCL/PC) is the one that presents the highest PLA overall crystallization rate, the effect of PC on PLA cold crystallization in neat PLA/PC blends was examined. At the same time, considering that PLA crystallization is tunable upon copolymer addition, but it is weakly dependent on the miscibility between PLA and PCL (as G does not significantly change, except for the blend that contains the 50/50 PC-*b*-PCL copolymer), the ability of PLA phase within the blends to form active nuclei below Tg, and thus promote the subsequent cold crystallization, was examined by annealing tests.

3.3.4 Effect of PC on the cold crystallization rate of PLA

Figure 3.11 clearly shows an enhancement effect on the cold crystallization rate of the PLA phase within PLA/PCL/PC, if compared with the cold crystallization rate of the PLA phase within all others blends characterized by the same amount of PCL (i.e., 20% wt).
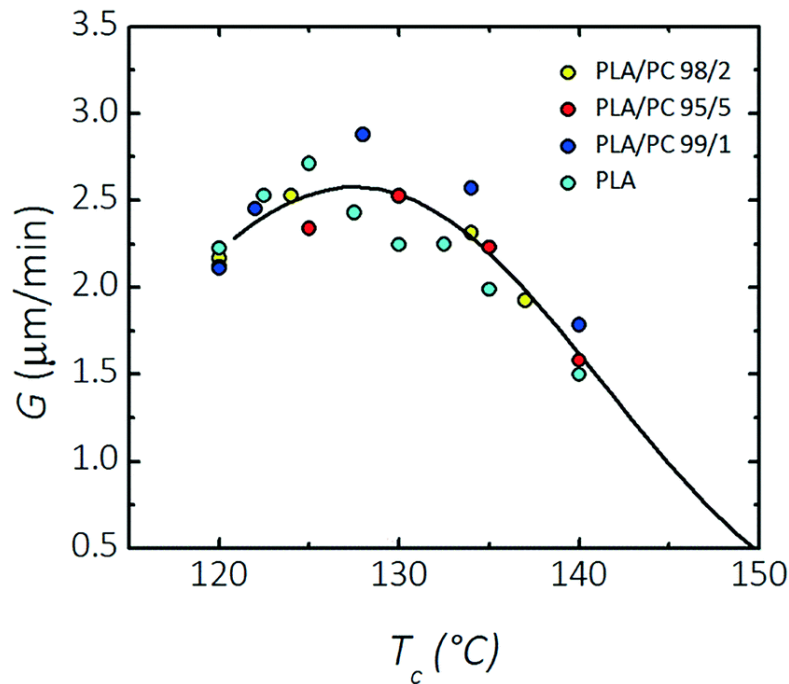
Figure 3.12: Spherulitic growth rate G as a function of isothermal crystallization temperature T_c for neat PLA and PLA phase within PLA/PC blends. The solid lines represent arbitrary fits to guide the eye

As indicated in Table 3.4, PCL droplet size is not reduced upon PC addition, this means that PC does not migrate to the PLA-PCL interface, but is probably dispersed in one or both phases. It is therefore plausible that the acceleration of PLA overall crystallization kinetics directly derives from an increase in PLA nucleation rate induced by PC. As PC remains amorphous in these blends, its nucleation effect could be due to a migration of heterogeneities during the blending process, that are capable of nucleating PLA.[182] In an effort to confirm our hypothesis, the spherulitic growth rate and the overall crystallization rate of neat PLA and the PLA phase within neat PLA/PC blends (increasing the amount of PC from 1 to 5%) were measured.

Figure 3.12 shows spherulitic growth rate values (G) at different isothermal crystallization temperatures (Tc) from the melt, fitted by an arbitrary function to guide the eye. In all samples, PLA spherulites grow linearly with time, indicating that no diffusion problems at the growth front are induced by blending.[144] At temperatures lower than 120°C, it is not possible to collect any data since the nucleation rate is too high.
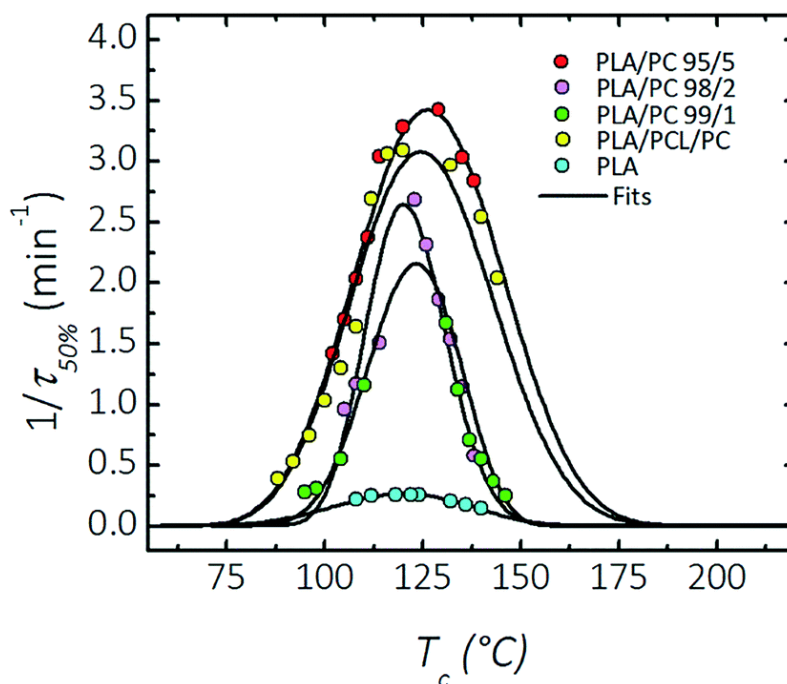

Figure 3.13: Isothermal crystallization experiments performed after the samples were heated from the glassy state to T_c. Overall crystallization rate ($1/t_{50\%}$) as a function of isothermal crystallization temperature T_c in neat PLA and PLA phase within PLA/PCs blends. The solid lines represent arbitrary fits to guide the eye.

Figure 3.12 shows that G values for the PLA phase within PLA/PC blends are close to those obtained for neat PLA. This result confirms the reported immiscibility of PLA with PC.[207] Otherwise, a change in spherulitic growth kinetics of PLA would be detected, as any amount of dissolved PC chains within a PLA-rich phase would reduce molecular diffusion (as PC is a rigid polymer characterized by a Tg of approximately 140°C). [144]

Figure 3.13 shows the overall crystallization rate (expressed as the inverse of half-crystallization time) as a function of temperature for neat PLA and PLA/PC blends. The solid lines correspond to arbitrary fits. The DSC isothermal crystallization experiments

were conducted after heating the samples from the glassy state, employing the same protocol used for performing the isothermal crystallization experiments whose results are reported in Figure 3.10.

Taking neat PLA as a reference material, an acceleration of its crystallization rate is clearly evident when it is blended with PC. Considering that PLA spherulitic growth is not affected by PC addition (see Figure 3.12 and its discussion), the increase in overall crystallization rate must be due to a nucleation effect caused by PC. Furthermore, the crystallization rate of the PLA phase increases with the amount of PC in the blend. In the case of the PLA/PC 99/1 blend, the PLA phase completes its crystallization at Tc = 125°C (i.e., the Tc value for which the crystallization rate is maximal) in 1 min. For PLA/PC 98/2, the PLA phase completes its crystallization at the same temperature in 0.75 m, while in the PLA/PC 95/5, the PLA component crystallizes in half a minute

If the values obtained for PLA/PC blends are compared with the ones obtained PLA/PCL/PC (see overlapped in Figure 2.13) it is clearly evident that the enhancement effect on crystallization rate of PLA within PLA/PCL/PC is mainly due to the presence of PC, confirming our hypothesis.

3.3.5 Annealing DSC experiments

The DSC results presented above clearly demonstrate that PLA cold crystallization, under non-isothermal and isothermal conditions (see Figure 3.8 and Figure 3.10, and their discussion), is accelerated in the blends with PCL. At the same time, Figure 3.7 demonstrated that the acceleration of PLA cold crystallization is due to an increase in the nucleation rate of PLA. Otherwise, a change in spherulitic growth kinetics of the PLA component in the blends would have been detected.

Several authors have reported that the enhancement of PLA cold crystallization in PLA/PCL blends could be attributed to increased PLA chain mobility induced by partial miscibility with PCL.[46–48] As previously discussed, in our case, the experimental evidences obtained by DSC and PLOM indicate that the neat PLA/PCL blends prepared here are totally immiscible. In spite of that, the PLA phase cold crystallization is accelerated.

In order to elucidate the mechanism that promotes the nucleation of the PLA phase upon PCL addition, annealing experiments were designed and implemented to study PLA nucleation in the blends.

Zhang *et al.*[205] investigated the structural evolution and kinetics of melt-quenched PLA during physical aging below Tg, finding that a local ordered structure develops during the aging time in glassy PLA. During the heating process at an appropriate rate, this local ordered structure phase transform into a stable crystal form. Lan *et al*,[208] using spectroscopic and microscopic techniques, found that the crystallization of PLA underwent a multistep process, in which the crystal formation was preceded by the formation of various metastable intermediate phases, including mesomorphic phase, preordering, and even metastable crystal in the glassy state. When grown in contact with an intermediate preordering and mesomorphic phase, the metastable crystal underwent gradually slow reorganization and densification to form crystals during subsequent heating.

Regardless of the type of precursor structures that may be formed by PLA during annealing below Tg, it is a well-known experimental fact that cooling the polymer until vitrification or annealing it below Tg promotes nucleation. This fact is reflected in the observation of cold-crystallization during heating from the glassy state, while no crystallization can be observed during cooling from the melt state.[96,202–205]

PCL crystallizes in a range of temperature below the Tg of PLA (the crystallization of PCL happens in a temperature range in between 30°C and 0°C). Therefore, it is proposed that the crystallization of PCL droplets could have a role in the nucleation of the adjacent glassy PLA matrix.

In order to confirm our hypothesis, an annealing test was performed (see Figure 3.4), as it mainly reflects the ability of the PLA phase to form nuclei during aging below Tg. The samples were quenched from the melt at 60°C/min (so that the PLA phase cannot crystallize during cooling and remains amorphous) until specific annealing temperatures (T_a), below the Tg of PLA, and kept at this temperature for 15 minutes. Reheating the samples from T_a to 200°C at 20°C/min, it is possible to correlate the effect of aging at different annealing temperatures with the cold crystallization temperatures of PLA, Tcc (Figure 3.11). At the same, by using the melting area of PCL during the heating scan after

annealing, it is possible to calculate the degree of crystallinity of PCL (X_{PCL}) as a function of the annealing temperature (T_a)

The following formula was used:

$$X_C(\%) = \frac{\Delta H_m}{(\Delta H_m^\circ w_f)}$$ Eq. (3.1)

where ΔH_m corresponds to the measured fusion enthalpies of PCL and ΔH_m° is the melting enthalpy of 100% crystalline PCL (136 J/g according to the literature[209]) and w_f is the weight fraction of PCL in the sample.

Figure 3.14 shows T_{cc} of neat PLA and PLA phase within the blends as a function of the annealing temperature (T_a), while Figure 3.15 shows the degree of crystallinity of PCL (X_{PCL}) as a function of the annealing temperature (T_a).

The Tcc of neat PLA (see Figure 3.14) does not change upon reducing T_a, keeping a constant value around 135°C, since an aging time of 15 minutes below Tg is not enough to develop nuclei at the annealing temperatures employed. Androsch and Di Lorenzo[202]
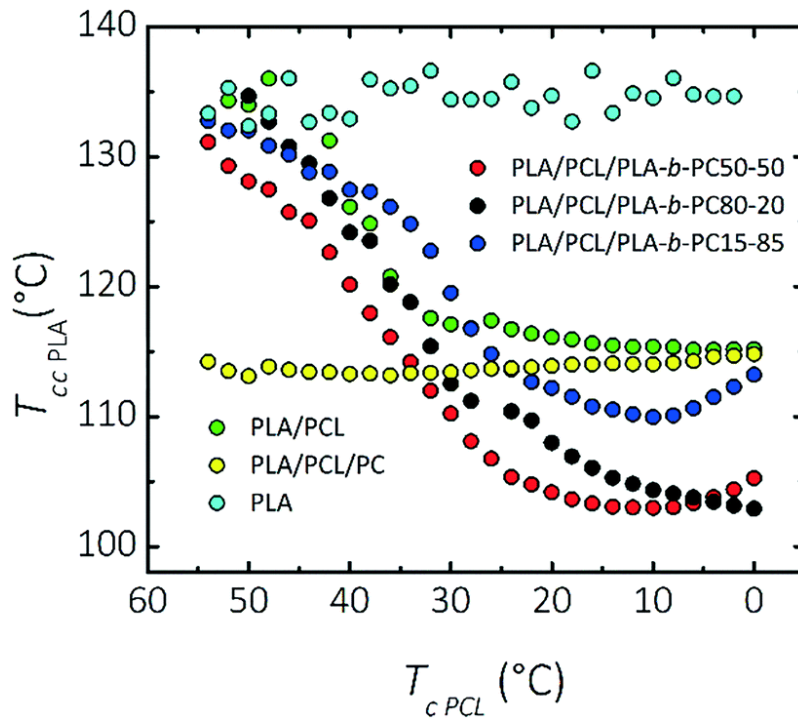

Figure 3.14: Annealing experiment. Temperature of cold crystallization (T_{cc}) of PLA and PLA phase within the blends as a function of the annealing temperature (T_a).

examined the kinetics of formation of nuclei in fully amorphous PLA samples aged below Tg for different periods of time and at different annealing temperatures. Their data are consistent with our results, since they found that aging at temperatures lower than 55°C, for periods of time less than about 100 min, cannot produce additional nuclei. The work by Androsh and Di Lorenzo clearly demonstrated that nucleation of PLA below Tg is possible even though chain mobility is restricted to local range. Only nucleation can occur during annealing below Tg, as the crystallization of PLA is obtained at temperatures substantially higher than Tg (i.e., after subsequent heating from the glassy state to Tc).

The cold crystallization of the PLA phase within PLA/PCL/PC blend does not change with T_a, and it is approximately constant at 114°C (Figure 3.14). In this case, the nuclei generated by the presence of PC droplets are more effective in promoting the PLA crystallization than those induced by PCL presence, as demonstrated above by the isothermal crystallization analysis on PLA/PC blends.

On the other hand, when PLA is blended with PCL, a clear reduction of its Tcc value is detected upon decreasing T_a (see Figure 3.14). A remarkable correspondence of this effect with an increase in crystallinity of PCL dispersed droplets can be observed in Figure
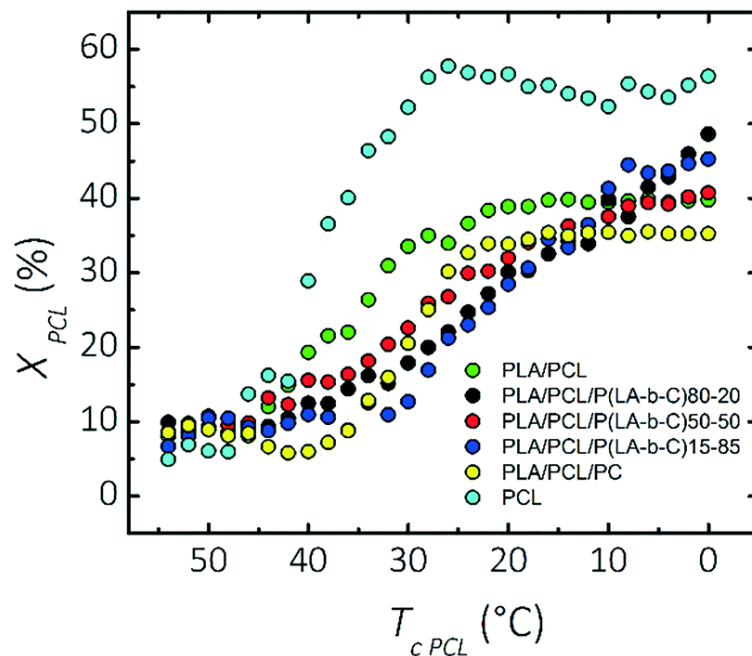

Figure 3.15: Annealing experiment. Degree of crystallinity of PCL (X_{PCL}) within the blends as a function of the annealing temperature (T_a).

3.13. This correlation clearly indicates that the acceleration of PLA cold crystallization, in neat 80/20 PLA/PCL blends, is due to a nucleation effect caused by PCL crystallization, at temperatures below the glass transition of PLA (i.e., glassy PLA).

It should be noted that PCL crystallization occurs only after the PLA matrix has vitrified. Nevertheless, PCL droplets crystallization can induce in the glassy PLA matrix that surround them, heterogeneous nuclei formation, in a similar process to the formation of nuclei that has been described during aging neat PLA below Tg [202,205,208]. The difference is that PCL crystals can induce nucleation of the glassy PLA matrix, in much shorter times as compared to the times involved for nucleation of neat glassy PLA[57]. It is noteworthy, that such nuclei (formed at temperatures below Tg) only generate crystals upon subsequent heating of PLA, during its cold crystallization, a process that takes place at temperatures that are above the melting temperature of the PCL droplets.

Figure 3.15 also shows that from 54°C to 30°C, the PCL component cannot complete its crystallization in the 15 minutes annealing time at T_a (i.e., the crystallinity degree is still increasing in Figure 3.15) and therefore the Tcc value of the PLA matrix shows a decreasing behaviour in this temperature range, for all blends (Figure 3.14). On the other hand, at T_a temperatures below 25°C, PCL has finished its crystallization during the allotted 15 min at T_a (Figure 3.15) and therefore the Tcc values of PLA phases within the blends are approximately constant (Figure 3.14).

Compatibilizer addition has an interesting effect in the data presented in Figure 3.14. The curves of Tcc versus T_a for the three samples that contain 2% of PLA-b-PC shift horizontally depending on the copolymer composition. The curves shift from left to right in the following order: PLA/PCL/PLA-b-PC50-50, PLA/PCL/PLA-b-PC80-20, PLA/PCL/PLA-b-PC15-85. If a constant T_a temperature is considered, Tcc values increase as the curves shift to the right, or in other words, the nucleation effect on cold-crystallization decreases. The nucleation order in the compatibilized blends correlates well with the reduction in PCL droplet sizes (see Table 3.4), which means that as the surface area of crystallized PCL increases (as particle drop decreases) the higher is the ability of PCL crystals to induce the formation of nuclei in the glassy PLA phase close to or at the interphase between PLA and PCL.

The blend without compatibilizers exhibits a less clear trend in the range of T_a temperatures between 50 and 30°C in comparison with those containing compatibilizers. In fact, it behaves somewhat similar to the blend compatibilized with the 80-20 PLA-b-PC copolymer. Table 3.4 shows that this sample exhibits the largest particle size, but also a larger size dispersity, as compared to the compatibilized blends. This may be the reason of its peculiar behaviour.

In the case of Figure 3.15, the error that characterizes crystallinity measurements by DSC (typically 10 to 15% when errors of integration, baseline drift and calibration are added up) prevent a detailed analysis of observed trends.

From the results of the annealing experiments analysed above, we can conclude that PCL droplets crystallization within the vitrified PLA matrix is responsible for inducing nuclei formation within glassy PLA.

3.4 CONCLUSIONS

Poly(L-lactide-block-carbonate) diblock copolymers are effective in improving the miscibility between PLA and PCL depending on their composition. The symmetric diblock copolymer prepared here (i.e., P(LA-b-C)50-50) causes a threefold reduction of PCL particle size in the 80/20 PLA/PCL blend and a Tg depression of 10°C for the PLA phase, as compared to neat blend.

The acceleration of the cold crystallization kinetics of PLA upon blending with PCL, often reported in the literature, is not connected with the miscibility between PLA and PCL phases, as it is also present in the neat PLA/PCL blend.

The results of a specially designed annealing treatment below the Tg of PLA have clearly demonstrated that the acceleration of the cold crystallization of PLA is due to a nucleation effect induced by PCL crystals on glassy PLA. Such nuclei only become effective upon heating to PLA cold crystallization temperatures, at which PCL is already molten.

4 CRYSTALLIZATION BEHAVIOUR OF POLY(LACTIDE) IN IMMISCIBLE BLEND WITH POLY(E-CAPROLACTONE), COMPARISON WITH SOLUTION AND MELT-MIXED BLENDS

4.1 INTRODUCTION

Poly(lactide) is one of the most promising substitutes for petroleum based polymers, since it is at the same time bio-based, biocompatible and biodegradable. However, it has some drawbacks, such as a slow crystallization rate and low toughness, that are limiting its applications and commercial expansion.[1,2]

One possible solution to improve PLA properties is the blending with another polymer counterpart. In this context, poly(ε-caprolactone) (PCL) is one of the best candidates, since it is flexible, biodegradable and biocompatible and therefore able to induce a toughening of PLA without limiting the original applications.

At the same time, the blending with PCL can be useful in enhancing the PLA crystallization rate, but the prediction of this effect is not a trivial issue. PLA/PCL is an immiscible blend, and thus a multiphase system, and the crystallization rate of each component is strictly related to phase morphology, processing conditions, molecular characteristics and interfacial properties of the blend.

In previous works, we already demonstrated the effect of PCL on the crystallization behaviour of PLA phase within 80/20 PLA/PCL blend during both melt[3] and cold crystallization.[4] If PLA crystallization starts from the molten state, PCL has no effect on both nucleation and growth of the PLA crystal. On the other hand, If PLA crystallization starts from the glassy state, PCL can induce the formation of active nuclei in PLA during aging below Tg.

In this part of the work, the crystallization behaviour of PLA phase within 80/20 PLA/PCL immiscible blends has been correlated with both the PLA-PCL phases compatibility as well as the preparation method of the blend.

Two different poly(ε-caprolactone)-poly(carbonate) based copolymers, varying in the length of the sequential block units, have been used for the first time to tune the

compatibility between PLA and PCL. At the same, in order to study the effect of the blend preparation, blending has been carried out by both melt and solvent mixing.

4.2 EXPERIMENTAL

4.2.1 Materials and methods

Poly(L-lactide) PLA (Ingeo index: 4032D, 1.2-1.6 % of D-LA isomer, Mw= 200 KDa) was purchased from NatureWorks™ and was dried overnight under vacuum at 60°C before processing to avoid degradation reactions induced by moisture. Poly(ε-caprolactone) PCL (CAPA 6800 Mw= 80 KDa) was purchased from Solvay™ and was used as received. Poly(carbonate) (PC, TARFLON® IV1900R) was purchased from Idemitsu Chemicals Europe and was used as received. ε-Caprolactone (Sigma-Aldrich-CAS Number: 502-44-3) and tin octanoate (Sigma Aldrich-CAS Number: 301-10-0) were used as received.

Two different random copolymers of BPA-Carbonate and ε-Caprolactone were used (Table 4.1) Both copolymers were synthetized by ring opening polymerization using tin (II) octanoate as catalyst and toluene as solvent. The detailed synthesis will be described in the next paragraph.

Table 4. 1: Molecular characteristics of copolymers. Composition (PCL content w/w%), PC and PCL units length, average molecular weights (Mw), polydispersity (D) and glass transition temperatures (T_g).

Sample	Comp. PCL[a] (w/w%)	PC length[b]	PCL length[b]	Mw (Da)[c]	D[d]	Tg (°C)[e]
PCL-*b*-PC	49	3	35	18500	1.4	-36
PCL-*ran*-PC	61	1	10	14600	2.3	-32

[a] Composition weight ratio between PCL and PC components determined by ^{1}H-NMR. [b] Length of PC and PCL unit determined by ^{1}H-NMR. [c] Determined by GPC. [d] Determined as Mw/Mn [e] Determined by DSC, heating curves at 10°C/min.

4.2.2 Synthesis of PCL-PC based copolymers

In a three-neck flask 10 g of poly(carbonate) were weighted and, under nitrogen atmosphere, 20 mL of ε-caprolactone were added. The mixture was stirred under nitrogen flux until complete dissolution of poly(carbonate). Maintaining inert atmosphere, 3 mL of Sn(Oct)$_2$ (5 mol catalyst /mol monomer %) and 35 mL of toluene

were added. The reaction mixture was immersed in an oil bath at 120°C for 2 hours under stirring to allow the polymerization.

The raw products were dissolved in 50 mL of dichloromethane and then poured into 400 mL of methanol. The precipitate collected by filtration was purified by a reprecipitation with dichloromethane and methanol and finally dried through a vacuum pump.
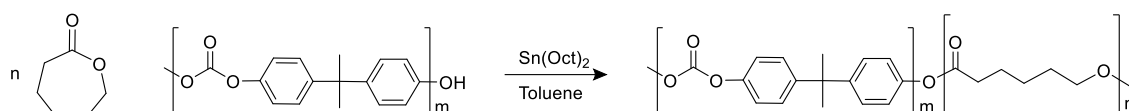

Figure 4. 1: Schematic representation of copolymers synthesis, from ε-caprolactone and polycarbonate olygomers

4.2.3 Blends preparation

A constant PLA/PCL weight ratio of 80/20 was employed. Block and random copolymers were used as compatibilizers by adding 10% with respect to the PCL phase. The composition of the final blends is approximately 80/20/2 PLA/PCL/PCL-*co*-PC. Table 4.2 reports the composition of the prepared blends.

Table 4.2: Composition of the prepared blends.

Sample	PLA	PCL	PCL-*b*-PC	PCL-*ran*-PC
PLA (m)	100	-	-	-
PLA (s)	100	-	-	-
PCL (m)	-	100	-	-
PCL (s)	-	100	-	-
PLA/PCL (m)	80	20	-	-
PLA/PCL (s)	80	20	-	-
PLA/PCL/PCL-*b*-PC (m)	79	19	2	-
PLA/PCL/PCL-*b*-PC (s)	79	19	2	-
PLA/PCL/PCL-*ran*-PC (m)	79	19	-	2
PLA/PCL/PCL-*ran*-PC (s)	79	19	-	2

The blends were prepared by both solution and melt mixing. The ones prepared by solution mixing have been designated with (s) while the corresponding ones prepared by melt blending have been designated with (m).

In the first case, PLA, PCL and PCL-*co*-PC based copolymers were dissolved in dichloromethane at the concentration of 1 g/dL and stirred at room temperature for 3

hours. The solutions were casted in Petri dishes (diameter = 5 cm) obtaining films that were dried for 24 hours at room temperature and for another 24 hours at 60°C under vacuum in order to remove any solvent residue.

In the second case, neat homopolymers and the PCL-*co*-PC based copolymers were melted and blended in a Collin twin-screw extruder (Teachline, L/D ratio 18, screw diameter 25 mm). Melt blending was obtained at a screw speed of 200 rpm, a temperature of 200°C with a residence time of approximately 1 minute. The extruded filaments were quenched in a water bath and pelletized. The pellets were dried overnight at 60 °C under vacuum and were compression moulded in a Collin P-200-E compression moulding machine at 200°C (3 minutes without pressure followed by 3 minutes at 100 bar). Tensile testing specimens (ASTM D 638 type IV, average thickness 1.84 mm) of the blends were obtained.

4.2.4 Spectroscopic analysis

Commercial poly(carbonate) and the synthetized copolymers were analysed by ^{1}H-NMR experiments. ^{1}H-NMR spectra have been recorded with a spectrometer Varian "Mercury 400" operating at 400 MHz on samples prepared in CDCl$_3$ at the 1.0 wt%. Chemical shifts (δ) for ^{1}H are given in ppm relative to the know signal of the internal reference (TMS).

4.2.5 Molecular weight analysis

Block and random copolymers and all the prepared blends were analysed by Gel Permeation Chromatography (GPC). The samples were analysed by a Waters column with 717 Autosampler equipped with a double detector: Waters 2487 Dual λ Absorbance Detector and Waters 2410 Refractive Index Detector. The column works at 25°C using THF as eluent. The samples were prepared at a concentration of about 0.07-0.10 (%w/V) weighting 3.5-5 mg subsequently dissolved in 5 mL of THF.

4.2.6 Morphological analysis

The morphology of the blends was investigated by Scanning Electron Microscopy (SEM). The tensile test specimens and the films were cryogenically fractured after 3 hours of immersion in liquid nitrogen. Fracture surfaces were observed after gold coating under

vacuum, using a Zeiss EP EVO 50 electron microscope equipped with a EDS detector classifiable as Oxford Instrument INCA ENERGY 350 [z>4 (Be), resolution 133eV (MnKa @ 2500cps)].

Micrographs of the most representative inner regions of the specimens were obtained. PCL droplet diameters were measured on at least 100 particles. Number (d_n) and volume (d_v) average diameters and particles size polydispersity (D_p) were calculated by the following equations.

$$d_n = \frac{\sum n_i d_i}{\sum n_i}$$
Eq. (4.1)

$$d_v = \frac{\sum n_i d_i^4}{\sum n_i d_i^3}$$
Eq. (4.2)

$$D = \frac{d_v}{d_n}$$
Eq. (4.3)

where n_i is the number of droplets 'i' of diameter d_i.

Polarized Light Optical Microscopy (PLOM) was employed to observe the morphology and growth kinetics of PLA spherulites. Micrographs were recorded by a LEICA DC 420 camera on film samples with a thickness of approximately 10 µm, cut from solvent casted films and tensile test specimens. By using a METTLER FP35Hz hot stage, the samples were firstly heated at 200°C and held at this temperature for 3 minutes to erase previous thermal histories, finally they were cooled to the crystallization temperature and the isothermal spherulitic growth was followed by PLOM.

4.2.7 Thermal analysis

The copolymers and all the blends were analysed by Thermogravimetric Analysis (TGA) and Differential Scanning Calorimetry (DSC).

The thermal stability of the blends was studied by TGA using a thermobalance TA Instruments, model TGAQ500. All measurements were conducted under nitrogen atmosphere and using sample masses of approximately 7 mg. All the samples were heated from 40 to 600°C at a rate of 10°C/min.

The thermal behaviour of the blends was studied by DSC using a Perkin Elmer DSC Pyris 1 calorimeter equipped with a refrigerated cooling system Intracooler 2P calibrated with indium. All measurements were performed under nitrogen atmosphere and using sample masses of approximately 5 mg. The analyses were conducted with different methods as a function of the experiments.

In non-isothermal analyses, the copolymers were heated from 25°C to 200°C at the rate of 10°C/min and held at 200°C for 3 minutes to erase the thermal history. Then they were cooled at 10°C/min until − 80°C (in order to see the glass transition temperature) and finally heated at 10°C/min to 200°C.

On the other hand, the blends were heated from 25°C to 200°C at the rate of 10°C/min and held at 200°C for 3 minutes to erase the thermal history. Then they were cooled at 10°C/min until -20°C and finally heated at 10°C/min to 200°C.

In isothermal analyses, the samples were heated from 25°C to 200°C at 20°C/min and held at this temperature for 3 minutes to erase the thermal history. Then they were cooled at 60°C/min (in order to avoid PLA crystallization during cooling) to the chosen isothermal crystallization temperature (T_c) and held at this temperature for 30 minutes while recording the evolved crystallization enthalpy.

The isothermal crystallization temperature range was determined by preliminary tests to ensure that no crystallization occurred during the cooling.

4.3 RESULTS AND DISCUSSION

4.3.1 Characterization of PCL-*co*-PC copolymers

The thermal behaviour of PCL-*co*-PC copolymers has been investigated by non-isothermal DSC and TGA experiments. The structure of the copolymers microdomains in the melt state depends on their segregation strength given by χN (where χ is the Flory–Huggins interaction parameter between different blocks and N the overall degree of polymerization of the entire block copolymer).[5] When χN is lower than 10, a single-phase melt is usually formed. On the other hand, when χN is higher than 10, copolymers segregate in two phases in the melt state.
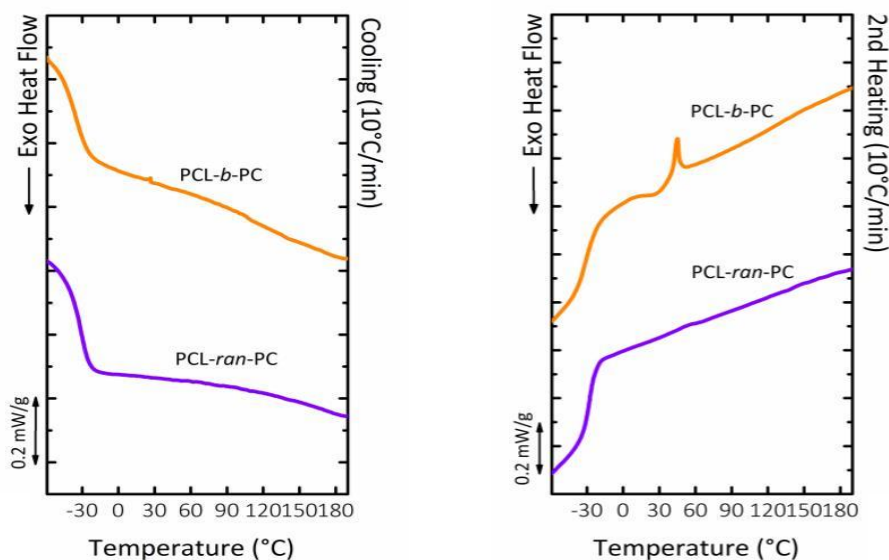
Figure 4.2: Non-isothermal DSC experiments on block and random copolymers. (a) cooling curves at 10°C/min from the melt state; (b) subsequent heating curves at 10°C/min. The curves have been normalized by the weight of the samples.

As Table 4. shows, for each copolymer a value lower than 10 is obtained. It is therefore assumable that the copolymers form a single phase system in the melt state. However, considering that in the second DSC heating curves

On the other hand, PCL-*ran*-PC does not show any evidence of crystallization of the PCL phase but it must be considered that in this case the relative PCL sequences are too short to crystallize, as expected for random copolymers.[6]

Table 4.3: Molecular characteristic of the copolymers. The Flory-Huggins enthalpic segmental interaction parameter χ; the overall degree of polymerization of the copolymer calculated by M_n/M_0 where M_n is the number average molecular weight of the entire copolymer and M_0 is the molecular weight of the repeating unit (taking into account the molar composition of the copolymer); glass transition temperature (T_g), temperature of crystallization (T_C) and melting (T_m) and relative enthalpy values.

Sample	χ	N	χN	T_g (°C)	T_c (°C)	ΔH_c (J/g)	T_m (°C)	ΔH_m (J/g)
PCL-*b*-PC	0.075	99.7	7.5	-36	22	0.8	44	1
PCL-*ran*-PC	0.075	124.4	8.8	-32	-	-	-	-

4.3 shows thermogravimetric curves of PCL-*b*-PC and PCL-*ran*-PC copolymers and the respective derivative curves dw/dT as function of temperature, while in Table 4.4 are reported the respective values obtained from the curves.

Both copolymers present a single degradation step, as result of formation of a single phase system in the melt state (χN is lower than 10 for both copolymers). However, the temperature at which PCL-*ran*-PC loses 10% of the total mass is 291°C, whereas for PCL-*b*-PC it is 315°C (Table 4.3).

Considering that the two copolymers have a similar composition, the different degradation behaviour is related to two factors. First of all, PCL-*ran*-PC has a lower molecular weight than PCL-*b*-PC, and in the latter case the longer polymer chains need higher temperature to start degradation. At the same time, in PCL-*ran*-PC the number of linkages between different sequences (i.e., PC and PCL blocks) is higher than in PCL-*b*-PC.

Table 4.4: Data obtained from TGA analysis for PCL-b-PC and PCL-ran-PC copolymers.

Sample	T 10% loss (°C)	T derivate peak (°C)
PCL-*b*-PC	315	339
PCL-*ran*-PC	291	329

Being PCL-PC linkage more susceptible to degradation than PC-PC or PCL-PCL linkages, PCL-*ran*-PC starts its degradation before PCL-*b*-PC.

4.3.2 Characterization of PLA/PCL based blends

4.3.2.1 Preparation of the blends

A constant PLA/PCL weight ratio of 80/20 was employed in order to obtain a well-balanced combination of stiffness and toughness. PCL-PC based copolymers were tested as compatibilizers by adding them at 10% by weight with respect to the minor phase. Thus, the final blends have an approximate composition of 80/20/2, weight ratio, PLA/PCL/PCL-*co*-PC. The blends were prepared by both solution and melt mixing.

In the first case, neat homopolymers and the PCL-*co*-PC based copolymers were dissolved in dichloromethane and stirred at room temperature. The film forming solutions were casted until constant weight was reached.

In the second case, neat homopolymers and the PCL-PC based copolymers were melted and blended in a twin-screw extruder (screw speed: 200 rpm, temperature: 200°C, residence time: 1 minute). The extruded filaments were rapidly quenched in a water bath and pelletized.

The blends prepared by solution mixing have been designated with: (s) while the corresponding ones prepared by melt blending have been designated with: (m).

It is worth noting that upon the two different blending techniques, different morphologies and thermal behaviours of the resulting blends are obtained. In melt mixing, samples are heated at a temperature higher than T_m and subjected to shear within the extruder. This process can cause a direct degradation of the polymer, which results in a shortening of the chains. On the other hand, in solution mixed samples, the blend components remain at room temperature in a hydrophobic solvent, which should prevent chain degradation. Because molecular weight has a key role in determining most of the properties of the blend, each of the following results must be correlated to a possible change in the molecular weight.

It is also important to consider that the migration of heterogenities from one phase to the other, which could change crystallization kinetics, in melt mixed blends happens directly from one phase to the other, whereas in solution mixed blends it could happen from one phase to the solvent.

At the same time, upon solution or melt blending a different morphology of the blend can be obtained. On one hand, in solution mixed blends, the size of the minor phase domains is mainly dependent on the respective interfacial tension between the phases during segregation upon solvent evaporation. On the other hand, in melt mixed samples, the size of the minor phase domains is also correlated with the balance between coalescence and mechanical breakup of the droplets and therefore to the processing parameters. Furthermore, as a general result, in solution mixed sample the size of the minor phase domains is typically higher than in melt mixed blend upon the mechanical dispersion of one phase in the other.

In the following paragraphs, results for both solution and melt mixed blends at the same respective compositions will be presented.

4.3.2.2 Molecular weight analysis

Table 4.4 reports average and numerical molecular weight of neat PLA and PLA phase within the blends. In all solution blended samples, the molecular weight of PLA phase does not change upon blending and it is maintained unchanged with respect to the nominal value reported by the producer (i.e., Mw = 180 KDa).

On the contrary in melt blended samples, PLA molecular weight is always lower than expected and it is even further influenced by copolymers addition. If on one hand, the molecular weight of neat PLA and PLA/PCL is only slightly decreased, on the other hand, copolymers addition causes a dramatic degradation of the polymers chains. In particular, in PLA/PCL/PCL-*b*-PC, the Mw value is decreased to 113 KDa while in PLA/PCL/PCL-*ran*-PC Mw is even decreased to 64 KDa. Considering that all melt blended samples have been processed in the same way, such reduction of the molecular weight must be induced by copolymer addition.

It is possible that PCL-co-PC based copolymers, characterized by low molecular weights , are more susceptible to degradation than the PLA phase at melt blending conditions. Once degraded to oligomers, they can undergo transesterification with PLA chains causing such molecular weight reductions.

As confirmation, it is worth noting that the copolymer characterized by the lowest molecular weight and thus the most susceptible to degradation (i.e., PCL-*ran*-PC, see molecular weight in Table 4.5) is the one that causes the highest PLA molecular weight reduction. In order to further confirm such hypothesis a thermogravimetric analysis was performed.

Table 4.5: Average and numerical molecular weight of melt blended and solvent mixed samples.

Sample	Mn (KDa)	Mw (KDa)	D
PLA(m)	123	153	1.2
PLA/PCL(m)	111	160	1.4
PLA/PCL/PCL-*b*-PC(m)	81	113	1.4
PLA/PCL/PCL-*ran*-PC(m)	38	64	1.7
PLA(s)	117	179	1.5
PLA/PCL(s)	116	178	1.5
PLA/PCL/PCL-b-PC(s)	132	179	1.4
PLA/PCL/PCL-ran-PC(s)	127	184	1.4

4.3.2.3 Thermogravimetric analysis

Figure 4.4 shows the thermograms and respective derivatives (dw/dT) of neat PLA, PLA/PCL and PLA/PCL/PCL-*co*-PC, for both the blends obtained by melt and solution mixing, while in Table 4.6 are reported the corresponding temperatures of 10% loss and derivative peak maximum.

Neat PLA starts its degradation at temperatures above 305°C in agreement with the study of Carrasco *et al.*[7] and without important differences between solvent cast and melt mixed samples.

Also, the PLA phase within PLA/PCL blends is not affected by processing condition

Table 4.6: Data obtained for TGA analyses for neat PLA, PLA/PCL and PLA/PCL/PCL-co-PC blends. Blends obtained by both melt and solution mixing.

Sample	T 10% loss (°C)	T derivate peak (°C)
PLA(m)	340	370
PLA/PCL(m)	345	368
PLA/PCL/PCL-*b*-PC(m)	280	306
PLA/PCL/PCL-*ran*-PC(m)	272	290
PLA(s)	334	370
PLA/PCL(s)	339	369
PLA/PCL/PCL-b-PC(s)	317	364
PLA/PCL/PCL-ran-PC(s)	310	365

(i.e., solution or melt blending) since in both blends PLA phase has a similar molecular weight (see Table 4.4) and thus the degradation is in the same temperature range.

On the other hand, the degradation temperature of PLA/PCL/PCL-*co*-PC depends on the processing condition (as reflection of the differences in molecular weight, see Table 4.3). According to Figure 4.4, PLA/PCL/PCL-*b*-PC(s) loses the 10% of the total mass at T=317°C whereas PLA/PCL/PCL-*b*-PC(m) at T=280°C. At the same time, PLA/PCL/PCL-*ran*-PC(s) loses the 10% of the total mass at T=310°C whereas PLA/PCL/PCL-*ran*-PC(m) loses the 10% of the total mass at T=272°C.

4.3.2.4 Morphological analysis

Figure 4.5 shows SEM micrographs of the cryogenically fractured surfaces of PLA/PCL and PLA/PCL/PCL-*co*-PC of the melt blended samples, while Figure 4.6 are reported the micrographs of the corresponding solution mixed samples. Table 4.7 reports average PCL

particles size within the blend measured by counting at least 100 particles for both the blends obtained by melt and solution.
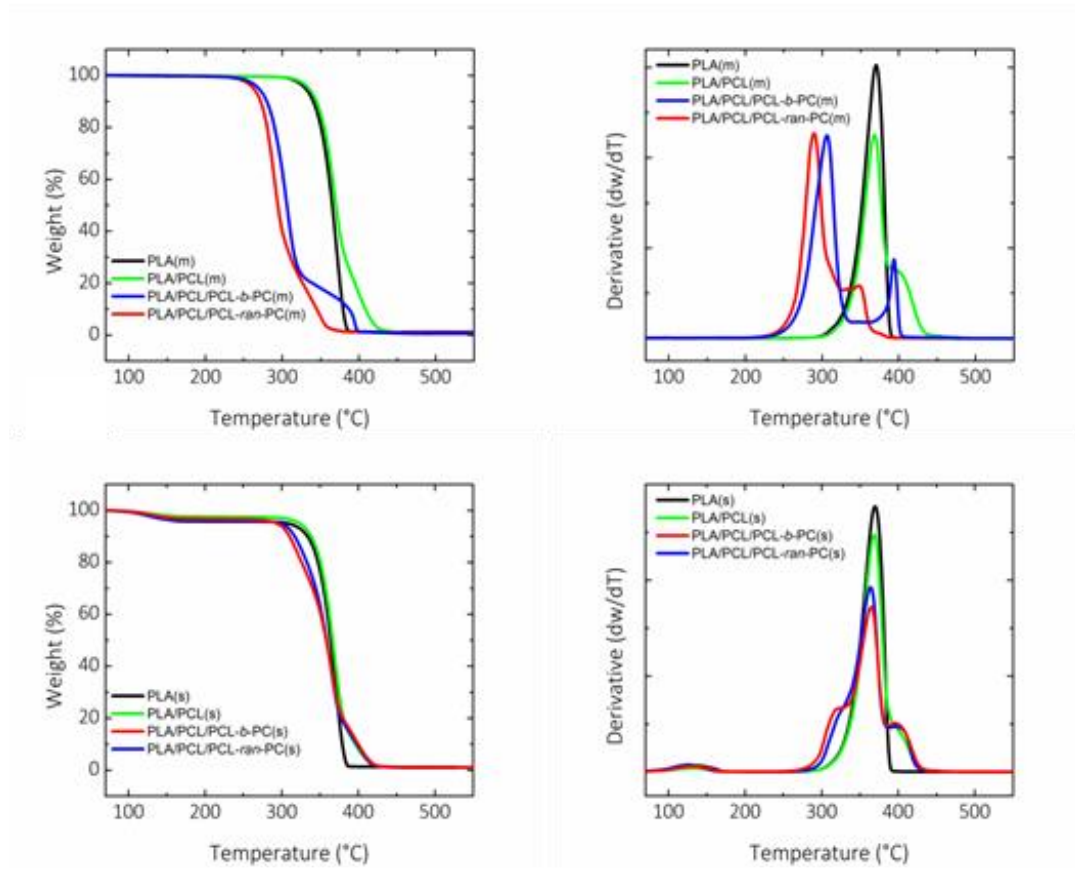

Figure 4.4: Thermograms of the blends. a) Weight reduction of neat PLA and PLA/PCL, PLA/PCL/PCL-co-PC blends, obtained by melt blending. b) Derivative curves (dw/dT) of neat PLA and PLA/PCL, PLA/PCL/ PCL-co-PC blends, obtained by melt blending. c) Weight reduction of neat PLA and PLA/PCL, PLA/PCL/ PCL-co-PC blends, obtained by solution blending. d) Derivative curves (dw/dT) of neat PLA and PLA/PCL, PLA/PCL/ PCL-co-PC blends, obtained by solution blending.

Table 4.7: Number average (d_n) and volume average (d_v) particle diameters, particle size distributions (D_p) and standard deviation (SD) of the PCL phase in PLA/PCL and PLA/PCL/PCL-co-PC blends. Blends obtained by both melt and solution mixing.

Sample	d_n (µm)	d_v (µm)	D_p	SD
PLA/PCL(m)	1.4	1.7	1.3	0.45
PLA/PCL/PCL-*b*-PC(m)	1.5	2.0	1.3	0.49
PLA/PCL/PCL-*ran*-PC(m)	1.7	2.3	1.4	0.52
PLA/PCL(s)	5.6	11.0	2.0	1.36
PLA/PCL/PCL-*b*-PC(s)	3.2	9.8	3.1	0.96
PLA/PCL/PCL-*ran*-PC(s)	6.2	13.2	2.1	2.48

A *sea island* morphology, typical of immiscible blends, is observable in all cases. PLA conforms the matrix, while PCL is dispersed in droplets. The cavities observed in all the micrographs are due to the interfacial debonding between PLA and PCL during the fracture confirming the immiscibility between phases.

The differences in PCL particle size are strictly related to the blending technique. When two immiscible polymers are blended, during melt mixing one phase is mechanically dispersed inside the other. The size and shape of the minor phase particles depend on the establishment of equilibrium between drop breakup and coalescence.

On the other hand, in solution mixing the two polymer phases are not mechanically dispersed one inside the other, but rather are dissolved in a common
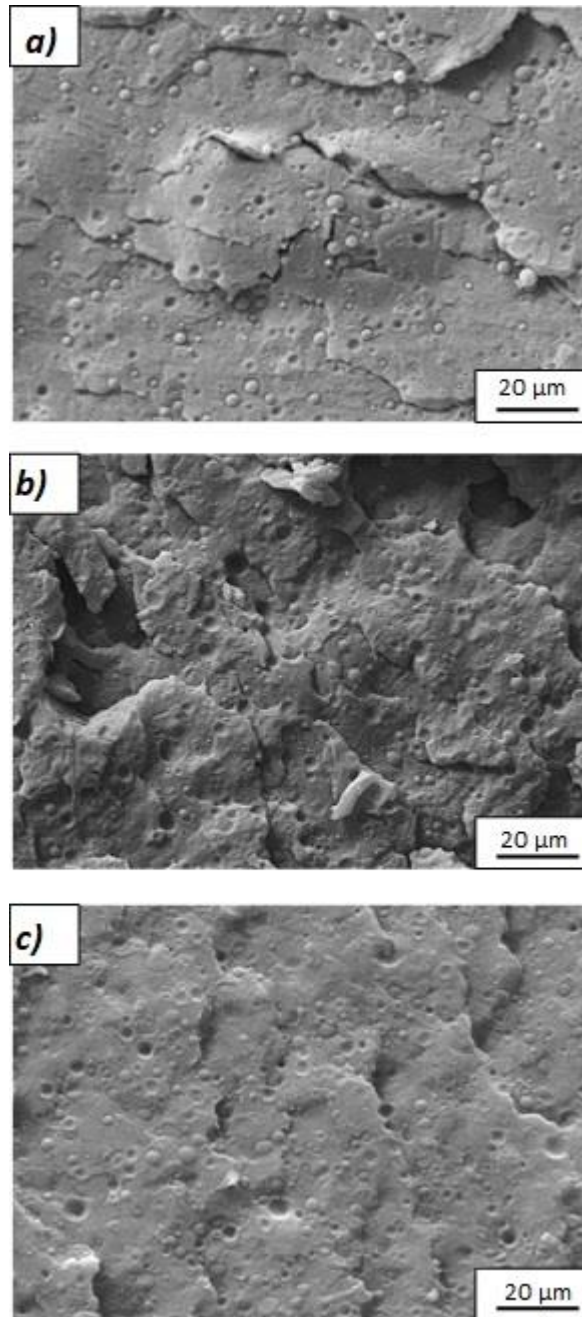
Figure 4.5: SEM micrographs of the cryogenically fractured surfaces of (a) PLA/PCL(m), (b) PLA/PCL/PCL-b-PC(m), (c) PLA/PCL/PCL-ran-PC(m) blends obtained by melt mixing.

solvent which provides to solubilize both the polymers. The absence of a direct mechanical dispersion is reflected in a general increase of the minor phase particles size and dispersion (D_p) as well.
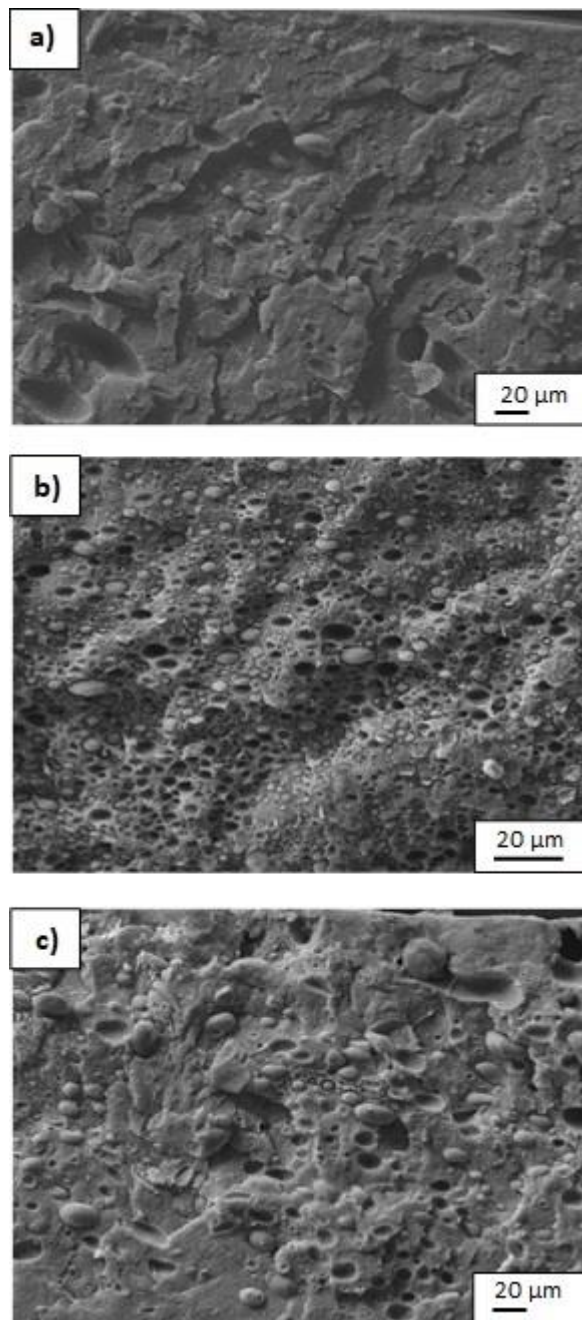
Figure 4.6: SEM micrographs of the cryogenically fractured surfaces of (a) PLA/PCL, (b) PLA/PCL/PCL-b-PC, (c) PLA/PCL/PCL-ran-PC blends obtained by solution mixing.

According to Table 4.7, in all cases (both melt and solution mixed blends) the size PCL particles size does not change upon copolymers addition. This indicates that the copolymers do not migrate to the PLA-PCL interphase, but, rather, are dispersed in one or both phases.

4.3.2.5 Non-isothermal DSC analysis - Cooling from the melt state

Figure 4.7 and Figure 4.8 show cooling DSC curves at 10°C/min from the melt state for all the blends: neat components, PLA/PCL and PLA/PCL/PCL-co-PC. While in Table 4.7 are reported the corresponding values of thermal transitions recorded during the scan.

In all the curves present in Figure 4.7 and Figure 4.8, the step recorded in the range between 59-61°C corresponds to the glass-transition temperature (T_g) of the PLA phase.

Upon blending with PCL, both in solution and melt mixing, the T_g of the PLA phase remains constant, proving that there is not an enhancement in miscibility between the PLA phase and the PCL one. Otherwise, a T_g depression would be detected, as a result of the interaction of PLA with the more flexible PCL chains (PCL T_g = -60°C).

It is worth noting that this result confirms the previous hypothesis, derived by morphological analysis of the blends, that copolymers do not migrate to the PLA-PCL interphase but, rather, are dissolved in one or both the phases.

Neat PCL crystallizes during cooling with a sharp exothermic peak, at 26°C in the case of melted sample (PCL(m)) and at 29°C in the case of solution mixed sample (PCL(s)). In the case of melt mixed PLA/PCL(m), PCL crystallization is fractionated into two peaks at 24°C and 35°C whereas in solution mixed PLA/PCL(s) the same phenomenon does not happen.

The fractionation of the crystallization is a common occurrence in immiscible blends. It happens when the number of droplets of a crystallizable phase is larger or of the same order of magnitude as the number of active heterogeneities in the bulk polymer before being dispersed. The smaller the droplets, the more difficult would be to find active heterogeneities in each droplet.

In melt mixed PLA/PCL(m), the first crystallization peak at 35°C corresponds to the crystallization of PCL droplets that have been nucleated by the same active heterogeneities present in the bulk polymer. The second crystallization peak at 24°C may be due to the crystallization of PCL droplets nucleated by less active heterogeneities.[8]

On the other hand, in solution mixed PLA/PCL(s) the same phenomenon does not happen since active heterogeneities probably migrate to the solvent during dissolution and therefore only one peak at 33°C is registered.

In the case of the mixed blends containing PCL-PC based copolymers (i.e., PLA/PCL/PCL-*b*-PC(m) and PLA/PCL/PCL-*ran*-PC(m)) a single PCL crystallization peak at 36°C is detected, even though the particle size is the same as the corresponding melt mixed PLA/PCL(m) blend. In this case, all PCL droplets crystallize at higher temperatures since the addition of the copolymers in the melt state probably causes a transfer of heterogeneities to the PCL phase.

Also in the case of solution mixed blends containing PCL-PC based copolymers (i.e., PLA/PCL/PCL-*b*-PC(s) and PLA/PCL/PCL-*ran*-PC(s) blends) a single PCL crystallization peak is detected. However in this case the temperature of crystallization is observed at 32°C, a temperature quite higher than that in the corresponding blends obtained by melt blending.

According to Figure 4.8 and 4.9, neat PLA does not crystallize during cooling at the scanning rate employed, both in the sample obtained by solution and melt blending. This is because the amount of D-units in PLA (i.e., PLA 4032D 1.2-1.6% of D-unit) is too high to allow chains alignments during crystallization at the employed scanning rates.[9]

PLA is able to crystallize only in the melt mixed blends (no crystallization exotherms are detected in solution mixed samples). In particular, a dramatic PLA phase
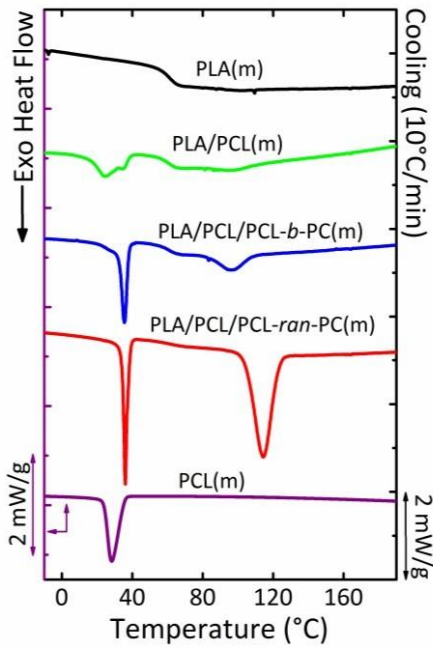
Figure 4.7: Non-isothermal DSC experiments curves. Cooling curves at 10°C/min from the melt state of neat PLA, neat PCL, PLA/PCL and PLA/PCL/PCL-*co*-PC blends obtained by melt mixing. The curves have been normalized by the weight of the samples.
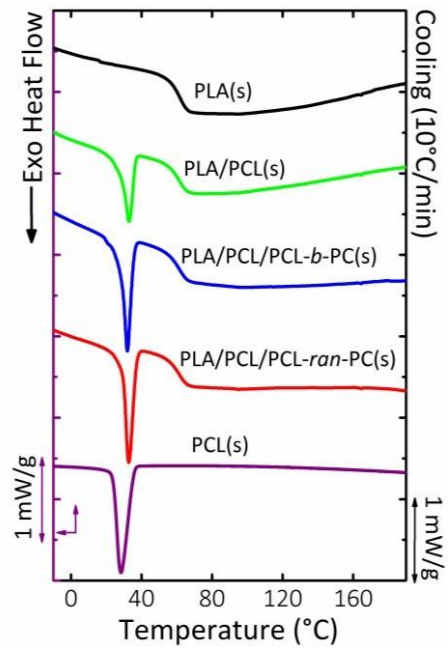
Figure 4.8: Non-isothermal DSC experiments curves. Cooling curves at 10°C/min from the melt state of neat PLA, neat PCL, PLA/PCL and PLA/PCL/PCL-co-PC blends obtained by solution mixing. The curves have been normalized by the weight of the samples.

Table 4.8: Thermal properties obtained from non-isothermal DSC cooling at 10°C/min. The enthalpies of crystallization and melting have been normalized by the weight fraction of the samples.

		Cooling				
Sample	Comp	PCL			PLA	
	w/w	T_c (°C)	ΔH_c (J/g)	T_g	T_c	ΔH_c (J/g)
PLA(m)	100	-	-	59.6	-	-
PLA/PCL(m)	80/20	24.3/34.5	8.7/36.1	59.3	94.3	4.1
PLA/PCL/PCL-*b*-PC(m)	80/20/2	35.5	49.9	59.6	96.5	9.1
PLA/PCL/PCL-*ran*-PC(m)	80/20/2	36.0	56.8	61.9	114.5	42.0
PCL(m)	100	25.9	45.7	-	-	-
PLA(s)	100	-	-	59.6	-	-
PLA/PCL(s)	80/20	32.9	26	59.5	-	-
PLA/PCL/PCL-*b*-PC(s)	80/20/2	31.9	41.5	59.4	-	-
PLA/PCL/PCL-*ran*-PC(s)	80/20/2	32.7	43.2	59.7	-	-
PCL(s)	100	28.8	57.2	-	-	-

is detected in the other blends.

Considering that no effect of increased miscibility between PLA and PCL phases are detected upon copolymers addition, the reason of this behaviour derives from the differences of processing condition between solution and melt mixing. In particular, it is assumable that the degradation of PLA phase upon melt blending is responsible of the increased crystallinity, as a result of the increased chain mobility upon molecular weight reduction.

As confirmation, it is worth noting that the blend characterized by lowest PLA phase molecular weight (i.e., PLA/PCL/PCL-*ran*-PC(m)) is the one that presents the largest crystallization enthalpy.

In any case, the crystallization of PLA phase within the blends, being the topic of this work, will be further analysed by isothermal analysis.

4.3.2.6 Non-Isothermal DSC analysis - Second Heating

Figure 4.9 and Figure 4.10 show second heating DSC curves at 10°C/min for neat components and all the blends, both obtained for melt and solution mixing. While in Table 4.8 the corresponding values obtained from the scans are reported.

Neat PLA undergoes cold crystallization and subsequent fusion of the produced crystals at respectively 115°C and 167°C for PLA(m), and 129°C and 166°C for PLA(s). In any case, the direct correspondence of enthalpy of crystallization and melting indicate that PLA remains completely amorphous during previous cooling in both the samples (see Table 4.8).

Upon blending with PCL, the cold crystallization exothermic peak is sharper and shifted to lower temperatures for both solution and melt mixed samples. This occurs because PCL can nucleate PLA during aging below T_g.

This occurrence was already demonstrated in our previous work,[10] where the decrease in T_{cc} of PLA upon blending with PCL in solution mixed sample was attributed to a nucleation effect of PCL on the glassy PLA matrix.

The melting temperature of PLA phase is maintained almost identical in all the samples, with the exception of PLA/PCL/PCL-*ran*-PC(m), where a double melting peak is

detected, which could be a result of PLA polymorphism. As it is reported in the literature, depending on the conditions (i.e., crystallization temperature), the most common and stable PLA polymorph, the α-form crystals can be formed. At temperatures below 120°C, α-form can be replaced by pseudohexagonal α'-form. In this case the chain segments have the same 10_3 helical chain conformation adopted in α-form but with higher conformational disorder and lower packing density. More recent studies demonstrate that the α'-form crystal is preferentially formed only at crystallization temperatures below 100°C, while at crystallization temperature between 100 and 120°C α'-form coexist with α-form.[11]

In PLA/PCL(m) and PLA/PCL/PCL-*b*-PC(m), PLA crystallizes at temperatures corresponding to α'-form crystal formation. However a small exotherm appears just before the single melting peak indicating a transformation of most disordered α'-form to the ordered α-form crystals.

On the other hand, in PLA/PCL/PCL-*ran*-PC(m), PLA crystallizes at the temperature of coexistence of the two crystals forms. Therefore a double melting peak appear during the scan. Any polymorphic behaviour would need to be corroborated by Wide Angle X ray Diffraction studies, which are outside the scope of the present work.

In order to understand the following results, another clarification must be carried out. As Table 4.3 shows, the molecular weight of PLA phase within the samples is not the same. In melt mixed blends, and especially in PLA/PCL/PCL-*ran*-PC(m), a lower molecular weight of PLA phase was found and thus a lower PLA melting temperature could have been anticipated. However, no significant change in melting temperature has been detected.

However, it must be considered that a change in the molecular weight does not necessarily provide a change in the melting temperature. In fact, T_m increases until reaching an asymptotical dependence with Mn values higher than 50 KDa.

Since in all the blends PLA has a high enough molecular weight T_m is not sensible to Mn variation.
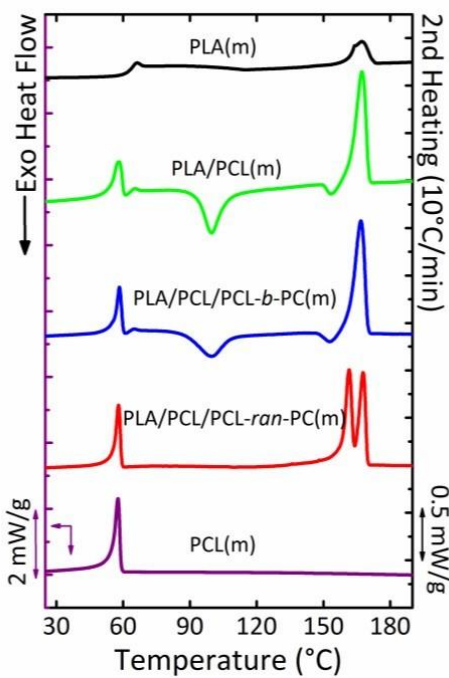
Figure 4.9: Non-isothermal DSC experiments. Second heating curves of neat PLA, neat PCL, PLA/PCL and PLA/PCL/PCL-*co*-PC blends obtained by melt mixing at 10°C/min. The curves have been normalized by the weight of the samples.
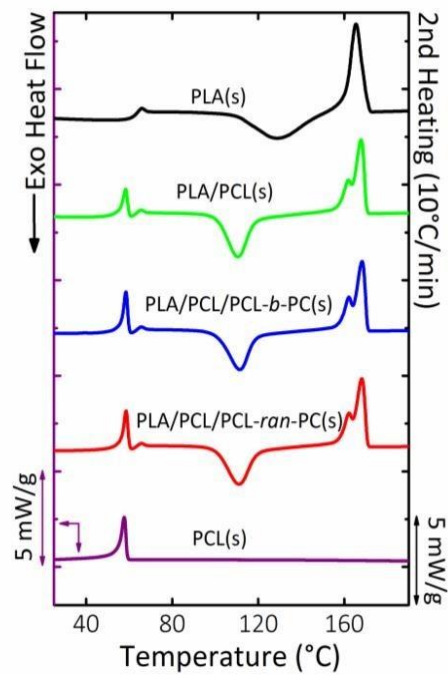
Figure 4.10: Non-isothermal DSC experiments. Second heating curves of neat PLA, neat PCL, PLA/PCL and PLA/PCL/PCL- co-PC blends prepared by solvent casting at 10°C/min. The curves have been normalized by the weight of the samples.

Table 4.8: Thermal properties obtained from non-isothermal DSC heating at 10°C/min. The enthalpies of crystallization and melting have been normalized by the weight fraction of the samples.

		Second Heating							
		PCL		PLA					
Sample	Comp w/w	T_m (°C)	ΔH_m (J/g)	T_{cc} (°C)	ΔH_{cc} (J/g)	T_{cc} (°C)	ΔH_{cc} (J/g)	T_m (°C)	ΔH_m (J/g)
PLA(m)	100	-	-	115.	8.5	-	-	167.3	9.0
PLA/PCL(m)	80/20	58.0	40.1	99.8	25.6	153.	2.9	167.3	36.9
PLA/PCL/PCL-*b*-PC(m)	80/20/2	58.4	42.2	99.7	21.4	152.	2.8	166.8	39.0
PLA/PCL/PCL-*ran*-	80/20/2	57.9	54.4	117.	3.3	-	-	161.6/167	27.3/19.5
PCL(m)	100	55.3	46.6	-	-	-	-	-	-
PLA(s)	100	-	-	128.	34.0	-	-	165.5	34.0
PLA/PCL(s)	80/20	58.4	30.0	110.	35.8	-	-	161.8/167	14.3/23.5
PLA/PCL/PCL-*b*-PC(s)	80/20/2	58.4	40.7	111.	31.5	-	-	162.3/168	12.1/21.7
PLA/PCL/PCL-*ran*-PC(s)	80/20/2	58.6	42.9	111.	32.3	-	-	162.1/168	12.7/21.4
PCL(s)	100	57.8	63.2	-	-	-	-	-	-

4.3.2.7 Spherulitic growth kinetics of PLA phase

Figure 4.10 shows PLOM micrographs of neat PLA and PLA samples obtained by melt blending, while in Figure 4.11 the micrographs of the corresponding samples obtained by solution mixing are shown. Upon blending spherulites get to be more fuzzy with a rougher morphology, furthermore some PCL droplets are evident inside the spherulities indicating that, although the two polymers are immiscible, a certain degree of compability is achieved during blending.

In all samples, PLA spherulites grow linearly with time, indicating that no diffusion problems at the growth front were induced by blending. The spherulitic growth rate G (μm min^{-1}) was thus calculated from the slope of the line obtained plotting the spherulitic radius (μm) against time (min).

Figure 4.12 shows G as a function of crystallization temperature T_c for neat PLA and samples obtained by melt blending, while in Figure 4.13 G as a function of crystallization temperature T_c is reported for the corresponding samples obtained by solution mixing. The values of G at different crystallization temperatures were fitted by an arbitrary function to guide the eye.

All the samples show the well know behaviour of G as a function of T_c. Decreasing the temperature from T_m, the growth rate increases as result of the increased thermodynamic driving force for secondary nucleation. After it passes through a maximum G decreases, upon the reduction of chain mobility with temperature.

Comparing Figure 4.12 with Figure 4.13, it is possible to see that for PLA/PCL/PCL-*b*-PC(m) and PLA/PCL/PCL-*ran*-PC(m) blends, G reaches values much larger than for neat PLA (in the case of PLA/PCL/PCL-*ran*-PC(m) a threefold increase of G is even detected). On the other hand, in the corresponding solution mixed sample (i.e., PLA/PCL/PCL-*b*-PC(s) and PLA/PCL/PCL-*ran*-PC(s)) the values of G are almost the same of neat PLA.

Considering that in none of the blends (both in melt and solution mixed samples as well) any evidence of increased miscibility between PLA and PCL phases is detected,
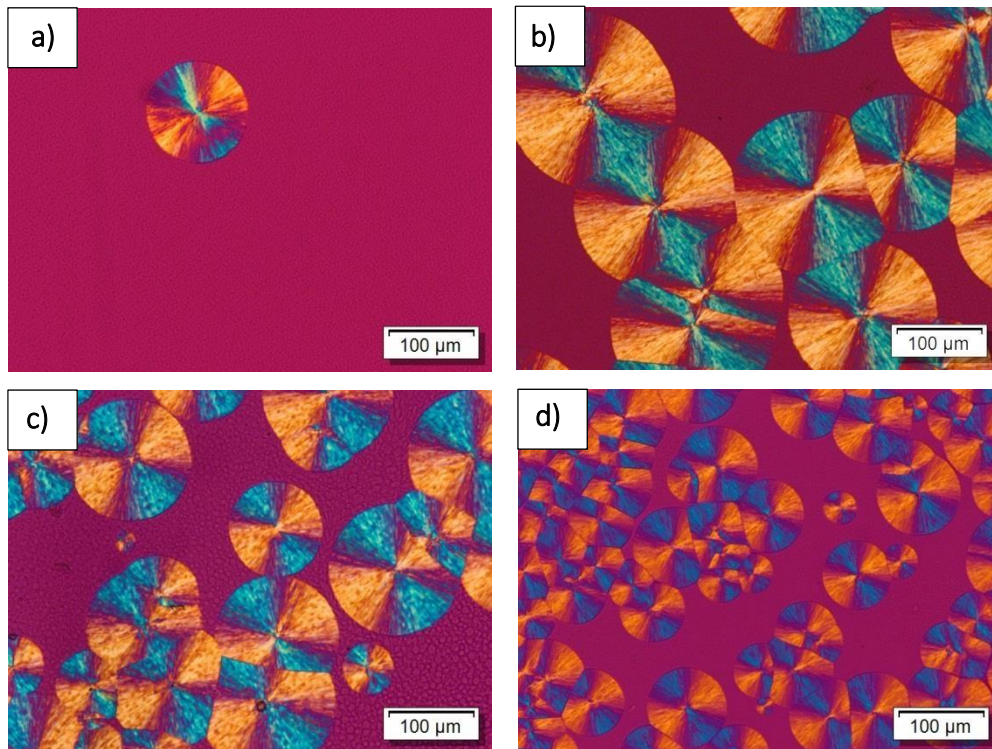
Figure 4.10: PLOM micrographs of (a) PLA(m) (b) PLA/PCL(m) (c) PLA/PCL/PCL-b-PC(m) (d) PLA/PCL/PCL-ran-PC(m) recorded at 130°C and after 25 minutes from the beginning of crystallization.
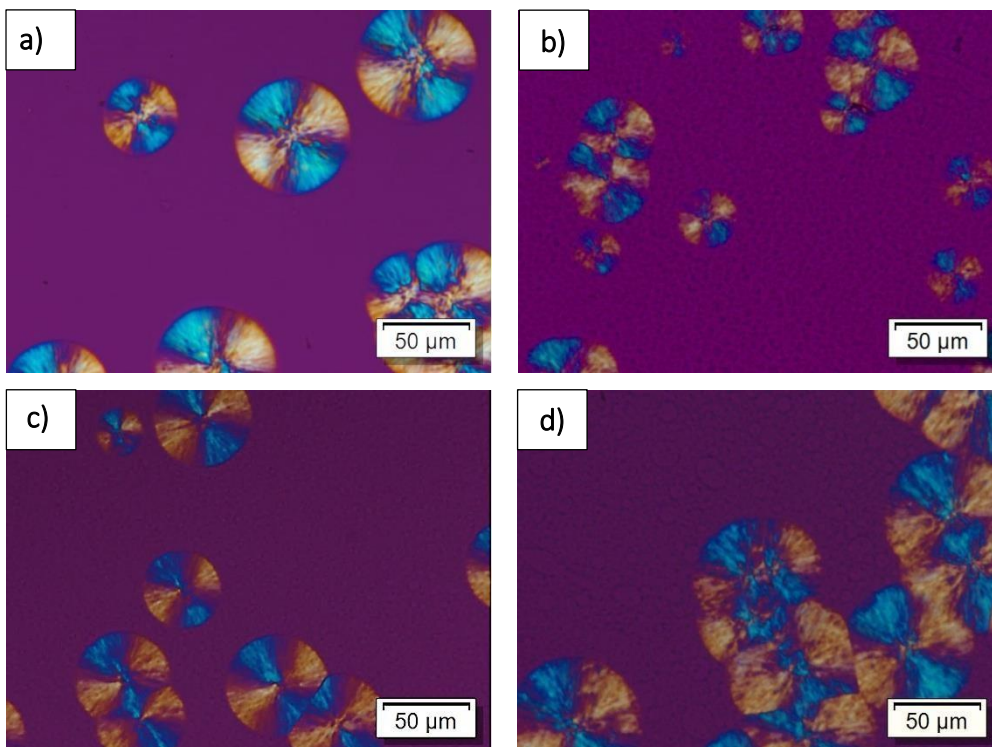

Figure 4.11: PLOM micrographs of (a) PLA(s) (b) PLA/PCL(s) (c) PLA/PCL/PCL-*b*-PC(s) (d) PLA/PCL/PCL-*ran*-PC(s) recorded at 130°C and after 25 minutes from the beginning of crystallization.
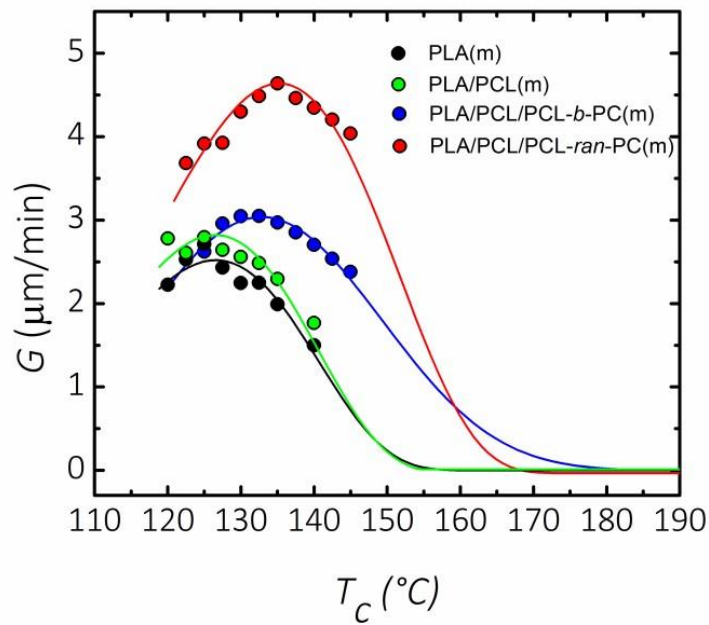
Figure 4.12: Spherulitic growth rate G as a function of isothermal crystallization temperature T_C for neat PLA and PLA phase within PLA/PCL and PLA/PCL/PCL-*co*-PC melt mixed blends. The solid lines represent an arbitrary fit to guide the eye.

chains within the samples.

(Mn > 100 KDa). In all cases the spherulites show the typical Maltese cross As it is well known, in a semicrystalline polymer the isothermal spherulitic growth rate decreases with molecular weight increases (in the molecular weight range larger than the critical molecular weight for entanglement formation), as expected from the more restricted chain mobility, whereas it reaches a constant value for high enough molecular weights

As reported in Table 4.8, in PLA/PCL/PCL-*b*-PC(m) and PLA/PCL/PCL-*ran*-PC(m), the PLA phase has a lower molecular weight than in the other blends, because of the increased degradation of the chains (i.e., 38 KDa and 81 KDa in comparison with the other blends where Mn is always among 130 KDa). As a result in PLA/PCL/PCL-*b*-PC(m) and PLA/PCL/PCL-*ran*-PC(m) the spherulitic growth rate is higher.

4.3.2.8 Isothermal overall crystallization of PLA phase

The inverse of the half-crystallization time, determined by isothermal crystallization from the melt employing DSC, provides an experimental measure of the overall crystallization rate, which includes both nucleation and spherulitic Figure 4.14 shows plots of the overall

crystallization rate (expressed as the inverse of half-crystallization time) as a function of temperature for melt blended samples, while in Figure 4.15 the plots are reported for the corresponding solution mixed samples.

The solid lines correspond to arbitrary fits performed to guide the eye. All the samples display the typical bell-shape trend, where the crystallization rate goes through a maximum as the kinetics changes from nucleation control at higher temperatures to diffusion control at lower temperatures.

Crystallization rate of neat PLA does not change upon different processing conditions. Both neat PLA samples, obtained by melt Figure 4.14) and solution (Figure 4.15) processing as well, achieve their maximum relative crystallinity in 16 minutes at T_c=104°C where the overall crystallization rate goes through a maximum. This result is consistent with the non-isothermal DSC cooling experiments, in which no crystallization of PLA was detected during cooling, for both melt and solution processing samples.
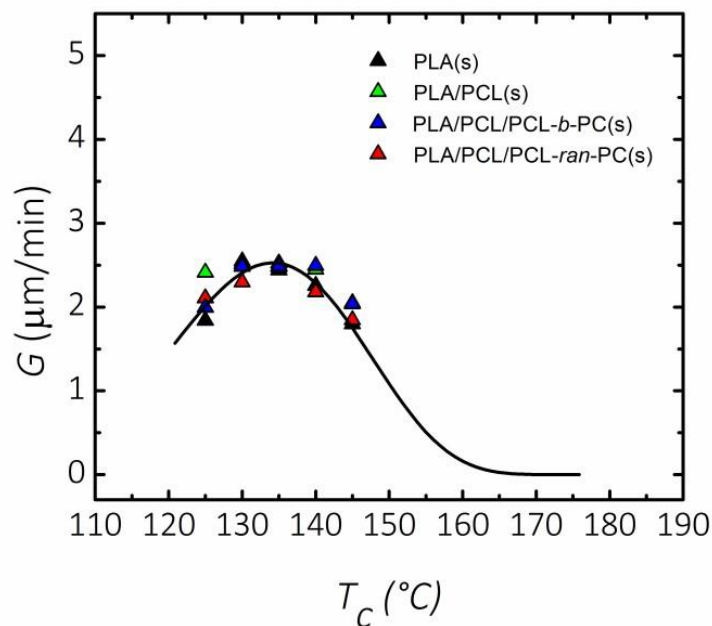

Figure 4.13: Spherulitic growth rate G as a function of isothermal crystallization temperature Tc for neat PLA and PLA phase within PLA/PCL and PLA/PCL/PCL-*co*-PC solvent mixed blends. The solid line represents an arbitrary fit to guide the eye.

Figure 4.14: Isothermal crystallization experiments from the melt state. Overall crystallization rate (1/t50%) as a function of isothermal crystallization temperature Tc in neat PLA and PLA phase within PLA/PCL and PLA/PCL/PCL-co-PC melt mixed blends. The solid lines represent arbitrary fits to guide the eye.
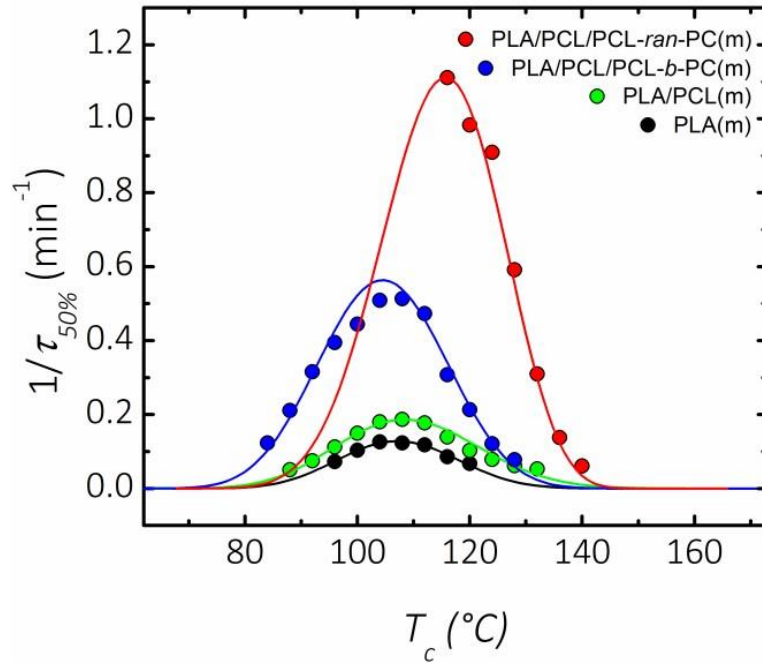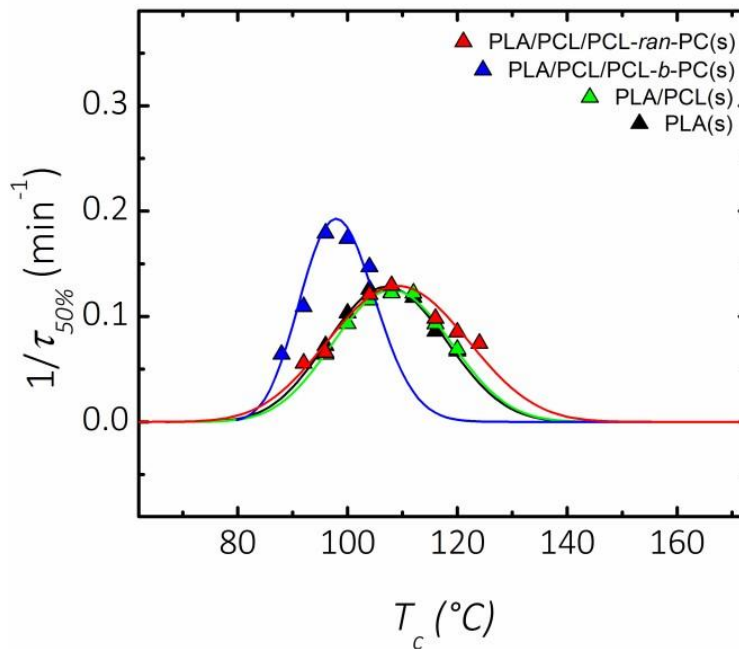

Figure 4.15: Isothermal crystallization experiments from the melt state. Overall crystallization rate (1/t50%) as a function of isothermal crystallization temperature Tc in neat PLA and PLA phase within PLA/PCL and PLA/PCL/PCL-co-PC solution mixed blends. The solid lines represent arbitrary fits to guide the eye.

At the same time, the effect of PCL blending to PLA phase crystallization rate is very similar for both melt and solution mixed sample. PLA/PCL(m) blend shows its maximum crystallization rate at $T_c=108°C$ and completes its crystallization after 10.8 minutes , while PLA/PCL(s) achieves its maximum relative crystallinity after 12 minutes at the same temperature.

Instead, upon the addition of PC-*co*-PCL based copolymers, the crystallization rate of PLA phase changes following the different processing condition (i.e., melt (Figure 4.14) or solution (Figure 4.15) blending).

As Figure 4.14 reports, PC-co-PCL based copolymers addition to melt mixed blends causes an enhancement of the crystallization rate. Taking neat PLA(m) as reference material, PLA/PCL/PCL-*b*-PC(m) shows a threefold increase, while in PLA/PCL/PCL-*ran*-PC(m) the crystallization rate is even ten times enhanced.

On the hand, PC-co-PCL based copolymers addition to solution mixed samples causes only small changes to PLA crystallization rate. Taking neat PLA(s) as reference material, both PLA/PCL/PCL-*b*-PC(s) and PLA/PCL/PCL-*ran*-PC(s) complete their crystallization after respectively 11.2 and 16 minutes, values quite similar to neat PLA(s).

As it was already detected, the differences of crystallization kinetics must be due to the different molecular weights of PLA chains and mainly reflects the behaviour detected by isothermal spherulitic growth rate.

4.4 CONCLUSION

In this part of the work, both melt and solution mixed 80/20 blends of PLA/PCL have been prepared in order to study the effect of the blending method on the crystallization behaviour of PLA. At the same time, in order to correlate the crystallization behaviour of PLA with PLA-*co*-PCL phases miscibility, poly(ε-caprolactone)-poly(carbonate) based copolymers, both block and random, have been tested as compatibilizers within the blends, by adding   at 10% with respect to the minor phase.

Poly(ε-caprolactone)-poly(carbonate) based copolymers were synthetized by ring opening polymerization (ROP), using commercial ε-caprolactone and preformed poly(carbonate), and characterized by spectroscopic and thermal analyses.

The copolymers do not cause any effect on PLA/PCL phases miscibility, since no reduction of PCL particles and PLA Tg value has been detected in both melt and solution mixed blends. Therefore, it is assumable that they do not migrate at the PLA-PCL interphase but are dispersed in one or both the phases.

At the same time copolymers addition causes a reduction of molecular weight in melt mixed blend. In particular, the random copolymer (PCL-ran-PC), characterized by a lower thermal stability than the block one (PCL-b-PC), causes a reduction of molecular weight from Mn=121 KDa to Mn=38 KDa during melt blending, whereas the same effect has not been detected in the corresponding solution mixed blends.

As result, PLA phase within melt mixed blends containing PCL-PC based copolymers has a higher tendency to crystallize during both isothermal and non-isothermal experiments. In particular, upon the addition of the random copolymer during melt blending (PLA/PCL/PCL-ran-PC(m)) an overall crystallization rate ten times higher than neat PLA (PLA(m)) has been detected, whereas no increase has been detected in the corresponding solution mixed blend PLA/PCL/PCL-ran-PC(s) (characterized by the same molecular weight of neat PLA). This effect has been attributed to an increase of the spherulitic growth rate due to the increase of chains mobility upon molecular weight reduction.

5 CONCLUSION

This thesis has been aimed to carry out a detailed investigation into poly(lactide) (PLA) crystallization within its immiscible blend with poly(ε-caprolactone) (PCL), upon the addition of different kind of compatibilizers. In particular, PLA crystallization cases has been examined through three diverse cases.

In the first case, two different kind of poly(lactide)-poly(ε-caprolactone) random copolymers, P(LA-*ran*-CL)s, (varying for composition and molecular weight) have been used as compatibilizers. Our results demonstrate that the addition of P(LA-*ran*-CL) to PLA/PCL blends induce a plasticization effect that increases the crystallization ability of the PLA phase. In particular the spherulitic growth rate of PLA has been increased two or three fold as compared to neat PLA, depending on the Tg of the random copolymer employed. At the same time, the crystallization of the PCL phase has also been investigated. A combined non-isothermal – isothermal experiment was designed in order to demonstrate that copolymer incorporation in the blends leads to an anti-plasticization effect of the PCL droplets.

In the second case, three different kinds of poly(L-lactide-*block*-carbonate) copolymers, PLA-co-PC, (varying composition and molecular weight) have been used for the first time to tune the compatibility between PLA and PCL. Cold crystallization of PLA (i.e., the crystallization of PLA during heating from the glassy state) has been investigated, both under non-isothermal and isothermal conditions. The use of specially designed thermal protocols have allowed us to obtain results able to successfully explain that the acceleration of the cold crystallization kinetics of PLA upon blending with PCL, often reported in the literature, is not connected with the miscibility between PLA and PCL phases, as it is also present in uncompatibilitized PLA/PCL blend, but it is due to a nucleation effect induced by PCL crystals on glassy PLA. Such nuclei only become effective upon heating to PLA cold crystallization temperatures, at which PCL is already molten.

In the last case, two different poly(ε-caprolactone)-poly(carbonate) based copolymers, PCL-co-PC, (varying for the length of the sequential block units) have been used for the first time to tune the compatibility between PLA and PCL. At the same time, in order to study the effect of the blend preparation, blending has been carried out by

both melt and solvent mixing. The copolymers do not cause any effect on PLA/PCL phases miscibility, since no reduction of PCL particles and PLA Tg value has been detected in both melt and solution mixed blends. However their addition causes a reduction of molecular weight in melt mixed blend. As result, PLA phase within melt mixed blends containing PCL-PC based copolymers has a higher tendency to crystallize during both isothermal and non- isothermal experiments.

6 REFERENCES

1   L. Mandelkern, *Biophys. Chem.*, 2004, 112, 109–116.

2   E. Piorkowska and G. C. Rutledge, *Handbook of Polymer Crystallization*, 2013.

3   P. G. Vekilov, *Cryst. Growth Des.*, 2010, **10**, 5007–5019.

4   M. Muthukumar, *Nucleation in polymer crystallization*, 2004, vol. 128.

5   J. Schmelzer, in *Nucleation Theory and Applications*, 2005, pp. 178–214.

6   J. M. Schultz, *Process. Polym.*, 2001, 270–342.

7   A. T. Lorenzo, M. L. Arnal, J. Albuerne and A. J. Müller, *Polym. Test.*, 2007, **26**, 222–231.

8   W. Banks and A. Sharples, *Die Makromol. Chemie*, 1963, **59**, 233–236.

9   J. N. Hay and Z. J. Przekop, *J. Polym. Sci. Polym. Phys. Ed.*, 1979, **17**, 951–959.

10   A. Maffezzoli, J. M. Kenny and L. Torre, *Thermochim. Acta*, 1995, **269–270**, 185–190.

11   M. Niaounakis, in *Biopolymers Reuse, Recycling, and Disposal*, 2013, pp. 1–75.

12   D. Marjadi and N. Dharaiya, *Search Res.*, 2011, **2**, 159–163.

13   M. Ashby and K. Johnson, *Mater. Today*, 2003, **6**, 24–35.

14   Ellen MacArthur Foundation, *Ellen MacArthur Found.*, 2016, 120.

15   G. Q. Chen and M. K. Patel, *Chem. Rev.*, 2012, 112, 2082–2099.

16   M. M. Reddy, S. Vivekanandhan, M. Misra, S. K. Bhatia and A. K. Mohanty, *Prog. Polym. Sci.*, 2013, **38**, 1653–1689.

17   L. Shen, E. Worrell and M. Patel, *Biofuels, Bioprod. Biorefining*, 2010, **4**, 25–40.

18   T. Iwata, *Angew. Chemie - Int. Ed.*, 2015, 54, 3210–3215.

19   European Bioplastics, Applications for bioplastics. European Bioplastics.

20   M. A. Abdel-Rahman, Y. Tashiro and K. Sonomoto, *Biotechnol. Adv.*, 2013, 31, 877–902.

21   R. P. Babu, K. O'Connor and R. Seeram, *Prog. Biomater.*, 2013, **2**, 8.

22   C. Purac, PLA bioplastics A Significance Contributor to Global Sustainability.

23   M. Carus, *Nov. Inst.*, 2012, 1–2.

24   M. Thielen, Bioplastics: Basics, Applications, Markets.

25   M. Murariu and P. Dubois, *Adv. Drug Deliv. Rev.*, 2016, **107**, 17–46.

26   S. Jacobsen and H. Fritz, *Polym. Eng. …*, 1999, **39**, 1311–1319.

27   J. M. Raquez, Y. Habibi, M. Murariu and P. Dubois, *Prog. Polym. Sci.*, 2013, **38**, 1504–1542.

28   H. R. Kricheldorf, I. Kreiser-Saunders, C. Jürgens and D. Wolter, *Macromol. Symp.*, 1996, **103**, 85–102.

29   S. Slomkowski, S. Penczek and A. Duda, *Polym. Adv. Technol.*, 2014, 25, 436–447.

30   J. Ahmed, J. X. Zhang, Z. Song and S. K. Varshney, in *Journal of Thermal Analysis and Calorimetry*, 2009, vol. 95, pp. 957–964.

31   N. Berezina, N. Landercy, P. Mariage and B. Morea, *World J. Org. Chem.*, 2013, **1**, 20–23.

32   E. Castro-Aguirre, F. Iñiguez-Franco, H. Samsudin, X. Fang and R. Auras, *Adv. Drug Deliv. Rev.*, 2016, **107**, 333–366.

33   W. Groot, J. Van Krieken, O. Sliekersl and S. De Vos, in *Poly(Lactic Acid): Synthesis, Structures, Properties, Processing, and Applications*, 2010, pp. 3–18.

34   D. L. Kaplan, *Biopolymers from Renewable Resources*, 2013.

35   G. Reddy, M. Altaf, B. J. Naveena, M. Venkateshwar and E. V. Kumar, *Biotechnol. Adv.*, 2008, 26, 22–34.

36   G. Q. Chen, *Plastics from Bacteria*, 2010, vol. 14.

37   Y. M. Harshe, G. Storti, M. Morbidelli, S. Gelosa and D. Moscatelli, *Macromol. React. Eng.*, 2007, **1**, 611–621.

38   O. Dechy-Cabaret, B. Martin-Vaca and D. Bourissou, *Chem. Rev.*, 2004, **104**, 6147–6176.

39   R. Mehta, V. Kumar, H. Bhunia and S. N. Upadhyay, *J. Macromol. Sci. Part C Polym. Rev.*, 2005, **45**, 325–349.

40   F. Achmad, K. Yamane, S. Quan and T. Kokugan, *Chem. Eng. J.*, 2009, **151**, 342–350.

41   A.-C. Albertsson and I. K. Varma, *Biomacromolecules*, 2003, **4**, 1466–1486.

42   K. Madhavan Nampoothiri, N. R. Nair and R. P. John, *Bioresour. Technol.*, 2010, 101, 8493–8501.

43   A. P. Dove, H. Li, R. C. Pratt, B. G. G. Lohmeijer, D. A. Culkin, R. M. Waymouth and J. L. Hedrick, *Chem. Commun.*, 2006, 2881.

44   H. Tsuji, *Macromol. Biosci.*, 2005, 5, 569–597.

45   R. Slivniak and A. J. Domb, *Biomacromolecules*, 2002, **3**, 754–760.

46   J. Coudane, C. Ustariz-Peyret, G. Schwach and M. Vert, *J. Polym. Sci. Part A Polym. Chem.*, 1997, **35**, 1651–1658.

47   N. Nomura, R. Ishii, Y. Yamamoto and T. Kondo, *Chem. - A Eur. J.,* 2007, **13**, 4433–4451.

48   A. Kowalski, A. Duda and S. Penczek, *Macromolecules*, 2000, **33**, 689–695.

49   S. Sosnowski and P. Lewinski, *Polym. Chem.*, 2015, 1–3.

50   J. W. Leenslag and A. J. Pennings, *Die Makromol. Chemie*, 1987, **188**, 1809–1814.

51   N. E. Kamber, W. Jeong, R. M. Waymouth, R. C. Pratt, B. G. G. Lohmeijer and J. L. Hedrick, *Chem. Rev.*, 2007, 107, 5813–5840.

52   M. Jamshidian, E. A. Tehrany, M. Imran, M. Jacquot and S. Desobry, *Compr. Rev. Food Sci. Food Saf.*, 2010, **9**, 552–571.

53   N. Peelman, P. Ragaert, B. De Meulenaer, D. Adons, R. Peeters, L. Cardon, F. Van Impe and F. Devlieghere, *Trends Food Sci. Technol.*, 2013, 32, 128–141.

54   S. P. Lyu, J. Schley, B. Loy, D. Lind, C. Hobot, R. Sparer and D. Untereker, *Biomacromolecules*, 2007, **8**, 2301–2310.

55   S. Li and S. McCarthy, *Biomaterials*, 1999, **20**, 35–44.

56   I. C. McNeill and H. A. Leiper, *Polym. Degrad. Stab.*, 1985, **11**, 267–285.

57   S. Inkinen, M. Hakkarainen, A. C. Albertsson and A. Södergård, *Biomacromolecules*, 2011, 12, 523–532.

58   K. Fukushima and Y. Kimura, *J. Polym. Sci. Part A Polym. Chem.*, 2008, **46**, 3714–3722.

59   J. E. Mark, *J. Am. Chem. Soc.*, 1999, **131**, 1012.

60   B. E. DiGregorio, *Chem. Biol.*, 2009, **16**, 1–2.

61   J. J. Kolstad, *J. Appl. Polym. Sci.*, 1996, **62**, 1079–1091.

62   S. Li and S. McCarthy, *Macromolecules*, 1999, **32**, 4454–4456.

63   M. Drieskens, R. Peeters, J. Mullens, D. Franco, P. J. Lemstra and D. G. Hristova-Bogaerds, *J. Polym. Sci. Part B Polym. Phys.*, 2009, **47**, 2247–2258.

64   T. Kawai, N. Rahman, G. Matsuba, K. Nishida, T. Kanaya, M. Nakano, H. Okamoto, J. Kawada, A. Usuki, N. Honma, K. Nakajima and M. Matsuda, *Macromolecules*, 2007, **40**, 9463–9469.

65   T. Y. Cho and G. Strobl, *Polymer (Guildf).*, 2006, **47**, 1036–1043.

66   M. L. Di Lorenzo, *Eur. Polym. J.*, 2005, **41**, 569–575.

67   H. Abe, Y. Kikkawa, Y. Inoue and Y. Doi, *Biomacromolecules*, 2001, **2**, 1007–1014.

68   M. Cocca, M. L. Di Lorenzo, M. Malinconico and V. Frezza, *Eur. Polym. J.*, 2011, **47**, 1073–1080.

69   J. Puiggali, Y. Ikada, H. Tsuji, L. Cartier, T. Okihara and B. Lotz, *Polymer (Guildf).*, 2000, **41**, 8921–8930.

70   L. Cartier, T. Okihara, Y. Ikada, H. Tsuji, J. Puiggali and B. Lotz, *Polymer (Guildf).*, 2000, **41**, 8909–8919.

71   R. J. Young and C. I. Chung, *J. Eng. Mater. Technol.*, 1982, **104**, 297.

72   T. G. Fox and P. J. Flory, *J. Polym. Sci.*, 1954, **14**, 315–319.

73   S. Saeidlou, M. a. Huneault, H. Li and C. B. Park, *Prog. Polym. Sci.*, 2012, **37**, 1657–1677.

74   Witzke DR., 1997.

75   D. M. Bigg, *Adv. Polym. Technol.*, 2005, **24**, 69–82.

76   H. Tsuji and Y. Ikada, *Macromol. Chem. Phys.*, 1996, **197**, 3483–3499.

77   K. Jamshidi, S. H. Hyon and Y. Ikada, *Polymer (Guildf).*, 1988, **29**, 2229–2234.

78   D. W. Oxtoby, *J. Phys. Condens. Matter*, 1992, **4**, 7627.

79   Y. Long, R. A. Shanks and Z. H. Stachurski, *Prog. Polym. Sci.*, 1995, 20, 651–701.

80   P. H. Geil, *J. Chem. Educ.*, 1981, **58**, 879.

81   B. Crist and J. M. Schultz, *Prog. Polym. Sci.*, 2016, **56**, 1–63.

82   H. D. Keith and F. J. Padden, *J. Appl. Phys.*, 1964, **35**, 1270–1285.

83   M. Yasuniwa, S. Tsubakihara, K. Iura, Y. Ono, Y. Dan and K. Takahashi, *Polymer*

(Guildf)., 2006, **47**, 7554–7563.

84   X. J. Li, Z. M. Li, G. J. Zhong and L. Bin Li, *J. Macromol. Sci. Part B Phys.*, 2008, **47**, 511–522.

85   S. K. Hideto Tsuji, Hiroki Takai and Saha, *Polymer (Guildf).*, 2006, **47**, 3826–3837.

86   H. Tsuji and Y. Ikada, *Macromol. Chem. Phys.*, 1996, **197**, 3483–3499.

87   J. Huang, M. S. Lisowski, J. Runt, E. S. Hall, R. T. Kean, N. Buehler and J. S. Lin, *Macromolecules*, 1998, **31**, 2593–2599.

88   S. Baratian, E. S. Hall, J. S. Lin, R. Xu and J. Runt, *Macromolecules*, 2001, **34**, 4857–4864.

89   I. C. Sanchez and R. K. Eby, *Macromolecules*, 1975, **8**, 638–641.

90   *,† Hideki Abe, †,‡ Yoshihiro Kikkawa, ‡ and Yoshio Inoue and ‡ Yoshiharu Doi†, , DOI:10.1021/BM015543V.

91   R. Vasanthakumari and A. J. Pennings, *Polymer (Guildf).*, 1983, **24**, 175–178.

92   L.-T. Lim, R. Auras and M. Rubino, *Prog. Polym. Sci.*, 2008, **33**, 820–852.

93   F. Carrasco, P. Pagès, J. Gàmez-Pèrez, O. O. Santana and M. L. Maspoch, *Polym. Degrad. Stab.*, 2010, **95**, 116–125.

94   *Polym. Degrad. Stab.*, 2010, **95**, 2508–2514.

95   R. Pantani, F. De Santis, A. Sorrentino, F. De Maio and G. Titomanlio, *Polym. Degrad. Stab.*, 2010, **95**, 1148–1159.

96   F. De Santis, R. Pantani and G. Titomanlio, *Thermochim. Acta*, 2011, **522**, 128–134.

97   J. Zhang, Yongxin Duan, H. Sato, H. Tsuji, I. Noda, S. Yan and Yukihiro Ozaki, , DOI:10.1021/MA051232R.

98   M. S. Sanchez, V. B. F. Mathot, G. Vanden Poel and J. L. G. Ribelles, *Macromolecules*, 2007, **40**, 7989–7997.

99   R. Legras, J. P. Mercier and E. Nield, *Nature*, 1983, **304**, 432–434.

100   X. Xu, C. L. Ting, I. Kusaka and Z.-G. Wang, *Annu. Rev. Phys. Chem.*, 2014, **65**, 449–475.

101   B. Fillon, A. Thierry, B. Lotz and J. C. Wittmann, *J. Therm. Anal.*, 1994, **42**, 721–731.

102   T. Ke and X. Sun, *J. Appl. Polym. Sci.*, 2003, **89**, 1203–1210.

103 J. Y. Nam, S. Sinha Ray and M. Okamoto, *Macromolecules*, 2003, **36**, 7126–7131.

104 K. U. Suprakas Sinha, Raya Kazunobu, Yamada Masami, Okamoto Youhei, Fujimotoa Akinobu, Ogami, *Polymer (Guildf).*, 2003, **44**, 6633–6646.

105 H. Nakajima, M. Takahashi and Y. Kimura, *Macromol. Mater. Eng.*, 2010, **295**, 460–468.

106 N. Kawamoto, A. Sakai, T. Horikoshi, T. Urushihara and E. Tobita, *J. Appl. Polym. Sci.*, 2007, **103**, 198–203.

107 L. WEN and Z. XIN, *Chinese J. Chem. Eng.*, 2010, **18**, 899–904.

108 A. M. Harris and E. C. Lee, *J. Appl. Polym. Sci.*, 2008, **107**, 2246–2255.

109 A. Pei, Q. Zhou and L. A. Berglund, *Compos. Sci. Technol.*, 2010, **70**, 815–821.

110 Z. Qiu and Z. Li, *Ind. Eng. Chem. Res.*, 2011, **50**, 12299–12303.

111 H. S. Xu, X. J. Dai, P. R. Lamb and Z. M. Li, *J. Polym. Sci. Part B Polym. Phys.*, 2009, **47**, 2341–2352.

112 Y. T. Shieh and G. L. Liu, *J. Polym. Sci. Part B Polym. Phys.*, 2007, **45**, 1870–1881.

113 Y.-T. Shieh, Y.-K. Twu, C.-C. Su, R.-H. Lin and G.-L. Liu, *J. Polym. Sci. Part B Polym. Phys.*, 2010, **48**, 983–989.

114 S. Brochu, R. E. Prud'homme, I. Barakat and R. Jérôme, *Macromolecules*, 1995, **28**, 5230–5239.

115 J. Yu and Z. Qiu, *Thermochim. Acta*, 2011, **519**, 90–95.

116 J. Yu and Z. Qiu, *ACS Appl. Mater. Interfaces*, 2011, **3**, 890–897.

117 P. Pan, Z. Liang, A. Cao and Y. Inoue, *ACS Appl. Mater. Interfaces*, 2009, **1**, 402–411.

118 S. Wang, C. Han, J. Bian, L. Han, X. Wang and L. Dong, *Polym. Int.*, 2011, **60**, 284–295.

119 R. M. Rasal, A. V. Janorkar and D. E. Hirt, *Prog. Polym. Sci.*, 2010, **35**, 338–356.

120 I. Pillin, N. Montrelay and Y. Grohens, *Polymer (Guildf).*, 2006, **47**, 4676–4682.

121 E. Piorkowska, Z. Kulinski, a. Galeski and R. Masirek, *Polymer (Guildf).*, 2006, **47**, 7178–7188.

122 L. V Labrecque, R. a Kumar, V. Dave, R. a Gross and S. P. McCarthy, *J. Appl. Polym. Sci.*, 1997, **66**, 1507–1513.

123 H. Xiao, W. Lu and J.-T. Yeh, *J. Appl. Polym. Sci.*, 2009, **113**, 112–121.

124 S. L. Yang, Z. H. Wu, B. Meng and W. Yang, *J. Polym. Sci. Part B Polym. Phys.*, 2009, **47**, 1136–1145.

125 V. P. Martino, A. Jiménez and R. A. Ruseckaite, *J. Appl. Polym. Sci.*, 2009, **112**, 2010–2018.

126 M. Murariu, A. Da Silva Ferreira, M. Alexandre and P. Dubois, *Polym. Adv. Technol.*, 2008, **19**, 636–646.

127 R. Gendron, J. Reignier and J. Tatibouët, *J. Appl. Polym. Sci.*, 2009, **112**, 1345–1355.

128 M. Mihai, M. A. Huneault and B. D. Favis, *J. Appl. Polym. Sci.*, 2009, **113**, 2920–2932.

129 M. Pracella, in *Handbook of Polymer Crystallization*, John Wiley & Sons, Inc., Hoboken, NJ, USA, 2013, pp. 287–326.

130 L. A. Utracki, in *Polymer blends handbook*, ed. L. A. Utracki, Springer Netherlands, Dordrecht, 2003, pp. 1–122.

131 P. J. Flory, *J. Chem. Phys.*, 1942, **10**, 51–61.

132 D. W. van (Dirk W. Krevelen and K. te. Nijenhuis, *Properties of polymers : their correlation with chemical structure ; their numerical estimation and prediction from additive group contributions*, Elsevier, 2009.

133 C. Koning, *Prog. Polym. Sci.*, 1998, **23**, 707–757.

134 L. a. Utracki, *Can. J. Chem. Eng.*, 2002, **80**, 1008–1016.

135 J.-B. Zeng, K.-A. Li and A.-K. Du, *RSC Adv.*, 2015, **5**, 32546–32565.

136 V. Mohanraj, Y. Chen and M. & Chen, *Trop. J. Pharm. Res. Trop J Pharm Res*, 2006, **5**, 561–573.

137 R. Jerome R., in *Macromolecular Engineering: Precise Synthesis, Materials Properties, Applications*, 2011, vol. 3, pp. 1753–1782.

138 M. Arnal and M. Matos, *Macromol. Chem. Phys.*, 1998, **1999(10)**, 2275–2288.

139 D. Garlotta, *J. Polym. Environ.*, 2001, **9**, 63–84.

140 A. Jiménez, M. A. Peltzer and R. A. Ruseckaite, *Poly(lactic acid) Science and Technology: Processing, Properties, Additives and Applications*, 2015.

141 D. J. David and T. F. Sincock, *Polymer (Guildf).*, 1992, **33**, 4505–4514.

142   G. Groeninckx, M. Vanneste and V. Everaert, *Polym. Blends Handb.*, 2003, 203–294.

143   F. Sakai, K. Nishikawa, Y. Inoue and K. Yazawa, *Macromolecules*, 2009, **42**, 8335–8342.

144   M. L. Di Lorenzo, *Prog. Polym. Sci.*, 2003, **28**, 663–689.

145   F. J. Li, S. D. Zhang, J. Z. Liang and J. Z. Wang, *Polym. Adv. Technol.*, 2015, **26**, 465–475.

146   A. C. Vieira, A. T. Marques, R. M. Guedes and V. Tita, in *Procedia Engineering*, 2011, vol. 10, pp. 1597–1602.

147   H. Liu and J. Zhang, *J. Polym. Sci. Part B Polym. Phys.*, 2011, **49**, 1051–1083.

148   M. E. Broz, D. L. VanderHart and N. R. Washburn, *Biomaterials*, 2003, **24**, 4181–4190.

149   M. M. Coleman, C. J. Serman, D. E. Bhagwagar and P. C. Painter, *Polymer (Guildf).*, 1990, **31**, 1187–1203.

150   J. Lu, Z. Qiu and W. Yang, *Polymer (Guildf).*, 2007, **48**, 4196–4204.

151   D. Wu, Y. Zhang, M. Zhang and W. Zhou, *Eur. Polym. J.*, 2008, **44**, 2171–2183.

152   R. Dell'Erba, G. Groeninckx, G. Maglio, M. Malinconico and A. Migliozzi, *Polymer (Guildf).*, 2001, **42**, 7831–7840.

153   J.-M. Yang, H.-L. Chen, J.-W. You and J. C. Hwang, *Polym. J.*, 1997, 29, 657–662.

154   J. Urquijo, G. Guerrica-Echevarría and J. I. Eguiazábal, *J. Appl. Polym. Sci.*, 2015, **42641**, n/a-n/a.

155   C. L. Simões, J. C. Viana and A. M. Cunha, *J. Appl. Polym. Sci.*, 2009, **112**, 345–352.

156   G. Maglio, A. Migliozzi, R. Palumbo, B. Immirzi and M. G. Volpe, *Macromol. Rapid Commun.*, 1999, **238**, 236–238.

157   Y.-H. Na, Y. He, X. Shuai, Y. Kikkawa, Y. Doi and Y. Inoue, *Biomacromolecules*, 2002, **3**, 1179–1186.

158   M. Harada, K. Iida, K. Okamoto, H. Hayashi and K. Hirano, *Polym. Eng. Sci.*, 2008, **48**, 1359–1368.

159   T. Takayama, M. Todo and H. Tsuji, *J. Mech. Behav. Biomed. Mater.*, 2011, **4**, 255–260.

160   Y. I. Tsuji, Hideto, *J. Appl. Polym. Sci.*, 1996, **60**, 2367–2375.

161   N. S. Choi, C. H. Kim, K. Y. Cho and J. K. Park, *J. Appl. Polym. Sci.*, 2002, **86**, 1892–1898.

162   C. H. Kim, K. Y. Cho, E. J. Choi and J. K. Park, *J. Appl. Polym. Sci.*, 2000, **77**, 226–231.

163   J. Odent, P. Leclère, J. M. Raquez and P. Dubois, *Eur. Polym. J.*, 2013, **49**, 914–922.

164   A. T. Lorenzo, M. L. Arnal, J. Albuerne and A. J. Müller, *Polym. Test.*, 2007, **26**, 222–231.

165   T. Ougizawa and T. Inoue, in *Morphology of Polymer Blends*, 2014, pp. 876–917.

166   R. M. Michell, I. Blaszczyk-Lezak, C. Mijangos and A. J. Müller, *Polym. (United Kingdom)*, 2013, 54, 4059–4077.

167   H. Li and M. a. Huneault, *Polymer (Guildf).*, 2007, **48**, 6855–6866.

168   M. Avrami, *J. Chem. Phys.*, 1939, **7**, 1103–1112.

169   K. a. Athanasiou, G. G. Niederauer and C. M. Agrawal, *Biomaterials*, 1996, **17**, 93–102.

170   R. Auras, B. Harte and S. Selke, *Macromol. Biosci.*, 2004, **4**, 835–864.

171   Y. Cheng, S. Deng, P. Chen and R. Ruan, *Front. Chem. China*, 2009, **4**, 259–264.

172   R. E. Drumright, P. R. Gruber and D. E. Henton, *Adv. Mater.*, 2000, **12**, 1841–1846.

173   M. Jamshidian, E. A. Tehrany, M. Imran, M. Jacquot and S. Desobry, *Compr. Rev. Food Sci. Food Saf.*, 2010, **9**, 552–571.

174   A. J. Müller, M. Avila, G. Saenz and J. Salazar, in *Poly(lactic acid) Science and Technology: Processing, Properties, Additives and Applications*, ed. R. Jimenez, A., Peltzer, M., Ruseckaite, The Royal Society of Chemistry, 2015, pp. 66–98.

175   M. Hiijanen-vainio, P. Varpomaa, J. Seppala and P. Tormala, *Macromol. Chem. Phys.*, 1996, **197**, 1503–1523.

176   A. V. Janorkar, A. T. Metters and D. E. Hirt, *Macromolecules*, 2004, **37**, 9151–9159.

177   G. Groeninckx, M. Vanneste and V. Everaert, in *Polymer Blends Handbook*, ed. L. A. Utracki, Springer Netherlands, Dordrecht, 2003, pp. 203–294.

178   R. M. Müller, A. J. and Michell, in *Polymer Morphology: Principles, Characterization, and Processing*, ed. Q. Guo, John Wiley & Sons, Hoboken, NJ,

USA, 2016, pp. 72–99.

179   Y. Zhang, F. Jiang, W. Wang and Z. Wang, *J. Phys. Chem. B*, 2014, **118**, 9112–7.

180   X.-F. Wei, R.-Y. Bao, Z.-Q. Cao, L.-Q. Zhang, Z.-Y. Liu, W. Yang, B.-H. Xie and M.-B. Yang, *Colloid Polym. Sci.*, 2014, **292**, 163–172.

181   P. Pan, G. Shan and Y. Bao, *Ind. Eng. Chem. Res.*, 2014, **53**, 3148–3156.

182   M. Pracella, in *Handbook of Polymer Crystallization*, ed. G. C. R. E. Piorkowska, John Wiley & Sons, Hoboken, NJ, USA, 2013, pp. 287–326.

183   R. M. Michell and A. J. Müller, *Prog. Polym. Sci.*, 2016, **54–55**, 183–213.

184   T. Patrício and P. Bártolo, *Procedia Eng.*, 2013, **59**, 292–297.

185   T. Patrício, M. Domingos, A. Gloria and P. Bártolo, *Procedia CIRP*, 2013, **5**, 110–114.

186   Y. Y. Chen, L. M. Geever, C. L. Higginbotham and D. M. Devine, *Eng. Technol. Res.*, 2014, **679**, 50–56.

187   I. Fortelný, A. Ostafińska, D. Michálková, J. Jůza, J. Mikešová and M. Šlouf, *Polym. Bull.*, 2015, **72**, 2931–2947.

188   M. Rizzuto, A. Mugica, M. Zubitur, D. Caretti and A. J. Müller, *CrystEngComm*, 2016, **18**, 2014–2023.

189   K. Chavalitpanya and S. Phattanarudee, *Energy Procedia*, 2013, **34**, 542–548.

190   L. Calandrelli, A. Calarco, P. Laurienzo, M. Malinconico, O. Petillo and G. Peluso, *Biomacromolecules*, 2008, **9**, 1527–1534.

191   L. Gardella, M. Calabrese and O. Monticelli, *Colloid Polym. Sci.*, 2014, **292**, 2391–2398.

192   A. S. Luyt and S. Gasmi, *J. Mater. Sci.*, 2016, **51**, 4670–4681.

193   F. Tuba, L. Oláh and P. Nagy, *Eng. Fract. Mech.*, 2011, **78**, 3123–3133.

194   S. Wachirahuttapong, C. Thongpin and N. Sombatsompop, *Energy Procedia*, 2016, **89**, 198–206.

195   L. Wang, W. Ma, R. a. Gross and S. P. McCarthy, *Polym. Degrad. Stab.*, 1998, **59**, 161–168.

196   R. V. Castillo, A. J. Müller, J. M. Raquez and P. Dubois, *Macromolecules*, 2010, **43**, 4149–4160.

197   N. López-Rodríguez, A. López-Arraiza, E. Meaurio and J. R. Sarasua, *Polym. Eng.*

Sci., 2006, **46**, 1299–1308.

198   M. Derakhshandeh, N. Noroozi, L. L. Schafer, D. Vlassopoulos and S. G. Hatzikiriakos, *Rheol. Acta*, 2016, **55**, 657–671.

199   Y. Zhang, Z. Wang, F. Jiang, J. Bai and Z. Wang, *Soft Matter*, 2013, **9**, 5771–5778.

200   A. J. Müller, V. Balsamo and M. L. Arnal, *Adv. Polym. Sci.*, 2005, **190**, 1–63.

201   Cardinaels, R., Moldenaers, P., in *Polymer Morphology: Principles, Characterization, and Processing*, ed. Q. Guo, John Wiley & Sons, Hoboken, NJ, USA, 2016, pp. 348–373.

202   R. Androsch and M. L. Di Lorenzo, *Macromolecules*, 2013, **46**, 6048–6056.

203   E. Quero, A. J. Müller, F. Signori, M. B. Coltelli and S. Bronco, *Macromol. Chem. Phys.*, 2012, **213**, 36–48.

204   R. Liao, B. Yang, W. Yu and C. Zhou, *J. Appl. Polym. Sci.*, 2007, **104**, 310–317.

205   T. Zhang, J. Hu, Y. Duan, F. Pi and J. Zhang, *J. Phys. Chem. B*, 2011, **115**, 13835–13841.

206   N. X. Sun, X. D. Liu and K. Lu, *Scr. Mater.*, 1996, **34**, 1201–1207.

207   B. Imre, K. Renner and B. Pukánszky, *Express Polym. Lett.*, 2014, **8**, 2–14.

208   Q. Lan and Y. Li, *Macromolecules*, 2016, **49**, 7387–7399.

209   M. Avella, M. E. Errico, P. Laurienzo, E. Martuscelli, M. Raimo and R. Rimedio, *Polym. Commun.*, 2000, **41**, 3875–3881.